SAPIENZA
UNIVERSITÀ DI ROMA

On Some Adventures in Dynamic Combinatorial Chemistry

Facoltà di Scienze Matematiche, Fisiche e Naturali

Ph.D. in Chemical sciences

XXXI cycle

Candidate

Simone Albano

1170088

Supervisor
Prof. Stefano Di Stefano

Dean of the Doctoral School
Prof. Osvaldo Lanzalunga

a.a. 2017-2018

Contents

1. An Introduction to Dynamic Combinatorial Chemistry

ABSTRACT

A brief introduction to the concepts and tools of dynamic combinatorial chemistry (DCC) is discussed. Particular attention is paid to the selection and amplification processes of library members induced by molecular recognition, with a special focus on the external template effect. Some considerations on the features of the dynamic covalent chemistries employed in the field are also presented. In conclusion a short overview on the current state of the discipline is given, along with some perspectives on future developments of the field.

INTRODUCTION

"Chemistry is the science of matter and its transformations"[1] and chemists have always put all their efforts in harnessing the interactions between atoms to efficiently produce molecules and materials (and always will). A wealth of methods has been developed for the making and breaking of covalent bonds between atoms in the most precise and controlled way possible. Moreover, these procedures and tools can be combined together and organized in suitable synthetic strategies for the achievement of increasingly complex molecular architectures and materials. Traditionally, reactions under kinetic control receive major attention in this respect, because they allow for the irreversible formation of covalent bonds and the products of these type of reactions can neither revert back to reactants nor convert into other products under the reaction conditions. These aspects are both of prime importance for the achievement of a single target product with the highest yield and the least effort in purification in each reaction.

Around fifty years ago a new groundbreaking field of chemistry took its very first steps, supramolecular chemistry,[2] whose aim is to study the complex and higher order discrete entities formed by selective association of two or more molecules or ions through non-covalent interactions. The non-covalent intermolecular interactions by which the recognition processes underlying the assembly of these supramolecules take place are reversible and, usually, labile, giving to them the feature of being dynamic. Nonetheless, it is also possible to endow molecular structures with dynamic features by the incorporation of reversible covalent bonds in the construction process, allowing to obtain more robust molecular structures, solely made of covalent bonds, that can undergo structural changes in response to the chemical and physical stimuli that influence or perturb these equilibria. This intriguing possibility led to the development of a set of tool and concepts, dynamic covalent chemistry (DCvC),[3] which is concerned with the synthesis and manipulation of molecules and materials having built-in reversible covalent bonds and which has already found application in numerous fields of research (Figure 1-1).[3]

DYNAMIC COMBINATORIAL CHEMISTRY

Relying on the basic concepts of DCvC is dynamic combinatorial chemistry (DCC),[4]

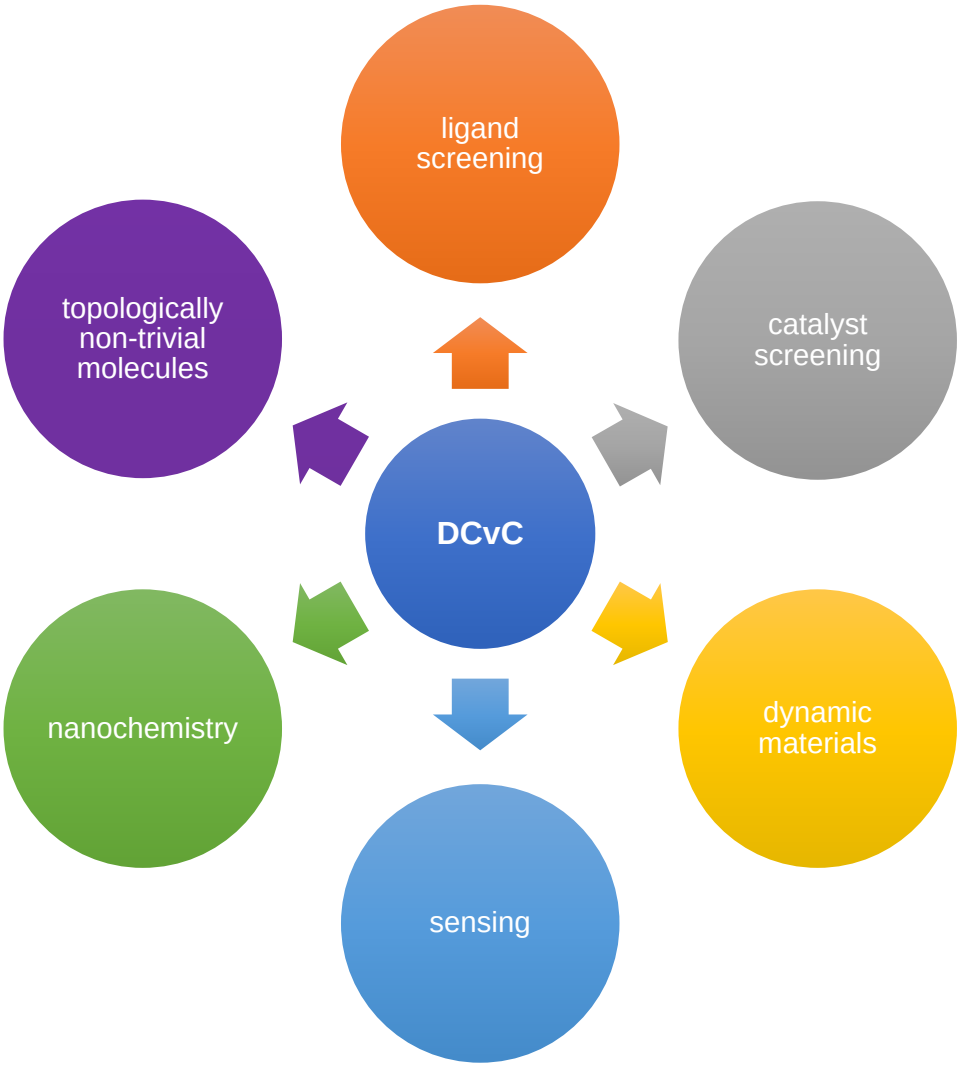

Figure 1-1. Some selected applications of dynamic covalent chemistry.[3]

briefly definable as combinatorial chemistry under thermodynamic control.[4d] Combinatorial chemistry (CC) is a discipline established in the early '90s of the past century that encompasses a variety of synthetic and analytical methods for the high-throughput preparation and screening of compounds (e.g. small organic molecules, peptides, oligonucleotides and oligosaccharides) to be investigated for their individual properties toward an intended target.[5] The quick generation and analysis of combinatorial libraries (CLs) having a large number of related compounds (up to millions) represents an extremely appealing way to obtain, among others, bioactive compounds and receptors in comparison with the rational design, synthesis and testing of single compounds. Dynamic combinatorial chemistry was somehow born to approach the same problems as combinatorial chemistry, but in a different way.[4c-d,6]

Dynamic combinatorial libraries and template effect

Indeed, the profound conceptual difference between CC and DCC resides in the dynamic combinatorial libraries (DCLs) being generated one-pot through reversible association reactions starting from one or more reactant molecular units. As a consequence of this, the members of a DCL can continuously interconvert between each other by reversible exchange of their molecular components (Figure 1-2). Of course, this is not possible in a traditional CL obtained through irreversible reactions.

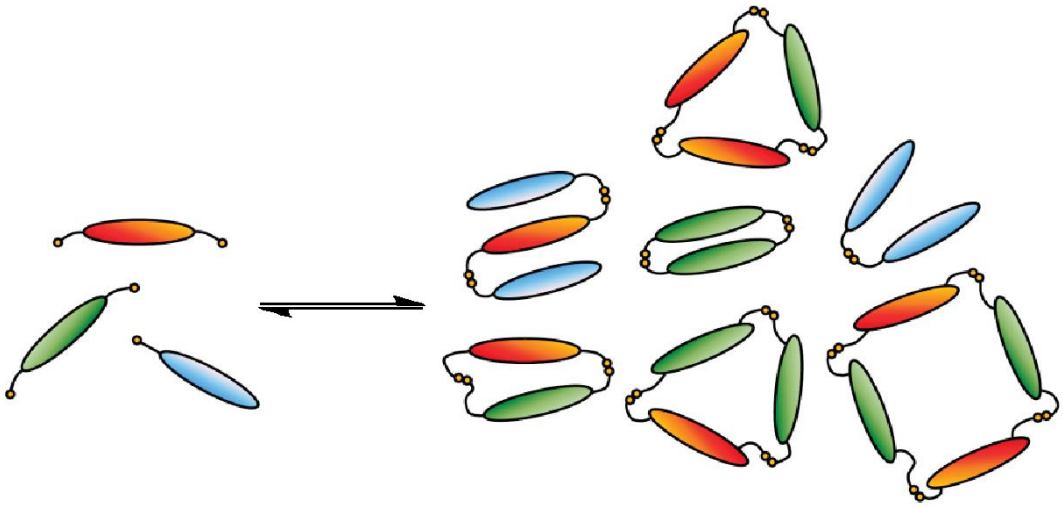

Figure 1-2. Schematic representation of the formation of a DCL from an initial set of starting compounds.[4f]

Therefore, a DCL is a mixture of compounds produced under thermodynamic control and its composition is determined by the standard chemical potentials of all the library members and the chosen experimental conditions (temperature, solvent etc.), thus reflecting their relative thermodynamic stabilities. All the physical and chemical factors that are able to influence or perturb the complex network of equilibria operating in a DCL induce a change in the library composition in a way that minimizes the total free energy of the system. In particular, the addition of an exogenous chemical species that is able to bind to one (or more) members of a DCL inevitably changes the composition of the library by virtue of the Le Châtelier-Braun principle for equilibrium systems,[7] because sequestration of a library member from the DCL to form a more or less stable supramolecular complex with such species pulls the underlying equilibria towards the amplification of this ligand or receptor. This phenomenon is called

thermodynamic template effect and the chemical species that causes it template agent (Figure 1-3).[8]

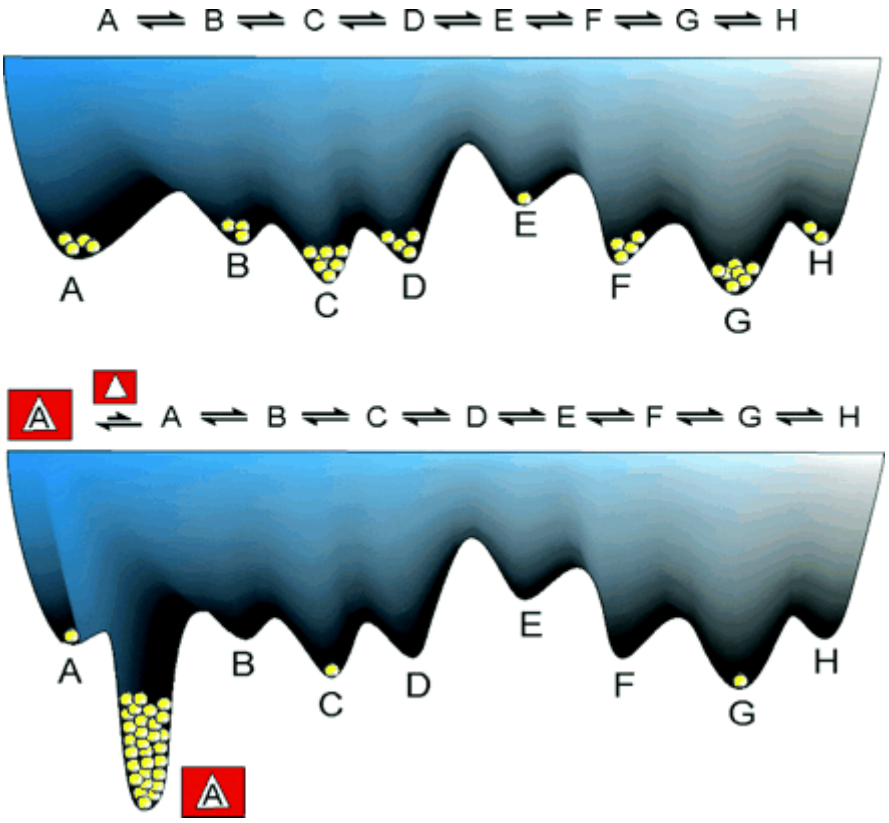

Figure 1-3. Pictorial representation of the thermodynamic template effect in a DCL. Each compound **A**-**H** of a DCL is associated to a minimum in the Gibbs free energy landscape and the number of the little yellow spheres lying in each minimum reflects the abundance of the related library member at equilibrium, before (top) and after (bottom) the addition of a template agent (the red square-shaped mold).[9]

This means that a well-designed DCL can be a very powerful system for the discovery of new receptors, in that it is able to autonomously re-organize its constitution in response to the presence of the target of interest (template agent), which picks out the best member(s) of the library through binding and allows for its selective amplification. In case that the template binds to more than one member of a DCL, the one that shows the highest affinity is, in general, the one that is most selectively amplified.[10] All these considerations about the possibility of a generic DCL to adapt to the experimental conditions and to respond to external influences, like the addition of a target substance, represent the highest advantage of DCC over traditional irreversible CC.[6c]

One of the most celebrated and impressive examples of DCL and template effect has been reported in 2005 by Sanders *et al*. (Figure 1-4).[11] The starting monomer in this study is a modified bifunctional L-prolyl-L-phenylalanine dipeptide (***p*PFm**) having a dimethyl acetal-protected aldehydic function and an hydrazidic function. Addition of an acid as a catalyst to a solution of the monomer enables the generation of a DCL of acyl hydrazones, made up, in principle, of linear and cyclic oligomers (Figure 1-4). However, at low concentration domains, cyclic species are in general highly favored (see Chapter 3).

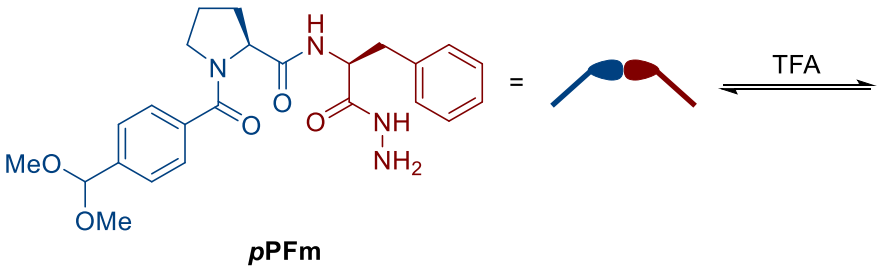

***p*PFm**

Figure 1-4. Preparation of a DCL of acyl hydrazones from ***p*PFm**, using trifluoroacetic acid (TFA) as a catalyst for acyl hydrazone formation and exchange.

The equilibrium condition for a 20 mM DCL of ***p*PFm** is reached in three days and cyclic oligomers up to at least the cyclic hexamer are detected, with no measurable trace of linear hydrazones. Next, the exposure of this DCL to 200 mM neurotransmitter acetylcholine chloride (ACh) as a template agent is found to bring about, after an equilibration period of 44 days, the diastereoselective amplification, up to 67% over the initial amount of the starting material, of a [2]catenane receptor consisting of two interlocked cyclic trimers (Figure 1-5). Importantly, this isomer of the cyclic hexamer could not be observed in absence of ACh. Measurement of the binding constant of ACh to the isolated [2]catenane receptor gave a value of 1.4×10^7 M^{-1}, showing marked affinity between the two species. Furthermore, in a previous work,[12] the same group reported that the addition of lithium and sodium ions (2.7 mM) to a 0.3 mM DCL prepared from the same building block leads to the selective amplification of the cyclic trimer, with a final yield of 98% over the amount of the starting material (Figure 1-5).

These two examples clearly show the ability of a DCL, in presence of a template, to selectively overexpress receptors with high affinity for a target species at the expense

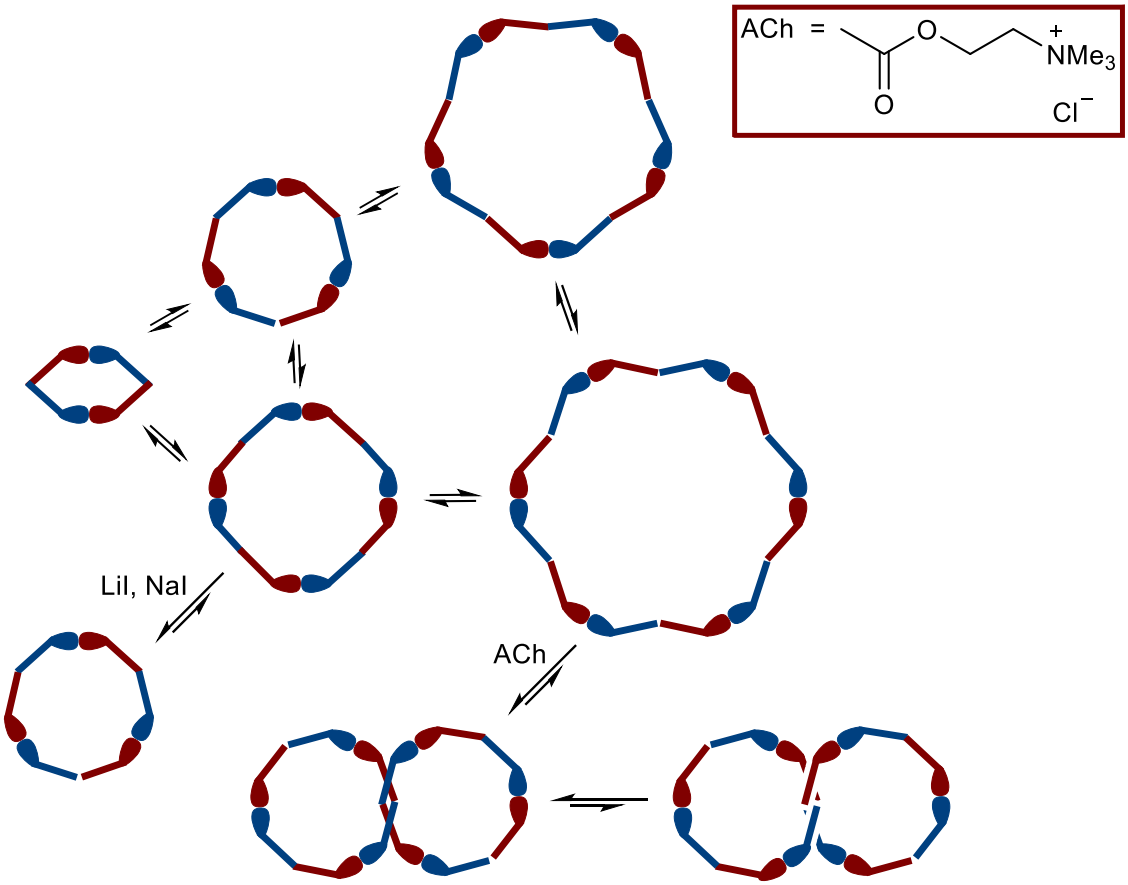

Figure 1-5. DCL obtained starting from bifunctional pseudodipeptide ***p*PFm** through acyl hydrazone formation and exchange. Template effects exerted by LiI, NaI and ACh are showed, along with the preference for one of the two diastereoisomeric [2]catenanes.[11,12]

of the other members of the library, with no need for the experimenter to have in advance much structural information on the desired structure. So, in DCC, the careful rational design that normally precedes the conventional synthesis of a molecule with possible recognition properties is partly sacrificed for a greater good, diversity and selective amplification. Moreover, in cases like the one previously described,[11] the member of the DCL that is amplified due to a favorable interaction with a template species is a compound that may not be present in significant amounts in absence of the template itself. According to the terminology introduced by Jean-Marie Lehn this kind of species may be termed virtual,[4c] because they are virtually accessible by the system but in practice, without the stabilization offered by a template, they are not produced in detectable amounts.

It is possible to include this external templating strategy to induce selection and amplification of any receptor in a DCL into a more general one characterized by

molecular recognition. Indeed, molecular recognition of a library member can take place not only in presence of a suitable added external species, but also intramolecularly, when stabilizing non-covalent interactions are established within a library member, or intermolecularly, when a library member establishes non-covalent interactions with other library members (Figure 1-6). These internal templating strategies produce, respectively, the amplification of species stabilized by folding into a conformationally ordered structure (foldamers)[13] or species involved in high-fidelity recognition and self-assembly with copies of themselves or with molecules of other library members (self-selection).[14]

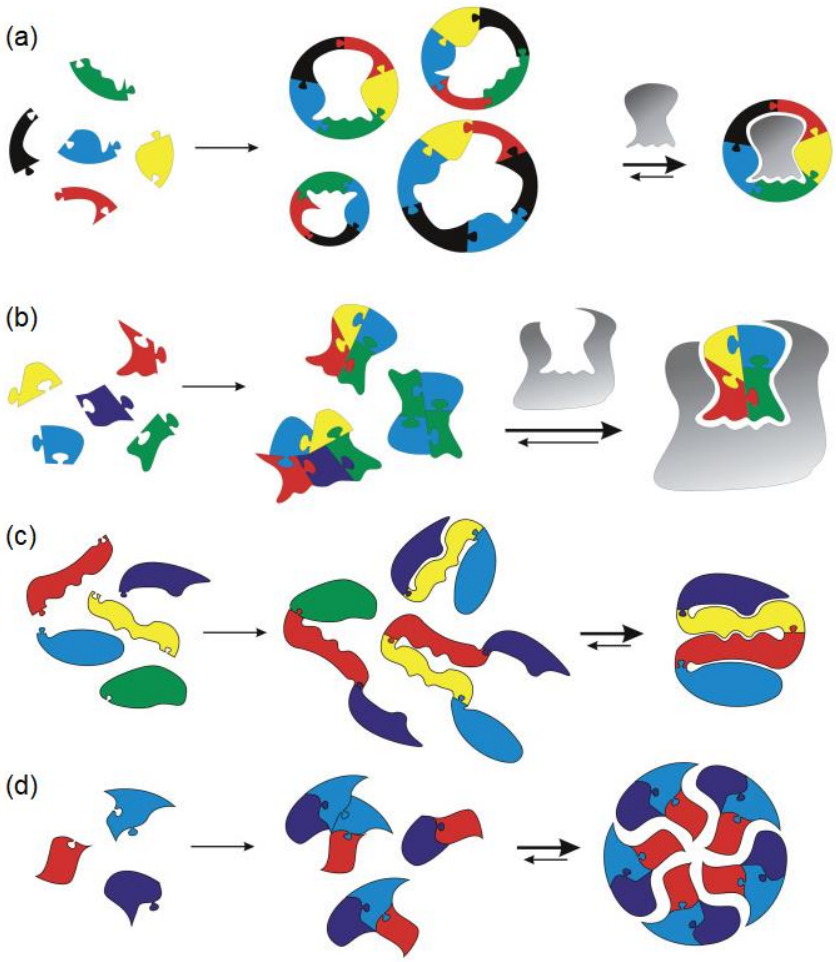

Figure 1-6. Pictorial representation of different molecular recognition-induced processes for the selection and amplification of DCL constituents: (a) external template acting as a guest (molding of the receptor);[4c] (b) external template acting as a host (casting of the receptor);[4c] (c) intramolecular self-templating; (d) intermolecular self-templating.[4b]

Many other ways are also known and have been practically used in DCC, other than molecular recognition, to control the composition of a DCL. Among these, it is possible to cite temperature changes, pH variations, electric field modulation, irradiation, modification of the solvent environment (both in single- and multi-phase systems) and supply of mechanical forces.[3a,4b] Nevertheless, molecular recognition remains unquestionably, from the outset of the discipline, the most employed and investigated approach to manipulate the complex distribution of chemical species expressed in a DCL.

Reversible reactions

An essential feature of DCC is the dynamic chemistries used to build up DCLs. Over the years dozens of different reversible reactions, leading not only to dynamic covalent bonds but also to non-covalent bonds, were adopted, the former being the most employed ones by far.[3d,4b,4d,15] A short collection of some of the more representative dynamic covalent chemistries employed in DCC is presented in Table 1-1.

It is possible to outline a number of criteria that should be examined when choosing a reversible reaction for a DCC study. First, the dynamic reaction should allow for reasonably fast formation and equilibration of the library, so that the single members are adequately stable for detection and, eventually, isolation, yet keeping their dynamic behavior. It is also desirable to have the possibility to quickly quench the reaction after equilibrium is attained, to facilitate isolation of the eventually selected library members, avoiding possible complications due to further exchange. For these reasons, weak and labile non-covalent bonds (hydrogen bonds and to some extent coordinative bonds) are rarely chosen when chromatographic analysis or separation is needed. Secondly, the conditions for the reversible chemistry to occur should be compatible with the specific conditions needed for selection (e.g. solubility of the template agent). In particular, sufficiently mild conditions are desirable to not interfere with molecular recognition-induced selection processes, which are based on weak non-covalent bonds.

CONCLUSIONS AND OUTLOOK

The discipline of DCC, in more than twenty years of history and continuous development, has surely proven as a powerful tool for the discovery of new molecules,

Table 1-1. Examples of reversible covalent reactions of historical value and widespread use (conditions and catalysts are omitted).

C−O bond exchange reactions
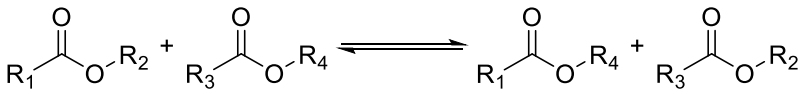 (a)
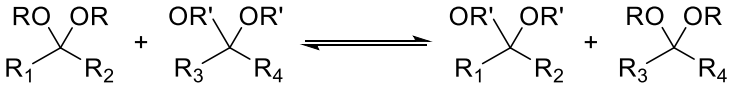 (b)
C=N bond exchange reactions
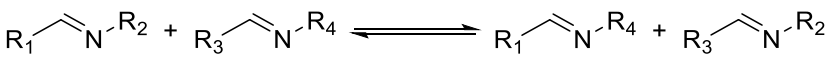 (c)
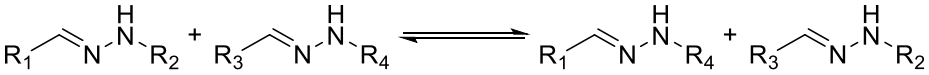 (d)
Other exchange reactions
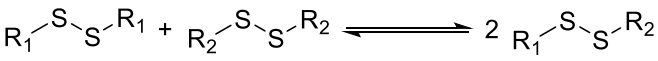 (e)
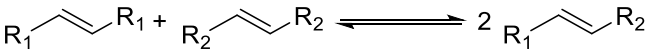 (f)

(a) Ester exchange; (b) acetal exchange; (c) imine metathesis; (d) hydrazone exchange; (e) disulfide exchange; (f) alkene metathesis.

mostly via selection induced by molecular recognition. Molecules with interesting binding properties, like receptors for a variety of ions and small molecules,[3a,4] ligands for biomolecules[3a,4a-b,4d,6,16] or catalysts[3a,4b,4d,4g,17] (employing a transition-state analog of the reaction to catalyze as a template agent), have been successfully discovered with this approach. Moreover, DCC has also showed great potential to provide molecules characterized by complex structures that are not as easily accessible with other means, like catenanes and molecular knots.[3a,4f-g,11,18] Unfortunately, the highly appealing and long-awaited goal of DCC-developed drugs, despite the great progresses made in this respect, has not been achieved so far.[3a,4a-b,6,16] In addition to this, DCC has also provided a vast number of results and applications in many other

fields, like sensing[4b,4e,4h19] and materials science[3a,3c,4a,19c,20] only to name a few examples, and more will surely follow.

In recent years, however, a new awareness is growing stronger in the field, inspired both by the scientific advancements in the discipline and the fascination for the complexity of living systems. Indeed, the behavior and the properties exhibited by complex networks of molecules can sometimes be more interesting than the individual properties of their constituents (e.g. like in DCL sensors). Moreover, the features of kinetically trapped and, especially, far-from-equilibrium systems can be extremely attractive. For these reasons, interest in DCC is now increasingly moving towards the study of DCLs at systems level, to investigate the emergent properties of molecular networks.[3a,4d,4g,21] Also, great efforts are being made to combine the equilibration processes of a DCL with kinetically controlled chemical or physical processes (e.g. in the development of dynamic combinatorial self-replicating systems),[3a,4b,4g,22] or to obtain dissipative DCLs by fuel supply.[23]

In conclusion, DCC is a vital discipline, still growing and evolving. Vast and yet unexplored lands are in sight. We can be confident that DCC will again deliver the promise: we can expect the unexpected.

NOTES AND REFERENCES

1 J.-M. Lehn, *Angew. Chem. Int. Ed.* **2015**, *54*, 3276-3289.

2 For a selection of books and reviews on the field, see for example: (a) J.-M. Lehn, *Supramolecular Chemistry – Concepts and Perspectives*, VCH, Weinheim (Germany), **1995**; (b) J. W. Steed, D. R. Turner, K. J. Wallace, *Core Concepts in Supramolecular Chemistry and Nanochemistry*, John Wiley & Sons, Chichester (U.K.), **2007**; (c) *Modern Supramolecular Chemistry: Strategies for Macrocycle Synthesis* (editors: F. Diederich, P. J. Stang, R. R. Tykwinski), Wiley-VCH Verlag, Weinheim (Germany), **2008**; (d) J. W. Steed, J. L. Atwood, *Supramolecular Chemistry (2nd edition)*, John Wiley & Sons, Chichester (U.K.), **2009**; (e) J.-M. Lehn, *Angew. Chem. Int. Ed. Engl.* **1988**, *27*, 89-112; (f) G. V. Oshovsky, D. N. Reinhoudt, W. Verboom, *Angew. Chem. Int. Ed.* **2007**, *46*, 2366-2393; (g) I. V. Kolesnichenko, E. V. Anslyn, *Chem. Soc. Rev.* **2017**, *46*, 2385-2390; (h) D. B. Amabilino, D. K. Smith, J. W. Steed, *Chem. Soc. Rev.* **2017**, *46*, 2404-2420; (i) A. J. Savyasachi, O. Kotova, S. Shanmugaraju, S. J. Bradberry, G. M. Ó'Máille, T. Gunnlaugsson, *Chem* **2017**, *3*, 764-811.

3 See for example: (a) *Dynamic Covalent Chemistry - Principles, Reactions, and Applications* (editors: W. Zhang, Y. Jin), John Wiley & Sons, Chichester (U.K.), **2018**; (b) S. J. Rowan, S. J. Cantrill, G. R. L. Cousins, J. K. M. Sanders, J. F. Stoddart, *Angew. Chem. Int. Ed.* **2002**, *41*, 898-952; (c) R. J. Wojtecki, M. A. Meador, S. J. Rowan, *Nat. Mater.* **2011**, *10*, 14-27; (d) Y. Jin, C. Yu, R. J. Denman, W. Zhang, *Chem. Soc. Rev.* **2013**, *42*, 6634-6654.

4 See for example: (a) *Dynamic Combinatorial Chemistry in Drug Discovery, Bioorganic Chemistry and Material Science* (editor: B. L. Miller), John Wiley & Sons, Hoboken, New Jersey (U.S.A.), **2009**; (b) *Dynamic Combinatorial Chemistry* (editors: J. N. H. Reek, S. Otto), Wiley-VCH Verlag, Weinheim (Germany), **2010**; (c) J.-M. Lehn, *Chem. Eur. J.* **1999**, *5*, 2455-2463; (d) P. T. Corbett, J. Leclaire, L. Vial, K. R. West, J.-L. Wietor, J. K. M. Sanders, S. Otto, *Chem. Rev.* **2006**, *106*, 3652-3711; (e) S. Ladame, *Org. Biomol. Chem.* **2008**, *6*, 219-226; (f) F. B. L. Cougnon, J. K. M. Sanders, *Acc. Chem. Res.* **2012**, *45*, 2211-2221; (g) J. Li, P. Nowak, S. Otto, *J. Am. Chem. Soc.* **2013**, *135*, 9222-9239; (h) A. Herrmann, *Chem. Soc. Rev.* **2014**, *43*, 1899-1933.

5 See for example: (a) C. D. Floyd, C. Leblanc, M. Whittaker, *Combinatorial Chemistry as a Tool for Drug Discovery in Progress in Medicinal Chemistry - Vol. 36* (editors: F. D. King, A. W. Oxford), Elsevier Science, Amsterdam (The Netherlands), **1999**; (b) G. Lowe, *Chem. Soc. Rev.* **1995**, *24*, 309-317; (c) F. Balkenhohl, C. von dem Bussche-Hünnefeld, A. Lansky, C. Zechel, *Angew Chem Int. Ed Engl,* **1996**, *35*, 2288-2337; (d) N. Srinivasan, J. D Kilburn, *Curr. Opin.*

Chem. Biol. **2004**, *8*, 305-310; (e) R. Liu, X. Li, K. S Lam, *Curr. Opin. Chem. Biol.* **2017**, *38*, 117-126.

6 (a) C. Karan, B. L. Miller, *Drug Discov. Today* **2000**, *5*, 67-75; (b) O. Ramström, J.-M. Lehn, *Nat. Rev. Drug Discov.* **2002**, *1*, 26-36; (c) S. Otto, R. L. E. Furlan, J. K. M. Sanders, *Drug Discov. Today* **2002**, *7*, 117-125; (d) J. D. Cheeseman, A. D. Corbett, J. L. Gleason, R. J. Kazlauskas, *Chem. Eur. J.* **2005**, *11*, 1708-1716; (e) P. Frei, R. Hevey, B. Ernst, *Chem. Eur. J.* **2018**, DOI: 10.1002/chem.201803365.

7 See for example: (a) I. N. Levine, *Physical Chemistry (6th edition)*, McGraw Hill, New York, New York (U.S.A.), **2009**, pp. 194-198; (b) J. de Heer, *J. Chem. Ed.* **1957**, *34*, 375-380; (c) R. S. Treptow, *J. Chem. Ed.* **1980**, *57*, 417-420.

8 See for example: (a) T. J. McMurry, K. N. Raymond, P. H. Smith, *Science* **1978**, *244*, 938-943; (b) D. H. Busch, N. A. Stephenson, *Coord. Chem. Rev.* **1990**, *100*, 119-154; (c) D. H. Busch, *J. Inclusion Phenom. Mol. Recognit. Chem.* **1992**, *12*, 389-395; (d) R. Hoss, F. Vögtle, *Angew. Chem. Int. Ed.* **1994**, *33*, 375-384; (e) J. E. Beves, B. A. Blight, C. J. Campbell, D. A. Leigh, R. T. McBurney, *Angew. Chem. Int. Ed.* **2011**, *50*, 9260-9327; (f) V. Martí-Centelles, M. D. Pandey, M. I. Burguete, S. V. Luis, *Chem. Rev.* **2015**, *115*, 8736-8834.

9 R. L. E. Furlan, S. Otto, J. K. M. Sanders, *Proc. Natl. Acad. Sci. U.S.A.* **2002**, *99*, 4801-4804.

10 It must be stressed, however, that there may be exceptions to this general observation due to the fact that the most selective amplification for the best binder does not always go hand in hand with the inevitable requirement for systems under thermodynamic control to minimize their total Gibbs free energy. For a deeper insight into this aspect of DCC, see for example: (a) Z. Grote, R. Scopelliti, K. Severin, *Angew. Chem. Int. Ed.* **2003**, *42*, 3821-3825; (b) K. Severin, *Chem. Eur. J.* **2004**, *10*, 2565-2580; (c) P. T. Corbett, S. Otto, J. K. M. Sanders, *Chem. Eur. J.* **2004**, *10*, 3139-3143; (d) P. T. Corbett, J. K. M. Sanders, S. Otto, *J. Am. Chem. Soc.* **2005**, *127*, 9390-9392.

11 R. T. S. Lam, A. Belenguer, S. L. Roberts, C. Naumann, T. Jarrosson, S. Otto, J. K. M. Sanders, *Science* **2005**, *308*, 667-669.

12 S. L. Roberts, R. L. E. Furlan, S. Otto, J. K. M. Sanders, *Org. Biomol. Chem.* **2003**, *1*, 1625-1633.

13 On foldamers, see for example: (a) *Foldamers: Structure, Properties and Applications* (editors: S. Hecht, I. Huc), Wiley-VCH, Weinheim (Germany), **2007**; (b) D. J. Hill, M. J. Mio, R. B. Prince, T. S. Hughes, J. S. Moore, *Chem. Rev.* **2001**, *101*, 3893-4011; (c) C. M Goodman, S. Choi, S. Shandler, W. F DeGrado, *Nat. Chem. Biol.* **2007**, *3*, 252-262.

14 Self-selection can be considered as a special example of a more general phenomenon called self-sorting (see also chapter 4 in reference 4a, and references 4g and 4h). On self-sorting, see

for example: (a) A. Wu, L. Isaacs, *J. Am. Chem. Soc.* **2003**, *125*, 4831-4835; (b) M. M. Safont-Sempere, G. Fernández, F. Würthner, *Chem. Rev.* **2011**, *111*, 5784-5814; (c) K. Osowska, O. Š. Miljanić, *Synlett* **2011**, 1643-1648; (d) Z. He, W. Jiang, C. A. Schalley, *Chem. Soc. Rev.* **2015**, *44*, 779-789.

15 K. Meguellati, S. Ladame, *Top. Curr. Chem*. **2012**, *322*, 291-314.

16 See for example: (a) C. R. Sherman Durai, M. M. Harding, *Aust. J. Chem.* **2011**, *64*, 671-680; (b) M. Mondal, A. K. H. Hirsch, *Chem. Soc. Rev.* **2015**, *44*, 2455-2488; (c) R. Huang, I. K. H. Leung, *Molecules* **2016**, *21*, 910-928.

17 See for example: (a) U. Lüning, *Pol. J. Chem.* **2008**, *82*, 1161-1174; (b) P. Dydio, P.-A. R. Breuil, J. N. H. Reek, *Isr. J. Chem.* **2013**, *53*, 61-74.

18 See for example: (a) C. J. Bruns, J. F. Stoddart, *The Nature of Mechanical Bond*, John Wiley & Sons, Hoboken, New Jersey (U.S.A.), **2017**, chapter 3; (b) L. Raehm, D. G. Hamilton, J. K. M. Sanders, *Synlett* **2002**, 1743-1761; (c) G. Gíl-Ramírez, David A. Leigh, A. J. Stephens, *Angew. Chem. Int. Ed.* **2015**, *54*, 6110-6150; (d) S. D. P. Fielden, D. A. Leigh, S. L. Woltering, *Angew. Chem. Int. Ed.* **2017**, *56*, 11166-11194; (e) F. B. L. Cougnon, K. Caprice, M. Pupier, A. Bauzá, A. Frontera, *J. Am. Chem. Soc.* **2018**, *140*, 12442-12450.

19 See for example: (a) S. Otto, K. Severin, *Top. Curr. Chem.* **2007**, *277*, 267-288; (b) A. Herrmann, *Chem. Eur. J.* **2012**, *18*, 8568-8577; (c) E. Moulin, G. Cormos, N. Giuseppone, *Chem. Soc. Rev.* **2012**, *41*, 1031-1049.

20 See for example: (a) J.-M. Lehn, *Prog. Polym. Sci.* **2005**, *30*, 814-831; (b) N. Giuseppone, *Acc. Chem. Res.* **2012**, *45*, 2178-2188. (c) F. García, M. M. J. Smulders, *J. Polym. Sci. Part A: Polym. Chem.* **2016**, *54*, 3551-3577; (d) Y. Liu, J.-M. Lehn, A. K. H. Hirsch, *Acc. Chem. Res.* **2017**, *50*, 376-386.

21 See for example: (a) R. F. Ludlow, S. Otto, *Chem. Soc. Rev.* **2008**, *37*, 101-108; (b) R. A. R. Hunt, S. Otto, *Chem. Commun.* **2011**, *47*, 847-858; (c) J.-M. Lehn, *Angew. Chem. Int. Ed.* **2013**, *52*, 2836-2850; (d) O. Š. Miljanić, *Chem* **2017**, *2*, 502-524. For more information on systems chemistry, see for example: (e) G. M. Whitesides, R. F. Ismagilov, *Science* **1999**, *284*, 89-92; (f) J. R. Nitschke, *Nature* **462**, 736-738; (g) K. Ruiz-Mirazo, C. Briones, A. de la Escosura, *Chem. Rev.* **2014**, *114*, 285-366; (h) E. Mattia, S. Otto, *Nat. Nanotechnol.* **2015**, *10*, 111-119; (i) G. Ashkenasy, T. M. Hermans, S. Otto, A. F. Taylor, *Chem. Soc. Rev.* **2017**, *46*, 2543-2554.

22 See for example: (a) J. J. P. Peyralans, S. Otto, *Curr. Opin. Chem. Biol.* **2009**, *13*, 705,713; (b) V. del Amo, D. Philp, *Chem. Eur. J.* **2010**, *16*, 13304-13318; (c) E. Moulin, N. Giuseppone, *Top. Curr. Chem.* **2012**, *322*, 87-106; (d) S. Otto, *Acc. Chem. Res.* **2012**, *45*, 2200-2210; (e) J. W. Sadownik, E. Mattia, P. Nowak, S. Otto, *Nat. Chem.* **2016**, *8*, 264-269; (f) S. M. Morrow, A. J. Bissette, S. P. Fletcher, *Tetrahedron* **2017**, *73*, 5005-5010. For more information on self-

replication, see for example: (g) L. E. Orgel, *Nature* **1992**, *358*, 203-209; (h) M. M. Conn, J. Rebek Jr., *Curr. Opin. Struct. Biol.* **1994**, *4*, 629-635; (i) V. Patzke, G. von Kiedrowski, *Arkivoc* **2007**, *5*, 293-310; (j) N. Paul, G. F Joyce, *Curr. Opin. Chem. Biol.* **2004**, *8*, 634-639; (k) G. Clixby, L. Twyman, *Org. Biomol. Chem.* **2016**, *14*, 4170-4184.

23 See for example: (a) C. G. Pappas, I. R. Sasselli, R. V. Ulijn, *Angew. Chem. Int. Ed.* **2015**, *54*, 8119-8123; (b) M. Tena-Solsona, C. Wanzke, B. Riess, A. R. Bausch, J, Boekhoven, *Nat. Commun.* **2018**, *9*: 2044.

2. Formation of Imidazo[1,5-*a*]pyridine Derivatives Due to the Action of Fe^{2+} on Dynamic Libraries of Imines

ABSTRACT

An imidazo[1,5-*a*]pyridine derivative was unexpectedly obtained through the action of Fe^{2+} on a dynamic combinatorial library of imines generated *in situ* via condensation of benzaldehyde and 2-picolylamine. The reaction product was easily isolated as the only nitrogen-containing product eluted from the chromatographic column. A reaction mechanism is proposed in which the combined kinetic and thermodynamic effects exerted by Fe^{2+} on the various steps of the complex reaction sequence are discussed. The nature of the added metal cation was found to be crucial for the achievement of this imidazo[1,5-*a*]pyridine product as well as its amount in the reaction mixture. When the electronic effects were evaluated, gratifying yields were obtained only in the presence of moderately electron-releasing or moderately electron-withdrawing groups on the aldehyde reactant. No traces of imidazo[1,5-*a*]pyridine derivatives were obtained for *p*-methoxy- and *p*-nitro-benzaldehyde.

Work published in:

S. Albano, G. Olivo, L. Mandolini, C. Massera, F. Ugozzoli, S. Di Stefano, *J. Org. Chem.* **2017**, *82*, 3820-3825.

INTRODUCTION

An imine is the condensation product of a primary amine with an aldehyde or a ketone, therefore having a carbon-nitrogen double bond to which carbon or hydrogen atoms are connected.

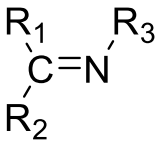

The chemistry of imines is one of the oldest[1] and most established in organic chemistry.[2] A major feature of the imine functionality is the reversibility of its formation and of many reactions in which it is involved. For this and other reasons, imines have always been considered as compounds of interest in many research fields, such as organic synthesis[3] and catalysis,[4] materials science[5] and, of course, supramolecular and dynamic combinatorial chemistry.[6] Some of the most relevant reversible reactions of imines are the following (Scheme 2-1):

(a) imine hydrolysis: the reversible reaction with a molecule of water, giving back a carbonyl compound and a primary amine;

(b) transimination: the reversible reaction with a second primary amine, resulting in the exchange of the amine portion in the imine reactant;

(c) metathesis: the reversible reaction with a second imine, resulting in the exchange of the amine portion in the imine reactants.

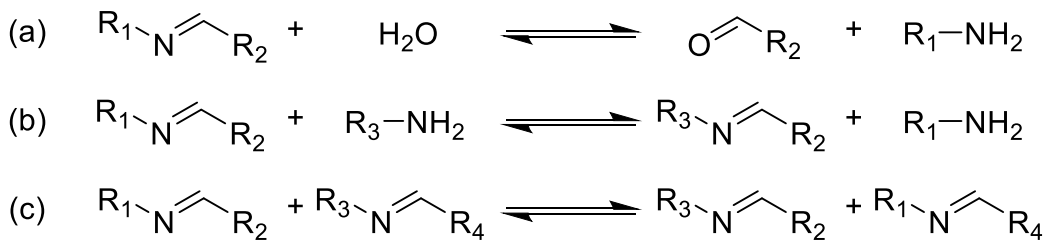

Scheme 2-1. Main reversible carbon-nitrogen exchange reactions involving imines: (a) imine hydrolysis, (b) transimination and (c) imine metathesis.

It was recently reported from our group that the imine-based complex **1**, quantitatively obtained in a one-pot procedure from an acetonitrile mixture of 2-picolylaldehyde, 2-picolylamine and iron(II) trifluoromethanesulfonate in a 2:2:1 molar ratio, respectively,

is a cheap and effective catalyst for the oxidation of nonactivated carbon-hydrogen bonds using hydrogen peroxide as the terminal oxidant (Scheme 2-2).[7]

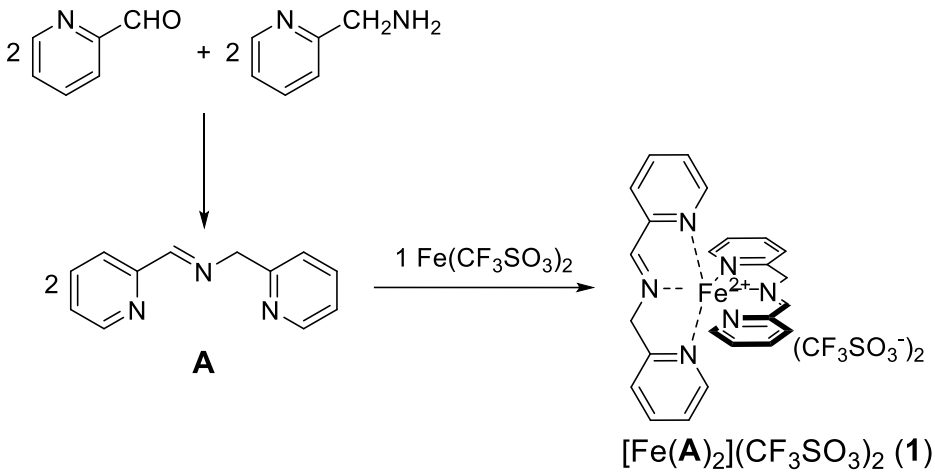

Scheme 2-2. One-pot procedure preparation of complex **1**.

When 2-picolylaldehyde derivatives X-substituted in the γ-position (X = −NO_2, −CH_3, −OCH_3) were used as starting materials, characterization of the resulting complexes was complicated by the transamination reaction showed in Equation 1, which occurred even in the absence of an added base other than 2-picolylamine.[7b] Obviously, no complication occurred in the case of complex **1** (X = −H), where transamination is degenerate.

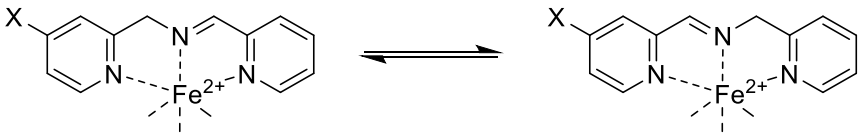

(1)

The reversible nature of transamination, that is the reversible base-induced 1,3-prototropic rearrangement of α-acidic imines, has been known for long.[2c,8] Ramström *et al.*[9] recently introduced the use of transamination as a new carbon-nitrogen exchange reaction in dynamic covalent chemistry. They reported that transamination, induced by a non-nucleophilic tertiary amine, can be carried out simultaneously with transimination, induced by primary amines and a Lewis acid,[2h,10] to yield a two-dimensional dynamic system[11] for which the acronym TATI (transamination−transimination) was coined. They showed that reaction of an *N*-benzylidene-benzylamine with a second primary benzylamine in the presence of a non-nucleophilic tertiary base and a

Lewis acid leads to an equilibrium mixture of nine imines and three amines when all three phenyl groups carry different substituents (Figure 2-1).

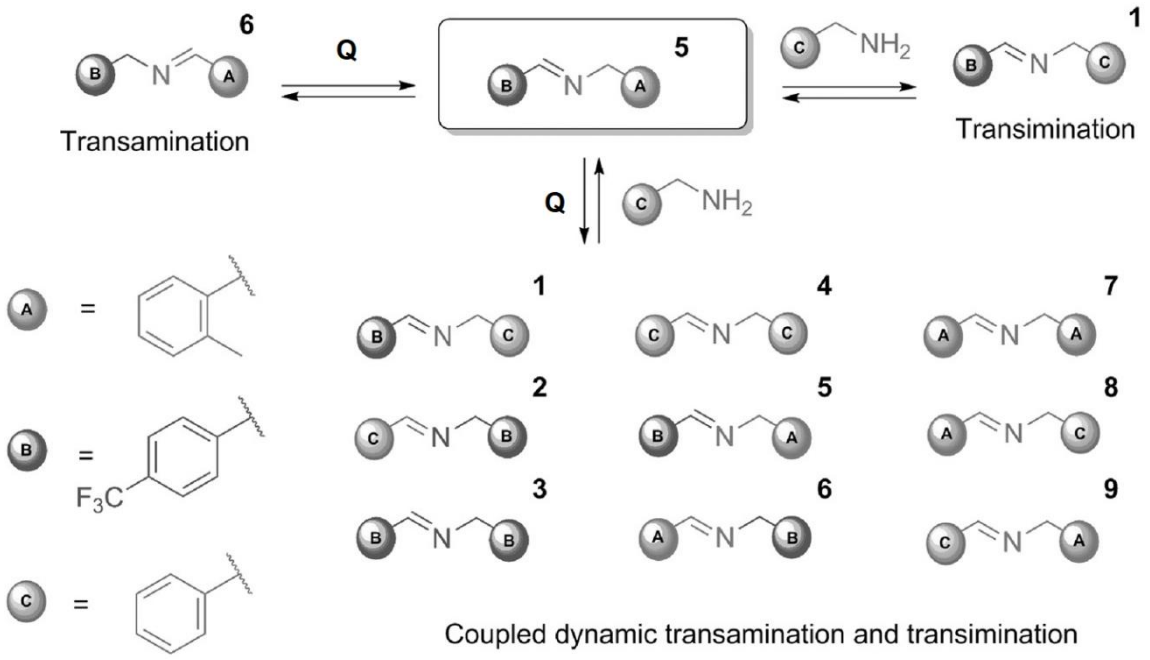

Figure 2-1. Representation of a generic TATI dynamic combinatorial library reported by Ramström *et al.* (**Q** represents quinuclidine, the base used to promote transamination reaction).[9]

The idea behind this work was to use DCC to develop a synthetic methodology, taking advantage of the effect of a template agent on a DCL to drive the network of equilibria toward the amplification of the fittest ligand for the template, necessarily together with the intended synthetic transformation.[12]

RESULTS AND DISCUSSION

Preliminary TATI experiment

Having in mind the possible use of the two-dimensional dynamic character of simultaneous transamination and transimination (TATI) for a synthetic application, we carried out a preliminary experiment to verify the generation of a dynamic combinatorial library of imines (Scheme 2-3) from a mixture of *N*-benzylidene-2-picolylamine (**C**), prepared *in situ* by condensation of benzaldehyde and 2-picolylamine, and 2-picolylamine. The results of the experiment are illustrated by the stacked ^{1}H NMR traces in Figure 2-2.

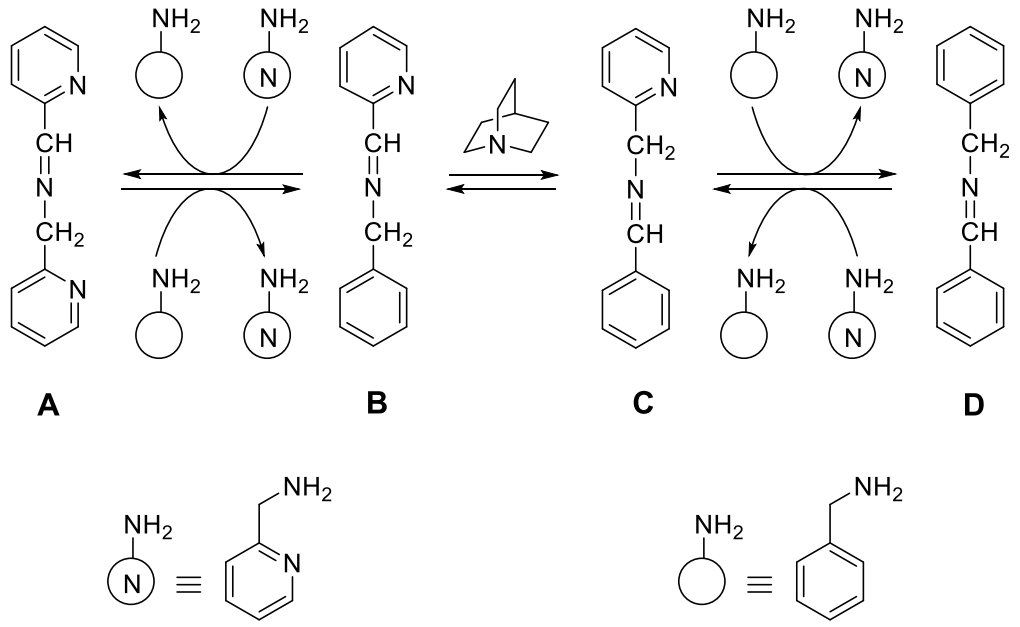

Scheme 2-3. Connected TATI system generated through the reaction of *N*-benzylidene-2-picolylamine (**C**) with 2-picolylamine in the presence of quinuclidine.

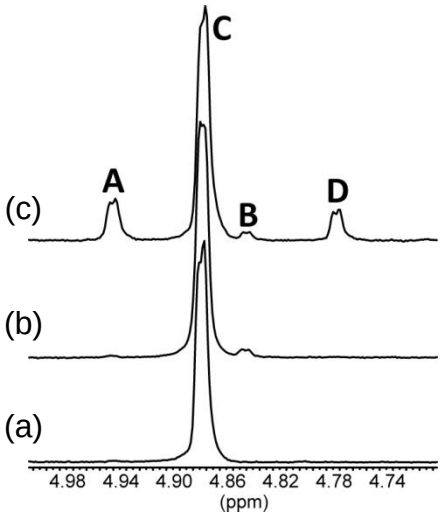

Figure 2-2. TATI of 10 mM *N*-benzylidene-2-picolylamine **C** and 10 mM 2-picolylamine in CD_3CN at 50 °C. ^1H NMR traces in the benzylic region: (a) *N*-benzylidene-2-picolylamine **C**; (b) 7 h after quinuclidine addition; (c) 17 h after 10 mM 2-picolylamine addition.

Trace (a) in the figure shows the benzylic proton signal of 10 mM **C** in CD_3CN at 50 °C. After 7 h from the addition of a ten-fold excess of quinuclidine the signal of transamination product **B** was clearly visible (trace b). Addition of one molar equivalent of 2-picolylamine after 36 h from the start triggered the transimination reactions **B** ⇄ **A** and **C** ⇄ **D**. The ^1H NMR spectrum taken after 17 h from the addition of 2-picolylamine (trace c) showed the expected mixture of four imines, by comparison with authentic

samples. The benzylic signals of benzylamine and 2-picolylamine (not visible in Figure 2-2) at 3.78 and 3.85 ppm, respectively, were also present.

Having ascertained the actual occurrence of the TATI process of Scheme 2-3 under relatively mild conditions, and considering that tridentate nitrogen ligand **A** is most likely the strongest ligand of the lot, we reasoned that addition of iron(II) trifluoromethanesulfonate would steer the DCL toward quantitative formation of the previously described complex **1**. Accordingly, a mixture of 2-picolylamine, benzaldehyde and Fe^{2+} in 4:2:1 molar ratio, respectively, should behave as shown in Equation 2.

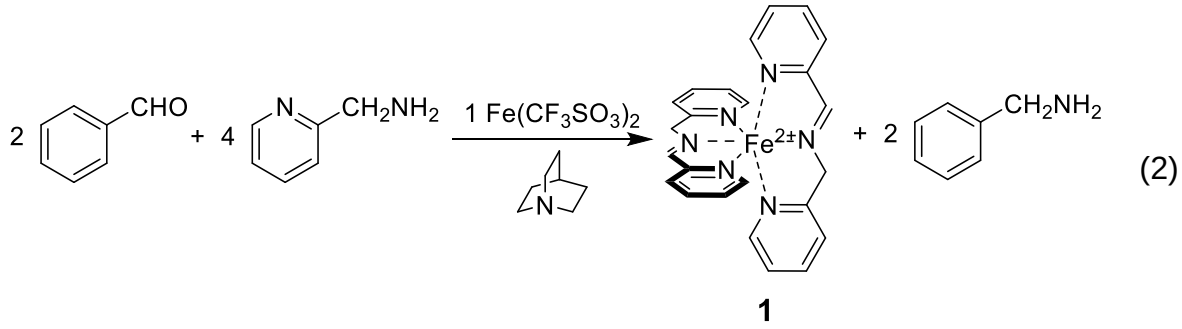

(2)

1

Complex **1** had been previously found to be easily removable from a reaction mixture by simple elution through a short silica pad.[7b] Consequently, if one looks at complex **1** as an easily removable byproduct, the net transformation is the reductive amination of benzaldehyde to benzylamine, in which the role of reductant is played by 2-picolylamine, through the formal isodesmic reaction of Equation 3. The latter compound undergoes oxidation to 2-picolylaldehyde, which should be found in the reaction mixture in the form of the Fe^{2+}−complexed tridentate nitrogen ligand **A** as a result of Fe^{2+} acting as a template agent.

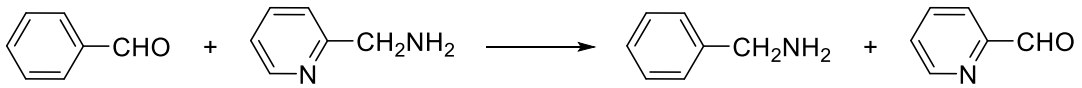

(3)

Based on the above considerations, we envisaged the possibility of realizing the actual transformation of benzaldehyde to benzylamine according to Equation 2, employing a suitable iminopyridine DCL formed through simultaneous TATI equilibria and the thermodynamic template effect exerted by Fe^{2+} to steer the library composition, thus

performing the transformation of an aldehydic function into a methylene amine function.

TATI experiment, structural characterization of the unexpected product and hypothesis of mechanism

The results, however, failed to meet our expectations as shown by the following experiment. A solution of benzaldehyde (15 mmol), 2-picolylamine (30 mmol), bis(acetonitrile)iron(II) trifluoromethanesulfonate (7.5 mmol) and quinuclidine (3 mmol)[13] in freeze-pump-thaw degassed acetonitrile (150 mL) was prepared under argon atmosphere and stirred for 40 h at 50 °C. Column chromatography on the crude product yielded a trace amount of benzaldehyde followed by 0.510 g of a pure yellow solid (mp: 92.0-92.5 °C), and no other compound was eluted from the column. The remaining materials, presumably strongly bound to Fe^{2+}, were trapped at the head of the column. Two additional runs, carried out under identical conditions, gave exactly the same results. A further experiment, carried out without paying attention to the exclusion of air but under otherwise identical conditions, yielded again the same amount of pure product.

Attempts at structure assignment to the isolated compound were based on standard spectrometric and spectroscopic techniques. Electron ionization (EI) and high-resolution electro-spray ionization (ESI) mass spectrometry were fully consistent with the molecular formula $C_{19}H_{15}N_3$ (Mw = 285 g mol^{-1}). The presence of an odd number of nitrogen atoms (namely three) in the product of a reaction between two reactants featuring an even number of nitrogen atoms (namely zero or two) is consistent with the occurrence of a TATI process along the reaction path. According to the formal stoichiometric Equation 4, 0.24 mol of unexpected product **2** per 2 mol of benzaldehyde was obtained.

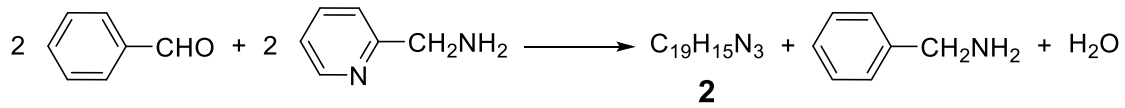

(4)

The ^{1}H NMR spectrum of compound **2** is shown in Figure 2-3. The existence of three different spin systems, involving four, four and seven protons, respectively, was clearly indicated by various bidimensional NMR techniques (COSY, TOCSY, and HSQC), but

this information was not sufficient for the unequivocal structure assignment, as several isomeric structures compatible with the spectroscopic data could be envisaged.

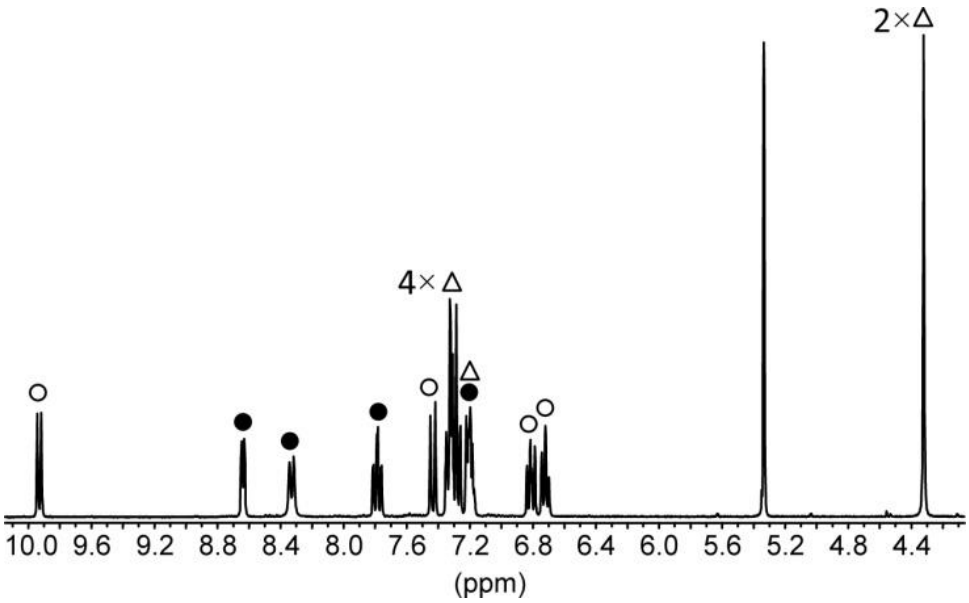

Figure 2-3. ^{1}H NMR spectrum (CD_2Cl_2, 25 °C) of the unknown compound **2**. Three spin systems including 4 (•), 4 (○) and 7 (Δ) protons respectively can be identified via bidimensional NMR techniques. The signal at 5.3 ppm is due to CHDCl.

A conclusive solution to this problem was offered by the obtaining of single crystals suitable for X-ray diffraction analysis, which were prepared by slow diffusion of pentane into a concentrated ethyl acetate solution of compound **2**. The molecular structure of **2** shown in Figure 2-4 was found to be characterized by the presence of an imidazo[1,5-*a*]pyridine bicyclic heteroaromatic nucleus.[14]

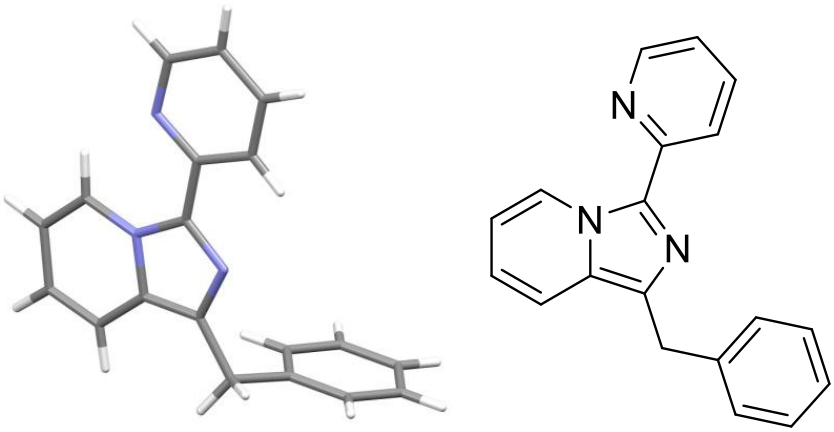

Figure 2-4. X-ray molecular structure of 3-(2-pyridyl)-1-benzylimidazo[1,5-*a*]pyridine (**2**). The three aforementioned spin systems are easily identifiable.

Synthetic strategies targeting a variety of imidazo[1,5-*a*]-pyridine derivatives receive considerable attention in view of potential applications of these compounds in pharmaceutical and materials chemistry as well as N-rich ligands for metal coordination.[15]

We suggest the mechanism outlined in Scheme 2-4 for the transformation of the iron(II) complex of the tridentate iminopyridine ligand **A** into the final product. The key step *a* is the base-catalyzed aldol-type condensation of benzaldehyde with the methylene group of **A**, whose acidity is enhanced by metal complexation. The hemilability of one of the pyridine ligands[7b] (step *b*) opens the way to the Fe^{2+}-activated intramolecular nucleophilic addition of the pyridine sp^2 nitrogen to the imine carbon atom (step *c*).[16] Step *d* is a prototropic rearrangement leading to an Fe^{2+} complex in which the ligand conformation suitable for metal chelation is disfavored by steric repulsion between hydrogen atoms of the pyridine units, as also suggested by the X-ray molecular structure (Figure 2-4) where the given hydrogen atoms are seen on opposite sides. It seems reasonable, therefore, that the complex loses the metal cation (step *e*), thus allowing the elution of free **2** from the chromatographic column.

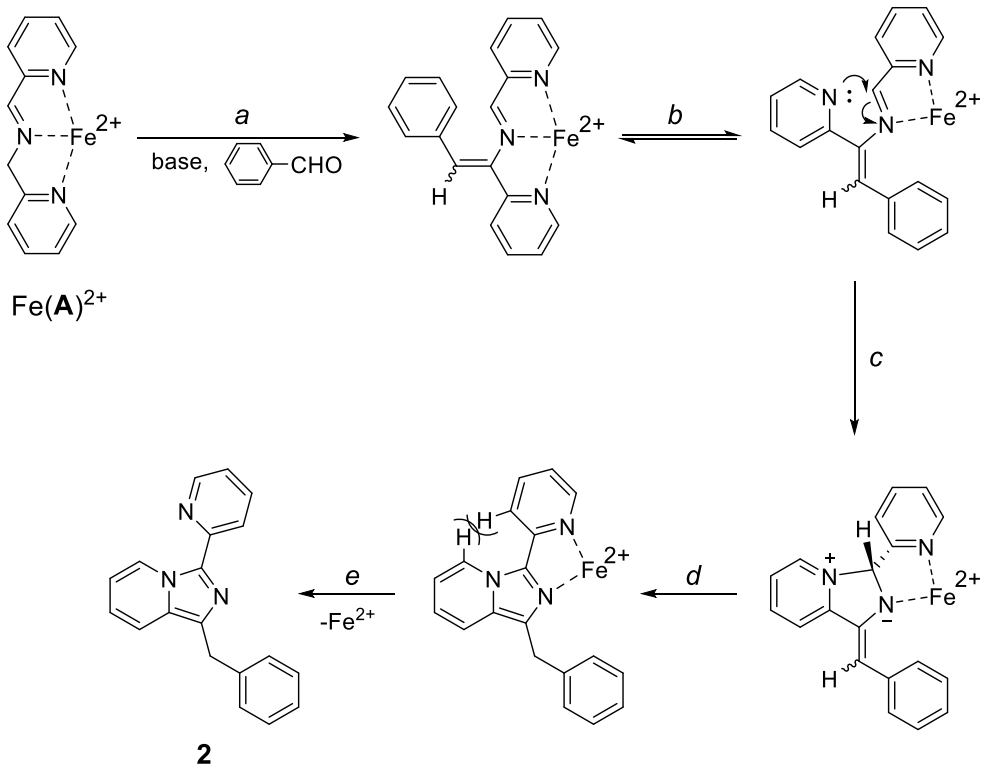

Scheme 2-4. Proposed mechanism for the formation of the unexpected imidazo[1,5-*a*]pyridine derivative **2**.

Optimization and scope of the reaction

Several attempts to optimize and enlarge the scope of the reaction were made. A decrease in yield was observed when shorter reaction times were applied, namely a 12% yield after 32 h to be compared with the 24% yield after 40 h, whereas longer reaction times did not afford any significant improvement (25% yield after 64 h). The yield of 3-(2-pyridyl)-1-benzylimidazo[1,5-*a*]pyridine (**2**) obtained in the presence of a substoichiometric amount of Fe^{2+} (Table 2-1, Entry 1) was lower than that obtained in the presence of the amount required by Equation 2 (Entry 2), but no traces of the expected product were found when the amount of Fe^{2+} was doubled (Entry 3), probably due to extensive complexation of the reactants. Replacement of Fe^{2+} with Zn^{2+}[17] or Co^{2+} (Entries 4 and 5) was completely unsuccessful, whereas Fe^{3+} (Entry 6) turned out to be effective, albeit to a lower degree compared to Fe^{2+}.

Table 2-1. Effect of the amount and nature of the metal ion on the yield of **2** obtained from a mixture of benzaldehyde (1.0 mmol) and 2-picolylamine (2.0 mmol) in 10 mL of acetonitrile held at 50 °C for 40 h.

Entry	Metal ion (mmol)	Yield %[a]
1	Fe^{2+} (0.1)[b]	10
2	Fe^{2+} (0.5)[b]	24
3	Fe^{2+} (1.0)[b]	nil
4	Zn^{2+} (0.5)[c]	nil
5	Co^{2+} (0.5)[d]	nil
6	Fe^{3+} (0.1)[b]	12

[a] Calculated according to Equation 4. [b] Trifluoromethanesulfonate salt. [c] Bromide salt. [d] Chloride salt.

In order to expand the scope of the procedure, a series of *para*-X-substituted benzaldehyde derivatives were reacted with 2-picolylamine in the presence of iron(II) trifluoromethanesulfonate (Table 2-2).

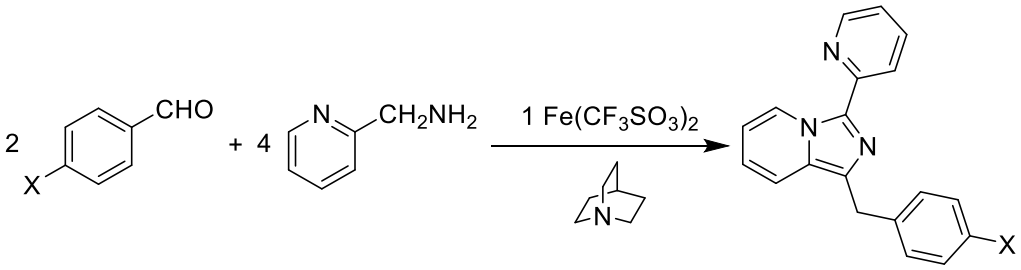

(5)

Table 2-2. Yields of 3-(2-pyridyl)-1-(4-X-benzyl)imidazo[1,5-*a*]pyridine derivatives obtained from a mixture of *p*-X-benzaldehyde (1.0 mmol), 2-picolylamine (2.0 mmol), and bis(acetonitrile)iron(II) trifluoromethanesulfonate (0.5 mmol) in 10 mL of acetonitrile held at 50 °C for 40 h (Equation 5).

X	Yield (%)
H	24
NO_2	nil
Cl	25
CH_3	14
OCH_3	nil

The results listed in Table 2-2 show that no traces of imidazo[1,5-*a*]pyridine products were eluted from the chromatographic column when X was $-OCH_3$ and $-NO_2$. However, significant amounts of the expected products, comparable to that related to the parent benzaldehyde, were obtained when X was $-CH_3$ and −Cl. The adverse effect of both strong electron-releasing and strong electron-withdrawing substituents, indeed, is well precedented in the field of imine chemistry.[10b] Thus, it is not unreasonable to believe that this is also the case in one or more of the steps involved in the multistep sequence of reversible exchange reactions of the TATI process. Furthermore, when X = $-OCH_3$, a strong retarding effect on the rate of aldol condensation (Scheme 2-4, step *a*) is expected. Unfavorable effects arising from

strong resonance interactions can possibly operate also in steps *b*, *c*, and *d* of the hypothesized mechanism illustrated in Scheme 2-4.

CONCLUSIONS

To sum up, a novel imidazo[1,5-*a*]pyridine derivative (**2**) was unexpectedly obtained from the reaction of benzaldehyde (2 equivalents) with 2-picolylamine (4 equivalents), and iron(II) trifluoromethanesulfonate (1 equivalent) in the presence of a catalytic amount of quinuclidine. The yield (24%) is moderate, but the product can be easily isolated in pure form and the starting materials are readily available commercial products. Due to its Lewis acid character, a variety of roles are played by the Fe^{2+} metal cation in the multistep reaction sequence leading from reactants to product. First of all, generation of the TATI system of imines starting from benzaldehyde and 2-picolylamine is most likely accelerated by Fe^{2+}.[18] In addition to this multiple kinetic effect, the high stability of the metal complex of the tridentate nitrogen ligand **A** is expected to drive the dynamic library toward the formation of complex **1**.[19] However, this is not the end of the story, as foreseen in our original project (Equation 2). Subsequent acts in which the role of Fe^{2+} is believed to be crucial are the aldol-type condensation with benzaldehyde (Scheme 2-4, step *a*) and closure of the five-membered imidazole ring (step *c*). Finally, detachment of the metal ion from the complex (step *e*) allows the free ligand **2** to be eluted from the chromatographic column.

In a sense, therefore, the results reported in this work may be viewed as a special application of dynamic combinatorial chemistry. Stabilization and amplification of a specific library member (imine **A**) through metal coordination, does not determine the final composition of the reaction mixture but the generation of a reaction intermediate, which unexpectedly undergoes a series of irreversible transformations leading to the ultimate formation of a complex structure such as that of the imidazo[1,5-*a*]pyridine derivatives isolated. Interestingly, the successful achievement of the imidazo[1,5-*a*]pyridine products was found to be strongly dependent on the nature of the metal cation, that must specifically be Fe^{2+} and must be added in the right amount, namely, 0.5 molar equivalents with respect to the aldehyde. When a series of benzaldehydes substituted in the *para* position were employed in the procedure, satisfactory yields

were obtained only in the presence of moderately electron-releasing or electron-withdrawing groups.

EXPERIMENTAL SECTION

Instruments, general methods and materials

NMR spectra were recorded with a 300 MHz spectrometer at room temperature and were internally referenced to the residual proton solvent signal. Mass spectra were recorded with an ESI-TOF mass spectrometer. UV−vis spectra were recorded with a double-beam spectrophotometer using a standard quartz cell (path length: 1 cm) at room temperature.

All reagents and solvents were purchased at the highest commercial quality and were used without further purification, unless otherwise stated. The glassware was either flame- or oven-dried. Acetonitrile used for the preparation of bis(acetonitrile)iron(II) trifluoromethanesulfonate was distilled over calcium hydride. Diethyl ether used for the preparation of bis(acetonitrile)iron(II) trifluoromethanesulfonate was distilled over sodium and benzophenone. Wet zinc bromide was dried at 250 °C under vacuum for 5 h.

Preparation of 3-(2-pyridyl)-1-benzylimidazo[1,5-*a*]pyridine 2

In a round-bottomed flask a solution of quinuclidine (0.33 g, 3 mmol), benzaldehyde (1.59 g, 15 mmol), 2-picolylamine (3.24 g, 30 mmol) and $[Fe(CH_3CN)_2](CF_3SO_3)_2$ (3.27 g, 7.5 mmol) in acetonitrile (150 mL) was prepared and stirred for 40 h at 50 °C. The solvent was evaporated and the dark brown crude material was chromatographed (silica gel, *n*-hexane/ethyl acetate 9:1) to obtain pure **2** (0.510 g, 1.8 mmol, yield: 24%). Mp: 92.0-92.5 °C. ^{1}H NMR (300 MHz, CD_2Cl_2) δ (ppm): 9.94-9.92 (m, 1H), 8.64-8.63 (m, 1H), 8.34-8.31 (m, 1H), 7.81-7.76 (m, 1H), 7.45-7.42 (m, 1H), 7.35-7.26 (m, 4H), 7.22-7.17 (m, 2H), 6.84-6.79 (m, 1H), 6.74-6.70 (m, 1H), 4.32 (s, 2H). ^{13}C{^{1}H} NMR (75 MHz, CD_2Cl_2) δ (ppm): 151.1, 148.0, 140.5, 136.3, 133.9, 132.2, 129.7, 128.4, 128.2, 125.9, 125.8, 121.3, 121.1, 119.0, 117.2, 113.2, 33.7. UV-vis (CH_2Cl_2) ε (mol^{-1} dm^3 cm^{-1}): 18700 at 362 nm, 12700 at 250 nm. HRMS (ESI-QTOF, *m*/*z*): $[M + H]^+$ calcd for $C_{19}H_{16}N_3$, 286.1344; found, 286.1331.

Preparation of 3-(2-pyridyl)-1-(4-methylbenzyl)imidazo[1,5-*a*]pyridine 3

In a round-bottomed flask a solution of quinuclidine (0.022 g, 0.2 mmol), *p*-methyl-benzaldehyde (0.12 g, 1 mmol), 2-picolylamine (0.22 g, 2 mmol) and $[Fe(CH_3CN)_2](CF_3SO_3)_2$ (0.22 g, 0.5 mmol) in acetonitrile (10 mL) was prepared and stirred for 40 h at 50 °C. The solvent was evaporated and the dark green crude material was chromatographed (silica gel, *n*-hexane/ethyl acetate 9:1) to obtain pure **3** (0.021 g, 0.07 mmol, yield: 14%). Mp: 95.5-96.0°C. ^{1}H NMR (300 MHz, $CDCl_3$) δ (ppm): 9.89-9.87 (m, 1H), 8.62-8.61 (m, 1H), 8.36-8.33 (m, 1H), 7.77-7.72 (m, 1H), 7.32-7.08 (m, 6H), 6.75-6.64 (m, 2H), 4.31 (s, 2H), 2.31 (s, 3H). ^{13}C{^{1}H} NMR (75 MHz, $CDCl_3$) δ (ppm): 151.0, 148.0, 137.1, 136.3, 135.4, 133.8, 132.5, 129.6, 129.0, 128.4, 125.7, 121.7, 121.4, 118.9, 117.5, 113.2, 33.7, 20.9. UV-vis (CH_2Cl_2) ε (mol^{-1} dm^3 cm^{-1}): 12200 at 361 nm, 11500 at 251 nm. HRMS (ESI-QTOF, *m*/*z*): $[M + H]^+$ calcd for $C_{20}H_{18}N_3$, 300.1501; found, 300.1527.

Preparation of 3-(2-pyridyl)-1-(4-chlorobenzyl)imidazo[1,5-*a*]pyridine 4

In a round-bottomed flask a solution of quinuclidine (0.022 g, 0.2 mmol), *p*-chloro-benzaldehyde (0.14 g, 1 mmol), 2-picolylamine (0.22 g, 2 mmol) and $[Fe(CH_3CN)_2](CF_3SO_3)_2$ (0.22 g, 0.5 mmol) in acetonitrile (10 mL) was prepared and stirred for 40 h at 50°C. The solvent was evaporated and the dark gray crude material was chromatographed (silica, *n*-hexane/ethyl acetate 9:1) to obtain pure **4** (0.041 g, 0.13 mmol, yield: 25%). Mp: 109.8-110.3°C. ^{1}H NMR (300 MHz, $CDCl_3$) δ (ppm): 9.90−9.88 (m, 1H), 8.63-8.61 (m, 1H), 8.33-8.31 (m, 1H), 7.78-7.72 (m, 1H), 7.31-7.15 (m, 6H), 6.78-6.66 (m, 2H), 4.30 (s, 2H). ^{13}C{^{1}H} NMR (75 MHz, $CDCl_3$) δ (ppm): 150.9, 148.1, 138.6, 136.3, 134.1, 131.7, 131.5, 129.8, 129.6, 128.4, 125.8, 121.7, 121.3, 119.3, 117.1, 113.3, 33.3. UV-vis (CH_2Cl_2) ε (mol^{-1} dm^3 cm^{-1}): 17400 at 359 nm, 14500 at 250 nm. HRMS (ESI-QTOF, *m*/*z*): $[M + H]^+$ calcd for $C_{19}H_{15}N_3Cl$, 320.0955; found, 320.0938.

Preparation of bis(acetonitrile)iron(II) trifluoromethanesulfonate

Bis(acetonitrile)iron(II) trifluoromethanesulfonate was prepared according to a laboratory procedure.[7b] In a three-neck round-bottomed flask equipped with a dropping funnel and containing freeze-pump-thaw degassed acetonitrile (40 mL), iron(II) chloride was added (2.48 g, 20 mmol) under argon atmosphere. Then trimethylsilyl trifluoromethanesulfonate (8.1 mL, 45 mmol) was slowly added through

the dropping funnel to the iron(II) chloride solution under magnetic stirring, and the resulting reaction mixture was kept at room temperature under inert atmosphere for 15 h. Next, the solvent was evaporated in a rotary evaporator previously flushed with nitrogen and the solid obtained was redissolved in degassed acetonitrile (8 mL). Then the mixture was filtered under argon atmosphere and freeze-pump-thaw degassed diethyl ether (16 mL) was added to the filtered solution, which was subsequently kept under argon atmosphere at -20 °C in a freezer for 16 h. A solid precipitate was collected by filtration of the mixture under argon atmosphere and dried under high vacuum, providing $[Fe(CH_3CN)_2](CF_3SO_3)_2$ as a white solid (6.34 g, 15 mmol, 74%).

NOTES AND REFERENCES

1 H. Schiff, *Ann. Chem. Pharm.* **1864**, *131*, 118-119.

2 For some books and reviews on the topic see: (a) W. P. Jencks, *Catalysis in Chemistry and Enzymology*, McGraw-Hill, New York, New York (U.S.A.), **1969**; (b) R. A. Y. Jones, *Physical and mechanistic organic chemistry (2nd edition)*, Cambridge University Press, Cambridge (U.K.), **1984**, pp. 254-260; (c) R. W. Layer, *Chem. Rev.* **1963**, 63, 489-510; (d) W. P. Jencks, *Prog. Phys. Org. Chem.* **1964**, *2*, 63-128; (e) R. B. Martin, *J. Phys. Org. Chem.* **1964**, *68*, 1369-1377; (f) W. P. Jencks, *Acc. Chem. Res.* **1976**, *9*, 425-432; (g) M. J. Mäkelä, T. K. Korpela, *Chem. Soc. Rev.* **1983**, *12*, 309-329; (h) S. Di Stefano, M. Ciaccia, *Org. Biomol. Chem.* **2015**, *13*, 646-654.

3 See for example: (a) S. F. Martin, *Pure Appl. Chem.* **2009**, *81*, 195-204; (b) M. Yus, J. C. González-Gómez, F. Foubelo, *Chem. Rev.* **2013**, *113*, 5595-5698; (c) A. L. Odom, T. J. McDaniel, *Acc. Chem. Res.* **2015**, *48*, 2822-2833; (d) J. R. Hummel, J. A. Boerth, J. A. Ellman *Chem. Rev.* **2017**, *117*, 9163-9227; (e) S. Morales, F. G. Guijarro, J. L. García Ruano, M. B. Cid, *J. Am. Chem. Soc.* **2014**, *126*, 1082-1089; (f) P. Ramaraju, N. A. Mir, D. Singh, V. K. Gupta, R. Kant, I. Kumar, *Org. Lett.* **2016**, *17*, 5582-5585; (g) W. W. Tan, Y. J. Ong, N. Yoshikai, *Angew. Chem.* **2017**, *129*, 8352-8356; (h) B. M. Trost, C.-I. Hung, M. J. Scharf, *Angew. Chem. Int. Ed.* **2018**, *130*, 11578-11582.

4 See for example: (a) G. J. P. Britovsek, V. C. Gibson, D. F. Wass, *Angew. Chem. Int. Ed.* **1999**, *38*, 428-447; (b) P. G. Cozzi, *Chem. Soc. Rev.* **2004**, *33*, 410-421; (c) V. C. Gibson, C. Redshaw, G. A. Solan, *Chem. Rev.* **2007**, *107*, 1745-1776; (d) B. L. Small, *Acc. Chem. Res.* **2015**, *48*, 2599-2611; (e) L. B. Schenkel, J. A. Ellman, *Org. Lett.* **2003**, *5*, 545-548; (f) G. J. P. Britovsek, J. England, S. K. Spitzmesser, A. J. P. White, D. J. Williams, *Dalton Trans.* **2005**, *5*, 945-955; (g) P. Shejwalkar, N. P. Rath, E. B. Bauer, *Dalton Trans.* **2011**, *40*, 7617-7631; (h) B. Zhou, K. Li, C. Jiang, Y. Lu, T. Hayashi, *Adv. Synth. Catal.* **2017**, *359*, 1969-1975.

5 See for example: (a) A.-J. Avestro, M. E. Belowich, J. F. Stoddart, *Chem. Soc. Rev.* **2012**, *41*, 5881-5895; (b) C.-J. Yang, S. A. Jenekhe, *Macromolecules* **1995**, *28*, 1180-1196; (c) M. Kathan, P. Kovaříček, C. Jurissek, A. Senf, A. Dallmann, A. F. Thünemann, S. Hecht, *Angew. Chem. Int. Ed.* **2016**, *55*, 13882-13886; (d) M. Matsumoto, R. R. Dasari, W. Ji, C. H. Feriante, T. C. Parker, S. R. Marder, W. R. Dichtel, *J. Am. Chem. Soc.* **2017**, *139*, 4999-5002; (e) X. Li, C. Zhang, S. Cai, X. Lei, V. Altoe, F. Hong, J. J. Urban, J. Ciston, E. M. Chan, Y. Liu, *Nat. Commun.* **2018**, *9*: 2998.

6 See for example: (a) J. R. Nitschke, *Acc. Chem. Res.* **2007**, *40*, 103-112; (b) A. Herrmann, *Org. Biomol. Chem.* **2009**, *7*, 3195-3204; (c) M. E. Belowich, J. F. Stoddart, *Chem. Soc. Rev.*

2012, *41*, 2003-2024; (d) I. Huc, J.-M. Lehn, *Proc. Natl. Acad. Sci. U.S.A.* **1997**, *94*, 2106-2110; (e) P. Kovaříček, J.-M. Lehn, *J. Am. Chem. Soc.* **2012**, *134*, 9446-9455; (f) M. Ciaccia, I. Tosi, R. Cacciapaglia, A. Casnati, L. Baldini, S. Di Stefano, *Org. Biomol. Chem.* **2013**, *11*, 3642-3648; (g) M. Ciaccia, I. Tosi, L. Baldini, R. Cacciapaglia, L. Mandolini, S. Di Stefano, C. A. Hunter, *Chem. Sci.* **2015**, *6*, 144-151; (h) R. Gu, K. Flidrova, J.-M. Lehn, *J. Am. Chem. Soc.* **2018**, *140*, 5560-5568; (i) M. Kathan, F. Eisenreich, C. Jurissek, A. Dallmann, J. Gurke, S. Hecht, *Nat. Chem.* **2018**, *10*, 1031-1036.

7 (a) G. Olivo, G. Arancio, L. Mandolini, O. Lanzalunga, S. Di Stefano*, Catal. Sci. Technol.* **2014**, *4*, 2900-2903; (b) G. Olivo, M. Nardi, D. Vìdal-Sanchez, A. Barbieri, A. Lapi, L. Gómez, O. Lanzalunga, M. Costas, S. Di Stefano, *Inorg. Chem.* **2015**, *54*, 10141-10152; (c) G. Olivo, O. Lanzalunga, S. Di Stefano, *Adv. Synth. Cat.* **2016**, *358*, 843-863.

8 P. A. S. Smith, C. Van Dang, *J. Org. Chem.* **1976**, *41*, 2013-2015.

9 F. Schaufelberger, L. Hu, O. Ramström, *Chem. Eur. J.* **2015**, *21*, 9776-9783.

10 For studies on the transimination reaction in organic solvents see: (a) M. Ciaccia, R. Cacciapaglia, P. Mencarelli, L. Mandolini, S. Di Stefano, *Chem. Sci.* **2013**, *4*, 2253-2261; (b) M. Ciaccia, S. Pilati, R. Cacciapaglia, L. Mandolini, S. Di Stefano, *Org. Biomol. Chem.* **2014**, *12*, 3282-3287. For Lewis acid-catalyzed transimination in organic solvents see: (c) N. Giuseppone, J.-L. Schmitt, E. Schwartz, J.-M. Lehn, *J. Am. Chem. Soc.* **2005**, *127*, 5528-5539; (d) P. Vongvilai, O. Ramström, *J. Am. Chem. Soc.* **2009**, *131*, 14419-14425.

11 On other double and multiple dynamic covalent systems, see for example: (a) A. Wilson, G. Gasparini, S. Matile, *Chem. Soc. Rev.* **2014**, *43*, 1948-1962; (b) V. Goral, M. I. Nelen, A. V. Eliseev, J.-M. Lehn, *Proc. Natl. Acad. Sci. U.S.A.* **2001**, *98*, 1347-1352; (c) J. Leclaire, L. Vial, S. Otto, J. K. M. Sanders, *Chem. Commun.* **2005**, 1959-1961; (d) H. M. Seifert, K. Ramirez Trejo, E. V. Anslyn, *J. Am. Chem. Soc.* **2016**, *138*, 10916-10924; (e) B. M. Matysiak, P. Nowak, I. Cvrtila, C. G. Pappas, B. Liu, D. Komáromy, S. Otto, *J. Am. Chem. Soc.* **2017**, *139*, 6744−6751.

12 (a) J.-M. Lehn, *Angew. Chem. Int. Ed.* **2015**, *54*, 3276-3289; (b) G. Vantomme, S. Jiang, J.-M. Lehn, *J. Am. Chem. Soc.* **2014**, *136*, 9509-9518.

13 Only a catalytic amount of quinuclidine was used in this case because the acidity of the imine methylene hydrogens is expected to be strongly enhanced by complexation with Fe^{2+}.

14 For the numbering system see: D. D. Davey, *J. Org. Chem.* **1987**, *52*, 1863-1869.

15 See for example: (a) J. D. Bower, G. R. Ramage, *J. Chem. Soc.* **1955**, 2834-2837; (b) K. C. Langry, *J. Org. Chem.* **1991**, *56*, 2400-2404; (c) M. E. Bluhm, M. Ciesielski, H. Görls, M. Döring, *Angew. Chem. Int. Ed.* **2002**, *41*, 2962-2965; (d) J. Wang, L. Dyers Jr., R. Mason Jr., P. Amoyaw, X. R. Bu, *J. Org. Chem.* **2005**, *70*, 2353-2356; (e) Y. Chen, L. Li, Z. Chen, Y. Liu, H. Hu, W.

Chen, W. Liu, Y. Li, T. Lei, Y. Kao, Z. Kang, M. Lin, W. Li, *Inorg. Chem.* **2012**, *51*, 9705-9713; (f) G. Pelletier, A. B. Charette, *Org. Lett.* **2013**, *15*, 2290-2293; (g) H. Wang, W. Xu, Z. Wang, L. Yu, K. Xu, *J. Org. Chem.* **2015**, *80*, 2431-2435; (h) Y.-J. Ou, Y. J. Ding, Q. Wei, X.-J. Hong, Z.-P. Zheng, Y.-H. Long, Y.-P. Cai, X.-D. Yao, *RSC Adv.* **2015**, *5*, 27743-27751; (i) H. Wang, W. Xu, L. Xin, W. Liu, Z. Wang, K. Xu, *J. Org. Chem.* **2016**, *81*, 3681-3687; (j) Y. Li, A. Chao, F. F. Fleming, *Chem. Commun.* **2016**, *52*, 2111-2113; (k) Z. Hu, J. Hou, J. Liu, W. Yu, J. Chang, *Org. Biomol. Chem.* **2018**, *16*, 5653-5660; (l) J. Sheng, J. Liu, H. Zhao, L. Zheng, X. Wei, *Org. Biomol. Chem.* **2018**, *16*, 5570-5574.

16 For a very similar metal-promoted intramolecular nucleophilic attack see: J. Wang, S. Onions, M. Pilkington, H. Stoeckli-Evans, J. C. Halfpenny, J. D. Wallis, *Chem. Commun.* **2007**, 3628-3630.

17 For successful use of Zn^{2+} in the stabilization of hemiacetals and hemiaminals/aminals in the field of DCC see: (a) D. Drahoňovský, J.-M. Lehn, *J. Org. Chem.* **2009**, *74*, 8428-8432; (b) L. You, S. R. Long, V. M. Lynch, E. V. Anslyn, *Chem. Eur. J.* **2011**, *17*, 11017-11023; (c) Y. Zhou, Y. Yuan, L. You, E. V. Anslyn, *Chem. Eur. J.* **2015**, *21*, 8207-8213.

18 Fe^{2+} was reported to enhance rates of imine formation from primary amine and carbonyl compounds (see reference 7a) as well as rates of transamination (see reference 7b). Transimination reactions are known to be catalyzed by a variety of Lewis acids (see references 10c and 10d).

19 Whether the actual stoichiometry of the ligand-metal complex is 2:1 or 1:1 is irrelevant to this argument.

3. An Introduction to the Jacobson-Stockmayer Theory for Macrocyclization Equilibria

ABSTRACT

A short introduction to the Jacobson-Stockmayer theory for macrocyclization equilibria is given, due to the special interest of dynamic combinatorial chemistry in the formation of macrocyclic compounds under thermodynamic control. A simple mathematical derivation of the mass-balance equation for a ring-chain system is presented, along with the description of the fundamental concepts of equilibrium effective molarity (*EM*) and critical monomer concentration (c_{mon}^{*}). Furthermore, a recent extension of the theory considering also the reversible formation of [2]catenanes is described.

INTRODUCTION

A major part of the dynamic combinatorial libraries described in literature is constituted by macrocyclic species, that form through ring-chain equilibria from suitable bifunctional compounds (Scheme 3-1).[1]

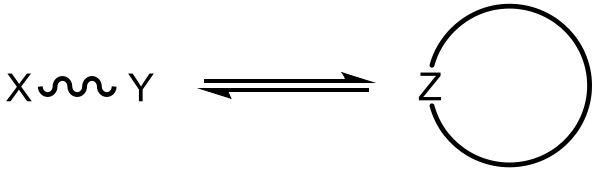

Scheme 3-1. Ring-chain equilibrium.

The reason behind this is that macrocyclic compounds are well-known to be more effective hosts and ligands compared to their non-cyclic counterparts due to the pre-organization of the binding motif that relieves the process of binding site organization of most of the conformational entropy cost.[2] Therefore, the knowledge of the rules of polymerization and macrocyclization reactions under thermodynamic control appears to be highly desirable in the field of dynamic combinatorial chemistry.

The first theoretical description of reversible polymerizations that took into account the occurring of intramolecular reactions that form macrocyclic species dates back to 1950 and is due to Homer Jacobson and Walter H. Stockmayer.[3] In 1993 a reformulation of this theory was proposed by Ercolani *et al.* with the aim to make the quantitative description of polymerization and macrocyclization processes under thermodynamic control more complete and easier to access to non-specialists.[4]

DISCUSSION

Ring-chain systems

A generic ring-chain system obtained from a linear bifunctional monomer $\mathbf{M_1}$ through reversible reactions between −X and −Y functional groups is represented in Scheme 3-2. Intermolecular reactions (reversible polymerizations) and intramolecular reactions (reversible cyclizations) occur simultaneously, producing linear ($\mathbf{M_i}$) and cyclic ($\mathbf{C_i}$) molecules respectively, where i denotes the polymerization degree of each species. When the equilibrium condition is reached all of the monomeric starting material $\mathbf{M_1}$

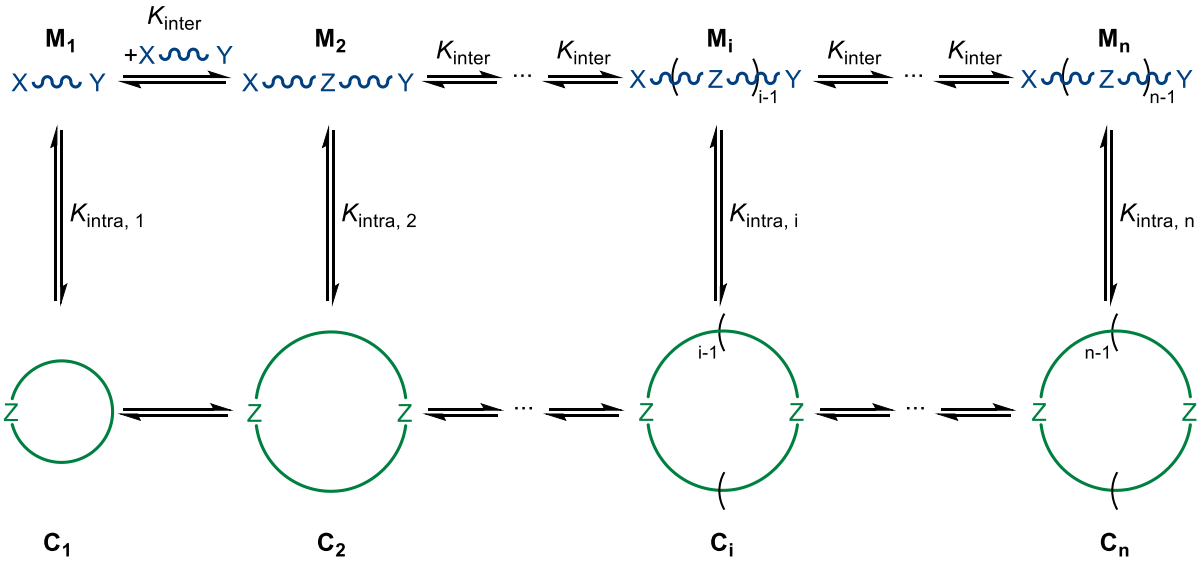

Scheme 3-2. Network of ring-chain equilibria occurring in a generic polymerization under thermodynamic control.

introduced is reversibly distributed among linear and cyclic species, and their concentration does not change anymore over time. Consequently, it is possible to write a mass-balance equation for the system at equilibrium (Equation 1).

$$[\mathrm{M}_1]_0 = \sum_{\mathrm{i}=1}^{\infty} \mathrm{i}[\mathrm{C}_\mathrm{i}] + \sum_{\mathrm{i}=1}^{\infty} \mathrm{i}[\mathrm{M}_\mathrm{i}] \tag{1}$$

If the functional groups −X e −Y react exclusively via a reversible reaction whose equilibrium constant K_{inter} is independent of the length of the chain to which they are attached, then it is possible to derive Equation 2 for the cyclic species and Equation 3 for the linear ones,[4]

$$[\mathrm{C}_\mathrm{i}] = EM_\mathrm{i} x^\mathrm{i} \tag{2}$$

$$[\mathrm{M}_\mathrm{i}] = \frac{x^\mathrm{i}}{K_{\mathrm{inter}}} \tag{3}$$

where EM_i, is defined by Equation 4,

$$EM_\mathrm{i} = \frac{K_{(\mathrm{intra})\mathrm{i}}}{K_{\mathrm{inter}}} \tag{4}$$

In these equations *x* constitutes the fraction of the reactive functional groups −X e −Y that reacted in the acyclic part of the ring-chain system at equilibrium and represents a measure of the extent of the polymerization reaction, whereas EM_i is the equilibrium effective molarity[5] for the i-th cyclic oligomer, a physical quantity that measures the thermodynamic ease of formation of a cyclic compound from its linear precursor compared to an analogous intermolecular reaction. This important quantity, related to the stability of a cyclic oligomer formed through a reversible reaction, also corresponds to the equilibrium constant for the macrocyclization reaction of Equation 5.

$$\mathbf{M_{i+j}} \xrightleftharpoons{EM_i} \mathbf{C_i} + \mathbf{M_j} \tag{5}$$

Then, substituting Equations 2 and 3 into Equation 1 a new expression for the mass-balance equation can be obtained (Equation 6).

$$[\mathrm{M}_1]_0 = \underbrace{\sum_{i=1}^{\infty} i EM_i x^i}_{\text{cyclic species}} + \underbrace{\frac{1}{K_{inter}} \sum_{i=1}^{\infty} i x^i}_{\text{linear species}} \tag{6}$$

The two series at the right-hand side of Equation 6 represent the amount of monomer **M₁** that is converted into cyclic and linear species respectively, expressed as concentration value.

If **Cᵢ** is a strainless ring, it can be demonstrated that its equilibrium effective molarity can be expressed in the form of Equation 7,

$$EM_i = B i^{-5/2} \tag{7}$$

where the parameter *B* represents the equilibrium effective molarity that the cyclic monomer **C₁** would have if it were a strainless ring.[6] Thus, substituting Equation 7 into Equation 6 and treating separately the contributions of strained[7] and strainless rings, the final expression of the mass-balance equation for a reversible ring-chain system according to the Jacobson-Stockmayer theory is obtained (Equation 8).

$$[\mathrm{M}_1]_0 = \underbrace{\sum_{i=1}^{n} i EM_i x^i}_{\text{strained rings}} + \underbrace{B \sum_{i=n+1}^{\infty} i^{-3/2} x^i}_{\text{strainless rings}} + \underbrace{\frac{1}{K_{inter}} \sum_{i=1}^{\infty} i x^i}_{\text{linear species}} \tag{8}$$

One of the most important results emerging from the Jacobson-Stockmayer theory is to predict the existence of a critical monomer concentration (c_{mon}^{*}), experimentally confirmed in a great number of studies.[4,8] For high values of the initial monomer concentration $[M_1]_0$ the extent of the polymerization reaction *x* tends towards 1. From a purely mathematical point of view, this translates into the fact that the two series associated to the cyclic species at the right-hand side of the mass-balance equation are convergent (Equation 9),[9] whereas the series associated to the linear species is divergent.

$$\sum_{i=1}^{\infty} i^{-3/2} = 2.612 \tag{9}$$

This means, physically, that only a finite number of monomeric units can be incorporated in the cyclic fraction of the polymeric material and, on the contrary, that a virtually infinite number of monomeric units can be incorporated in the acyclic fraction of the polymer, the only limit being the solubility of the material. Furthermore, for large values of the intermolecular equilibrium constant, $K_{inter} \geq 10^5$ M^{-1},[4] it is possible to precisely identify a cut-off value for the initial monomer concentration $[M_1]_0$ below which the system is exclusively constituted by cyclic species and above which the excess monomer produces acyclic species only. In the latter case the concentration of each cyclooligomer remains constant on increasing the initial monomer concentration and, recalling Equation 2, assumes a value that is equal to the respective effective molarity EM_i (Figure 3-1). This cut-off value for the total monomer concentration takes the name of critical monomer concentration (c_{mon}^{*}) and it is defined by the summation of the effective molarities of all the cyclic species times their corresponding degree of polymerization i (Equation 10).

$$c_{mon}^{*} = \sum_{i=1}^{n} i EM_i + B \sum_{i=n+1}^{\infty} i^{-3/2} \tag{10}$$

In order to better understand the behavior of a ring-chain system under thermodynamic control, a useful parallel can be made whose pictorial representation is showed in Figure 3-2.[1] In this analogy an infinite number of communicating vessels of finite total capacity, each of which having different size and shape, is assigned to store a liquid, in our case the linear monomer **M₁**. Each of these vessels is related to

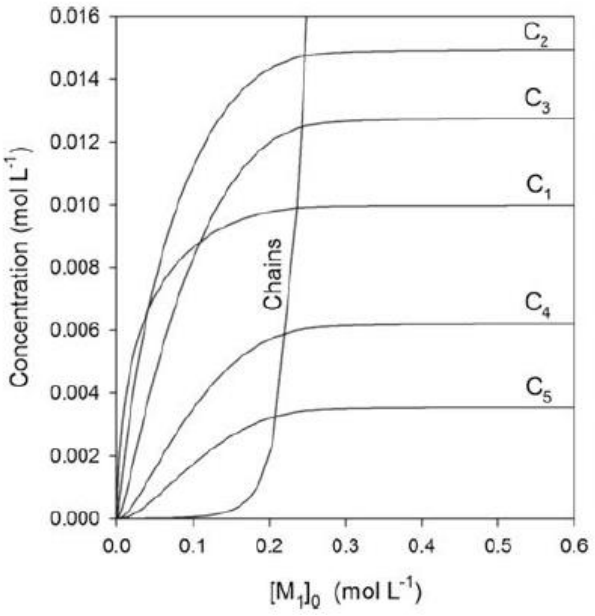

Figure 3-1. Equilibrium concentrations of rings (i from 1 to 5) and the chain fraction for a practical system (see reference 4 and 5b for details), showing evidence of the phenomenon of critical monomer concentration.

the degree of polymerization i of a particular cyclic species and has a finite capacity, corresponding to the value of the effective molarity EM_i of the cyclooligomer. Just like a liquid that is poured inside the communicating vessels until they are completely full, as monomer **M₁** is added to the solution and reacts, the starting material gets distributed into the different cyclic species until the critical monomer concentration is reached. At this point the concentration of every cyclic oligomer reaches its maximum value and equals the corresponding *EM* value. Above the critical monomer concentration, the monomer added in excess can only indefinitely be distributed into the linear polymeric material, similarly to an excess of liquid poured into the communicating vessels that overflows and is collected in a tank of infinite capacity underneath.

Ring-chain-catenane systems

Jacobson-Stockmayer theory takes into consideration only the formation of linear and cyclic species in reversible polymerization reactions. In principle, many other topologically non-trivial species[10] can be formed in these conditions, like catenanes, knots and other more exotic species, that probably remain hidden in the mass of the

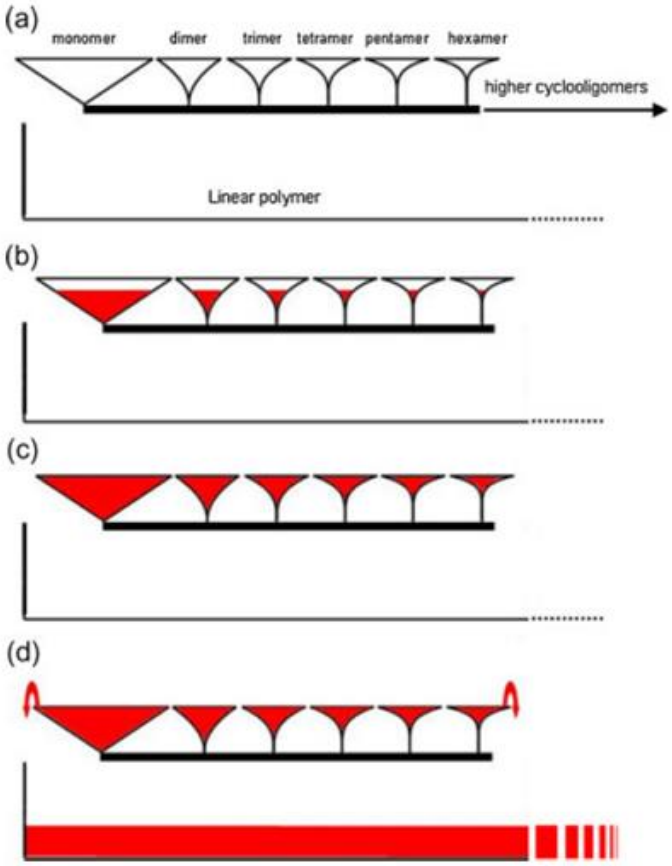

Figure 3-2. Visual representation of a generic ring-chain system at equilibrium having $K_{inter} \geq 10^5$ M^{-1}: (a) $[M_1]_0 = 0$ M, (b) $[M_1]_0 < c_{mon}$*, (c) $[M_1]_0 = c_{mon}$* and (d) $[M_1]_0 > c_{mon}$*.[1]

supposedly linear polymer in the experimental practice. Jacobson himself tried to correct the theory to consider the reversible formation of [2]catenanes, molecular links constituted by two interlocked macrocycles.[11] Other theoretical models were proposed to give an estimate of the probability of catenation of two macrocyclic species, either before and after Jacobson's attempt.[10a,12] Recently, these theoretical models, along with some computational methods elaborated with the same purpose,[13] were critically examined by Di Stefano and Ercolani and, in light of this, a new model was proposed.[14] This new model gives an expression for the catenation equilibrium constant (Scheme 3-3) under the condition that the process is dictated by entropy only, and thus it holds for interlocked rings that are large enough to be considered non-interacting (so-called statistical catenation).[10a,15] Of course, such an equilibrium is only possible if one or both macrocycles can undergo a reversible ring-opening reaction, that is the case in equilibrium polymerization reactions.

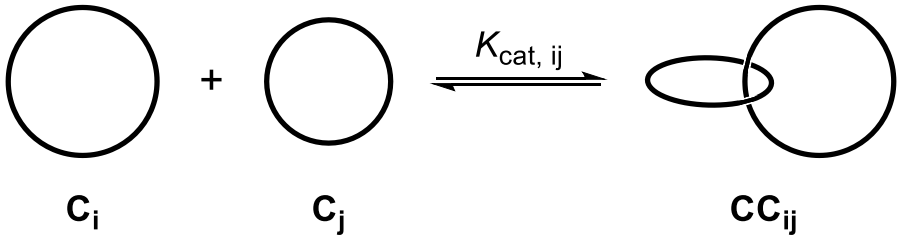

Scheme 3-3. Catenation equilibrium involving cyclic oligomers $\mathbf{C_i}$ and $\mathbf{C_j}$ to form [2]catenane $\mathbf{CC_{ij}}$.

According to this model the catenation constant takes the form of Equation 11,

$$K_{\mathrm{cat\ ij}} = \alpha \frac{2^{[1-\mathrm{INT(j/i)}]}}{\sigma B}\left(\mathrm{i}^{1/2} + \mathrm{j}^{1/2}\right)^3 \qquad (11)$$

where INT is a function that rounds the argument down to the nearest integer, so that $2^{[1\ -\ \mathrm{INT(j/i)}]}$ is equal to either 1 when i = j or 2 when i > j, σ is a symmetry factor equal to either 1 for monomers of the type X−Y or 2 for monomers of the type X−X,[6] and α is a parameter that takes into account the steric hindrance to catenation due to excluded volume effects of the polymer chains.

Taking this result as a starting point, an extension to the Jacobson-Stockmayer theory was later proposed by the same authors[16] to take into account the reversible formation of [2]catenanes in polymerization equilibria (Scheme 3-4). The formation of higher order catenanes ([3]catenanes, [4]catenanes etc.) is less likely to happen, from an entropic point of view, than that of [2]catenanes, and was neglected in this treatment. A new mass-balance equation for the system was derived that includes the contribution of [2]catenanes to the mixture of products at equilibrium when a long linear bifunctional monomer $\mathbf{M_1}$ is subjected to reversible polymerization, starting from Equation 12.

$$[\mathrm{M}_1]_0 = \sum_{\mathrm{i}=1}^{\infty} \mathrm{i}[\mathrm{C_i}] + \sum_{\mathrm{i}=1}^{\infty} \mathrm{i}[\mathrm{M_i}] + \sum_{\mathrm{i}=1}^{\infty}\sum_{\mathrm{j}=1}^{\mathrm{i}} (\mathrm{i}+\mathrm{j})\left[\mathrm{CC_{ij}}\right] \qquad \mathrm{i} \geq \mathrm{j} \qquad (12)$$

Combining Equation 2 and Equation 13 it is possible to obtain the expression for the equilibrium concentration of a generic catenane $\mathbf{CC_{ij}}$ (Equation 14).

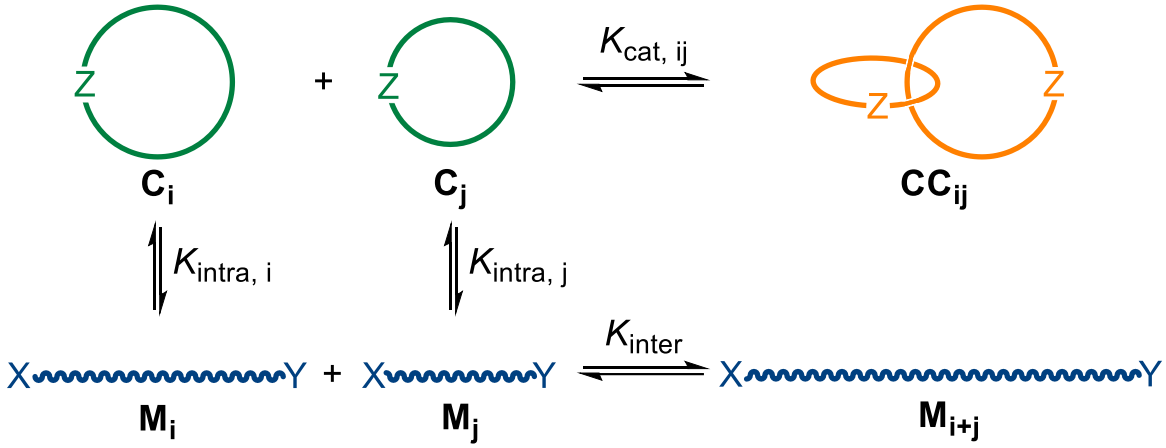

Scheme 3-4. Representation of a reversible ring-chain-catenane system.

$$K_{\mathrm{cat\,ij}} = \frac{[\mathrm{CC_{ij}}]}{[\mathrm{C_i}][\mathrm{C_j}]} \tag{13}$$

$$[\mathrm{CC_{ij}}] = K_{\mathrm{cat\,ij}} EM_{\mathrm{i}} EM_{\mathrm{j}} x^{\mathrm{i+j}} \tag{14}$$

Having the expressions for the equilibrium concentrations of cyclic species (Equation 2), linear species (Equation 3 and eq. 32 in reference 4) and catenanes (Equation 14), and recalling the expression for the *EM* of a strainless cyclic oligomer i (Equation 7) and the expression for the catenation constant (Equation 11), the mass-balance equation takes the form of Equation 15,

$$[\mathrm{M_1}]_0 = \frac{1}{K_{\mathrm{inter}}} \frac{x}{(1-x)^2} + BS_1 + \frac{B\alpha}{\sigma} \mathrm{S_2} \tag{15}$$

where S_1 and S_2 are given by

$$\mathrm{S_1} = \sum_{\mathrm{i=1}}^{\infty} \mathrm{i}^{-3/2}\, x^{\mathrm{i}} \tag{16}$$

$$\mathrm{S_2} = \sum_{\mathrm{i=1}}^{\infty} \sum_{\mathrm{j=1}}^{\mathrm{i}} 2^{[1-\mathrm{INT(j/i)}]} (\mathrm{i+j}) \left(\mathrm{i}^{1/2} + \mathrm{j}^{1/2}\right)^3 (\mathrm{ij})^{-5/2} x^{\mathrm{i+j}} \tag{17}$$

S_1 is the same series that is obtained with the traditional Jacobson-Stockmayer theory for systems consisting solely of strainless rings, like in this case where a suitably long linear monomer **M₁** is considered,[5,7] and it was already known to converge to 2.612

when $x = 1$ (see Equation 9).[9] The series S_2 is a series related to the equilibrium concentrations of [2]catenanes but, in contrast to the series S_1, is divergent for x = 1. This means that [2]catenanes, unlike rings and analogously to linear species, are predicted to not have a maximum total concentration in the limit of high monomer concentration.

Then, the authors[16] examined the reversible formation of [2]catenanes from a quantitative point of view, building distribution curves of the fractions of chains, rings, and catenanes as a function of the initial monomer concentration for two different scenarios: “thick” chains and “thin” chains. The term “thick” chain is used to identify a type of polymer chain characterized by non-negligible Kuhn segment[17] thickness with respect to its length (low Kuhn segment aspect ratio, ≈ 2-3)[18], which means that the co-volume of the polymer chain is not negligible, thus hindering the catenation process. A polymethylene chain, for example, can be included into this category. For such a flexible chain, the parameter α that takes into account the excluded volume effects on catenation is empirically estimated[14] as 6.6×10^{-5} by fitting the yield of Wasserman’s first reported statistical synthesis of a catenane (Figure 3-3).[19] On the contrary, the term “thin” chain is used to identify a type of polymer chain characterized by negligible Kuhn segment thickness with respect to its length. That is to say that the negligibly small co-volume of a “thin” polymer chain does not have a major detrimental effect on the catenation process. For example, double-stranded DNA, a locally rigid polymer chain featuring high Kuhn segment aspect ratio (66),[18] falls into this category. In this case, the value adopted for α is 9.6×10^{-3}, that appears to be the most reliable[14] when compared with the available experimental catenation constant for the catenation of 186 DNA and λcI857 DNA rings.[12]

The predicted distribution curves of chains, rings, and [2]catenanes for a “thick” unsymmetrical chain X−Y (σ =1, $\alpha = 6.6 \times 10^{-5}$ and B = 1 mol L^{-1})[20] as a function of the initial monomer concentration at increasing values of K_{inter} are showed in Figure 3-4. From these plots, it looks clear that the formation of catenanes in “thick” systems is negligible up to K_{inter} values as large as 10^5 mol^{-1} L (Figure 3-4a,c), implying that up to these values, the classical Jacobson-Stockmayer theory is still perfectly suited to

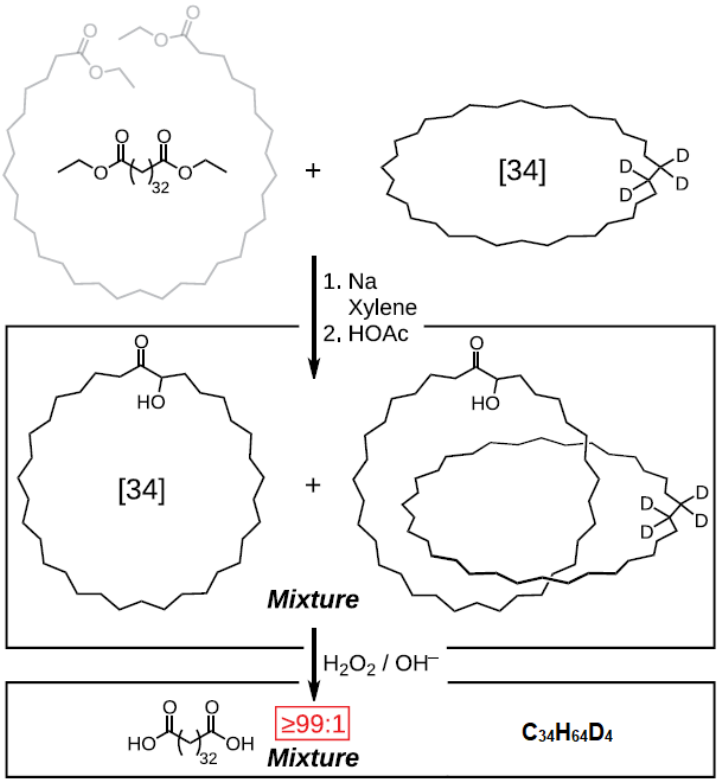

Figure 3-3. Wasserman's statistical synthesis of a catenane, obtained as a ≈ 1% mixture[19] together with cyclic acyloin. The value was determined by quantification of the deuterated macrocycle after oxidative cleavage of the acyloin functionalities.[15]

accurately treat such a system. Above this K_{inter} value (Figure 3-4d), however, the catenane fraction starts to increase at the expense of the linear fraction. Significant amounts of both fractions start to appear only when the total monomer concentration in the system reaches the critical monomer concentration value (c_{mon}*). Moreover, for K_{inter} values tending to infinity, it is predicted that the system transforms into a ring-catenane system, due to chains disappearing in favor of catenanes (Figure 3-5).

A very different scenario is predicted for "thin" chains. The distribution curves of chains, rings, and [2]catenanes for a "thin" unsymmetrical chain X−Y ($\sigma = 1$, $\alpha = 9.6 \times 10^{-3}$ and $B = 1$ mol L^{-1}) as a function of the initial monomer concentration at increasing values of K_{inter} are showed in Figure 3-6. Differently from the previous case, significant amounts of catenane material are expected already at lower values of K_{inter} (Figure 3-6a-b), so that the catenation process cannot be neglected and making the use of the extended Jacobson-Stockmayer theory necessary to have an accurate

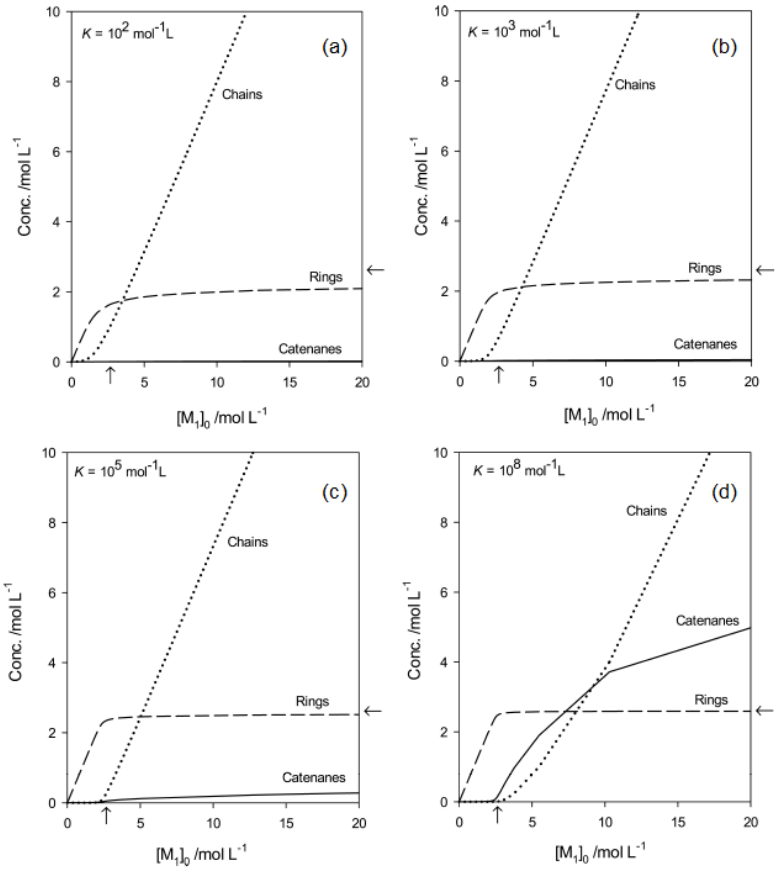

Figure 3-4. Weighted equilibrium concentrations of chains (dotted line), rings (dashed line), and catenanes (solid line) for a "thick" chain. Distributions are reported as a function of $[M_1]_0$ for B = 1 mol L^{-1}, σ = 1, α = 6.6 × 10^{-5}, and (a) K_{inter} = 10^2 mol^{-1} L, (b) K_{inter} = 10^3 mol^{-1} L, (c) K_{inter} = 10^5 mol^{-1} L and (d) K_{inter} = 10^8 mol^{-1} L. Arrows on abscissa and ordinate point to the value of 2.612 mol L^{-1}.

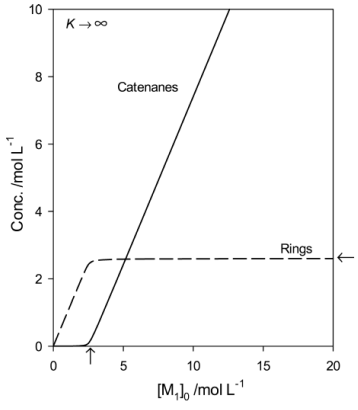

Figure 3-5. Weighted equilibrium concentrations of rings (dashed line) and catenanes (solid line) for a "thick" chain as a function of $[M_1]_0$, calculated for B = 1 mol L^{-1}, σ = 1, α = 6.6 × 10^{-5} and $K_{inter} \rightarrow \infty$. Arrows on the abscissa and ordinate point to the value of 2.612 mol L^{-1}.

quantitative description of the system. At higher K_{inter} values (Figure 3-6c-d), the linear fraction decreases drastically even at high total monomer concentration. Interestingly, it can be seen that the phenomenon of critical concentration is not observed neither for chains nor for catenanes (the steep increase occurring at c_{mon}*) and that rings do not reach, at any value of total monomer concentration, their limiting value.

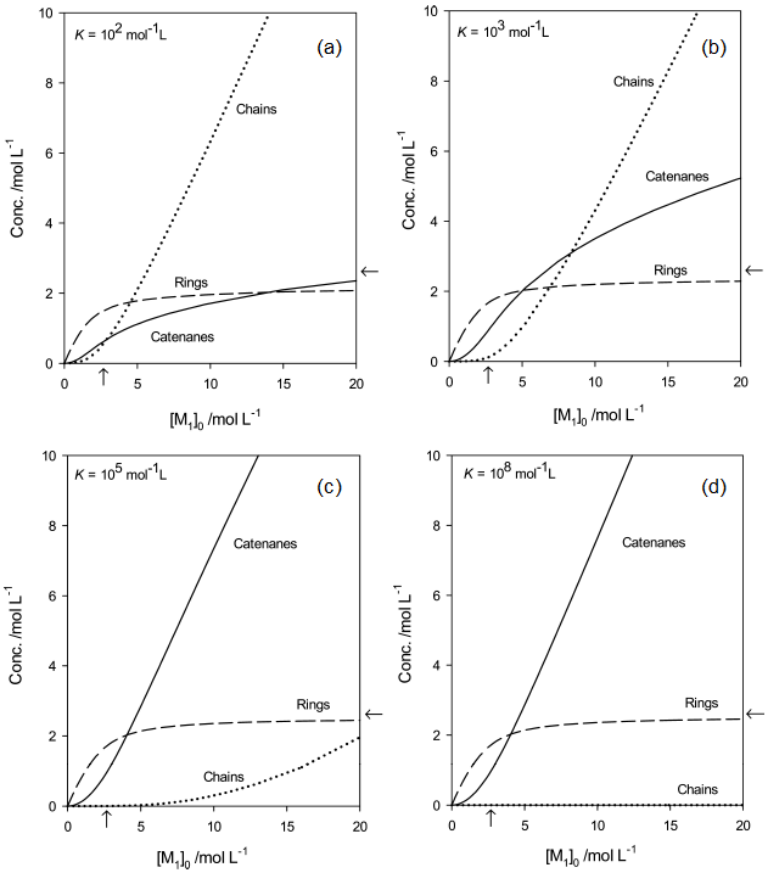

Figure 3-6. Weighted equilibrium concentrations of chains (dotted line), rings (dashed line), and catenanes (solid line) for a "thin" chain. Distributions are reported as a function of $[M_1]_0$ for B = 1 mol L^{-1}, σ = 1, α = 9.6 × 10^{-3}, and (a) K_{inter} = 10^2 mol^{-1} L, (b) K_{inter} = 10^3 mol^{-1} L, (c) K_{inter} = 10^5 mol^{-1} L and (d) K_{inter} = 10^8 mol^{-1} L. Arrows on abscissa and ordinate point to the value of 2.612 mol L^{-1}.

CONCLUSIONS AND PERSPECTIVES

An introduction to the Jacobson-Stockmayer theory for macrocyclization equilibria has been given, using the simpler formalism and the integrations reported in 1993 by Ercolani *et al.*.[4] The fundamental concepts of equilibrium effective molarity (*EM*) of a macrocycle and critical monomer concentration (c_{mon}^*) have been described and discussed.

Additionally, a recent extension to the theory[16] covering also the reversible formation of [2]catenanes has been presented, along with two different scenarios for the distribution of all species at equilibrium related to two different type of polymer chains ("thick" chains and "thin" chains). "Thin" chains, like dsDNA, are predicted to have a definite advantage over the "thick" ones, like polymethylene chains, in catenation processes. It is worth pointing out again that the above theory takes into account only the formation of [2]catenanes, the formation of higher order catenanes being considered not as relevant (unless the catenane fraction constitutes the main fraction of the system) than that of [2]catenanes, and thus safely neglectable in most of the cases.

Further advancements and improvements of the theory will most certainly come from expanding the current availability of data relative to the experimental values of the catenation equilibrium constants for both "thick" and "thin" chain polymers, to make more accurate quantitative predictions on the distribution of species - chains, rings and catenanes - for a larger scope of polymerization systems. Of course, an experimental confirmation of these new theoretical predictions on statistical catenation is highly desirable (see Chapter 5). Moreover, it would be interesting to eventually expand further the Jacobson-Stockmayer theory to include the contribution of the statistical formation of molecular knots in the study of macrocyclization equilibria (Scheme 3-5), starting from theoretical models and experimental data related to knotting equilibria (Equation 18).[8a;13a,21]

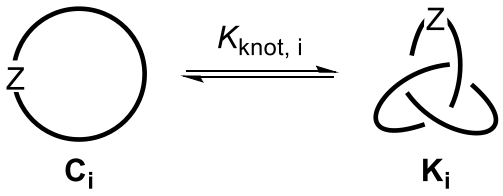

(18)

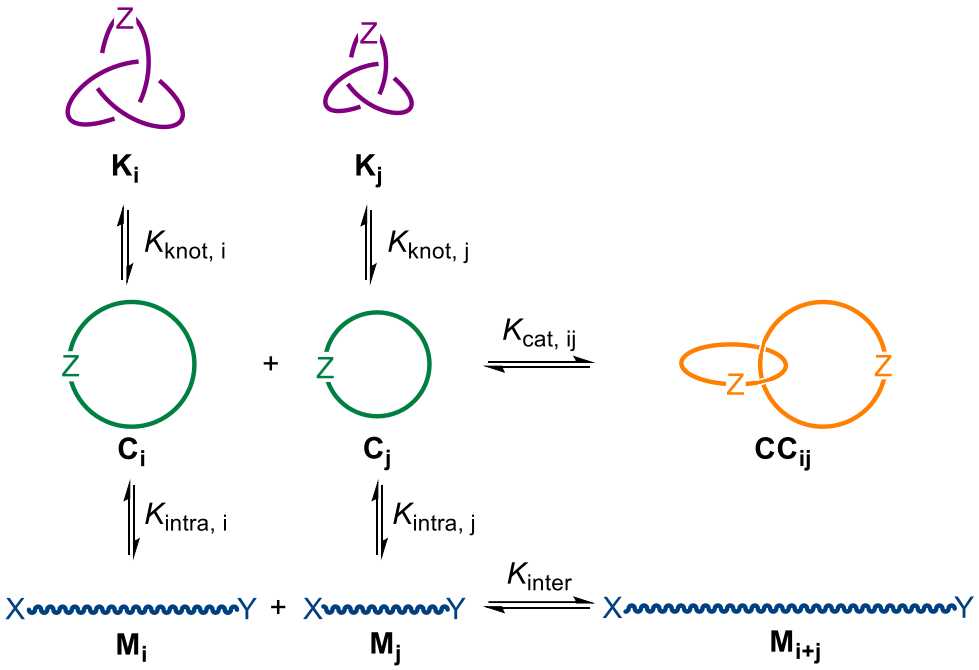

Scheme 3-5. Representation of a reversible ring-chain-catenane-knot system.

NOTES AND REFERENCES

1 S. Di Stefano, *J. Phys. Org. Chem.* **2010**, *23*, 797-805.

2 (a) J. D. Lamb, R. M. Izatt, J. J. Christensen, D. J. Eatough, *Thermodynamics and Kinetics of Cation-Macrocycle Interaction* in *Coordination Chemistry of Macrocyclic Compounds* (editor: G. A. Melson), Plenum Press, New York, New York (U.S.A.), **1979**; (b) A. E. Martell, R. D. Hancock, *The Chelate, Macrocyclic, and Cryptate Effects* in *ACS Symposium Series Vol. 565 - Coordination Chemistry. A Century of Progress* (editor: G. B. Kauffman), American Chemical Society, Washington, D.C. (U.S.A.), **1994**; (c) D. H. Busch, N. A. Stephenson, *Coord. Chem. Rev.* **1990**, *100*, 119-154; (d) V. Martí-Centelles, M. D. Pandey, M. I. Burguete, S. V. Luis, *Chem. Rev.* **2015**, *115*, 8736-8834; (e) D. K. Cabbiness, D. W. Margerum, *J. Am. Chem. Soc.* **1969**, *91*, 6540-6541.

3 H. Jacobson, W. H. Stockmayer, *J. Chem. Phys.* **1950**, *18*, 1600-1606.

4 G. Ercolani, L. Mandolini, P. Mencarelli, S. Roelens, *J. Am. Chem. Soc.* **1993**, *115*, 3901-3908.

5 (a) L. Mandolini, *Adv. Phys. Org. Chem.* **1986**, *22*, 1-111; (b) S. Di Stefano, G. Ercolani, *Adv. Phys. Org. Chem.* **2016**, *50*, 1-76.

6 The expression for *B* (given in mol L^{-1}), valid for polymer chains obeying Gaussian statistics, is the following:

$$B = \frac{1000}{N_A \sigma}\left(\frac{3}{2\pi C_\infty \upsilon l^2}\right)^{3/2}$$

where N_A is the Avogadro constant, σ is a symmetry factor equal to either 1 for monomers of the type X−Y or 2 for monomers of the type X−X, υ is the number of skeletal bonds of length *l*, measured in cm, per monomer, and C_∞ is the characteristic ratio in the limit of high chain length, which is a measure of the stiffness of a polymeric chain. For more detailed information on the macrocyclization constant of a strainless macrocycle, see references 5, 16, and references cited therein. For a deeper insight on single chain conformations of ideal polymer chains, see for example: M. Rubinstein, R. H. Colby, *Polymer Physics*, Oxford University Press, Oxford (U.K.), **2003**, chapter 2.

7 C. Galli, L. Mandolini, *Eur. J. Org. Chem.* **2000**, 3117-3125.

8 See for example: (a) *Cyclic Polymers* (editor: J. A. Semlyen), Elsevier, London (U.K.), **1986**; (b) J. A. Semlyen, *Adv. Polym. Sci.* **1976**, *21*, 41-75; (c) K. Ito, Y. Hashizuka, Y. Yamashita, *Macromolecules* **1977**, *10*, 821-824; (d) Y. Yamashita, J. Mayumi, Y. Kawakami, K. Ito, *Macromolecules* **1980**, *13*, 1075-1080; (e) L. Reif, H. Höcker, *Macromolecules* **1984**, *17*, 952-

956; (f) Z.-R. Chen, J. P. Claverie, R. H. Grubbs, J. A. Kornfield, *Macromolecules* **1995**, *28*, 2147-2154; (g) A. T. ten Cate, H. Kooijman, A. L. Spek, R. P. Sijbesma, E. W. Meijer, *J. Am. Chem. Soc.* **2004**, *126*, 3801-3808; (h) M. P. F. Pepels, P. Souljé, R. Peters, R. Duchateau, *Macromolecules* **2014**, *47*, 5542-5550; (i) R. Cacciapaglia, S. Di Stefano, L. Mandolini, *J. Am. Chem. Soc.* **2005**, *127*, 13666-13671.

9 C. Truesdell, *Ann. Math.* **1945**, *46*, 144-157.

10 (a) H. L. Frisch, E. Wasserman, *J. Am. Chem. Soc.* **1961**, *83*, 3789-3795; (b) R. S. Forgan, J.-P. Sauvage, J. F. Stoddart, *Chem. Rev.* **2011**, *111*, 5434-5464; (c) J.-P. Sauvage, *Angew. Chem. Int. Ed.* **2017**, *56*, 11080-11093.

11 a) H. Jacobson, *Macromolecules* **1984**, *17*, 705-709; b) H. Jacobson, *Macromolecules 1988*, *21*, 2842-2848.

12 a) J. C. Wang, H. Schwartz, *Biopolymers* **1967**, *5*, 953-966; b) J. C. Wang, *Acc. Chem. Res.* **1973**, *6*, 252-256.

13 (a) M. D. Frank-Kamenetskii, A. V. Lukashin, A. V. Vologodskii, *Nature* **1975**, *258*, 398-402; (b) N. Hirayama, K. Tsurusaki, T. Deguchi, *J. Phys. A: Math. Theor.* **2009**, *42*: 105001.

14 S. Di Stefano, G. Ercolani, *Macromol. Theory Simul.* **2016**, *25*, 63-73.

15 C. J. Bruns, J. F. Stoddart, *The Nature of Mechanical Bond*, John Wiley & Sons, Hoboken, New Jersey (U.S.A.), **2017**, pp. 62-65.

16 S. Di Stefano, G. Ercolani, *J. Phys. Chem. B* **2017**, *121*, 649-656.

17 The Kuhn segment of an ideal polymer chain is defined as the shortest portion of an equivalent freely-jointed polymer chain that is able to explore freely any direction in space. See: M. Rubinstein, R. H. Colby, *Polymer Physics*, Oxford University Press, Oxford (U.K.), **2003**, pp. 53-54.

18 F. Latinwo, C. M. Schroeder, *Soft Matter* **2011**, *7*, 7907-7913.

19 E. Wasserman, *J. Am. Chem. Soc.* **1960**, *82*, 4433-4434. For a disambiguation statement on the reported yield value, see note 7 in: D. A. Ben-Efraim, C. Batich, E. Wasserman, *J. Am. Chem. Soc.* **1970**, *92*, 2133-2135.

20 Observing the expression of Equation 15, it appears immediately that the ratio of catenanes to rings is independent of B (thus is independent of the size and stiffness of the cyclic monomer, i.e. of the ease of its formation), but only depends on α / σ and x. So, the value $B = 1$ mol L^{-1} is chosen for simplicity reasons only.

21 For some literature on molecular knots and knotting probability, see for example: (a) Alexander V. Vologodskii, *Circular DNA* in *Cyclic Polymers (2nd edition)* (editor: J. A. Semlyen), Kluwer Academic Publishers, Dordrecht (The Netherlands), **2000**; (b) A. Y. Grosberg. *Polym. Sci., Ser. A* **2009**, *51*, 70-79; (c) C. Micheletti, D. Marenduzzo, E. Orlandini, *Phys. Rep.* **2011**,

504, 1-73; (d) S. D. P. Fielden, D. A. Leigh, S. L. Woltering, *Angew. Chem. Int. Ed.* **2017**, *56*, 11166-11194; (e) K. Koniaris, M. Muthukumar, *Phys. Rev. Lett.* **1991**, *66*, 2211-2214; (f) L. Tubiana, A. Rosa, F. Fragiacomo, C. Micheletti, *Macromolecules* **2013**, *46*, 3669-3678; (g) E. Uehara, T. Deguchi, *J. Phys.: Condens. Matter* **2015**, *27*: 354104.

4. Influence of Topology on the Gelation Behavior of Metallo-supramolecular Polymers Prepared via Ring-Opening Metathesis Polymerization of Macrocyclic Olefins

ABSTRACT

This work reports on the consequences of copper(I)-templated concatenation of two identical phenanthroline-based macrocyclic olefins on the gelation behavior of metallo-supramolecular polymers obtained via ring-opening metathesis polymerization (ROMP). The influence of concatenation is evaluated by comparison with the gelation behavior of a non-interlocked model complex under the same reaction conditions. The suitability of the choice of the non-interlocked model complex is discussed in terms of molecular structure and effective molarity (*EM*). It is found that concatenation has a primary role in the gelation process, resulting in lower critical gelation concentrations for the endotopic, interlocked complex compared to the exotopic, non-interlocked one.

Work published in:

S. Albano, A. Fantozzi, J. A. Berrocal, S. Di Stefano, *J. Polym. Sci. Part A: Polym. Chem.* **2017**, *55*, 1237-1242.

INTRODUCTION

The discovery and development of the chemistry of mechanical bond has been undoubtedly a major breakthrough in modern chemistry.[1] The possibility to synthesize catenanes,[2] species formed by the interlocking of two or more macrocyclic components, or rotaxanes,[3] species formed by linear components enclosed and trapped by macrocyclic ones, has opened up new exciting possibilities in many fields of research (Figure 4-1).[4]

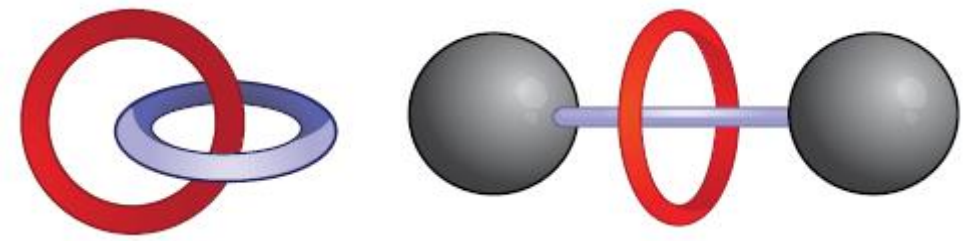

Figure 4-1. Graphical representations of a catenane (left) and a rotaxane (right), two of the main classes of mechanomolecules, that is molecules bearing one or more mechanical bonds.[1a]

One of these is polymer science, in which studies on polymers incorporating mechanical bonds,[5] such as polycatenanes[6] and polyrotaxanes,[7] have attracted great interest. This new family of polymeric materials (is expected to) present special or extraordinary mechanical, dynamic, rheological and thermal properties, compared to those related to conventional covalent polymers. In the case of catenane-based polymers, many strategies have been adopted thus far to achieve polycatenanes of different structural types but the preparation of catenane-only structures, solely formed from catenane subunits, still remains an open challenge.[8]

In our group it was recently found[9] that a polymeric material mainly consisting of interlocked cyclic molecules could be easily obtained by ring-opening metathesis polymerization (ROMP) of 30 mM catenate complex **1**[10] in the presence of 3 mol% 2nd generation Grubbs' catalyst **G2** in dichloromethane at 30 °C (Figure 4-2). After 30 min from the addition of **G2** to the solution of catenate **1**, a dark red gel was formed. When the reaction was carried out in a spinning NMR tube a rod-shaped material was produced which was easy to deform, flexible and mechanically stable in the wet state (Figure 4-3). Upon releasing the mechanical stress, the original shape was spontaneously restored due to the elasticity of the material. In stark contrast, the dry material showed antithetical mechanical properties, such as rigidity and brittleness. Importantly, solutions of the demetalated polycatenane at the same total monomer concentration were not able to produce a gel.[9]

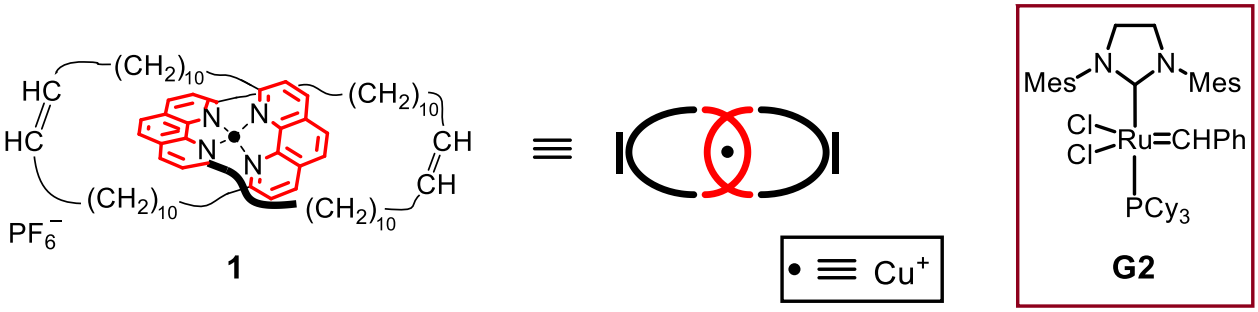

Figure 4-2. Structures of catenate **1** and catalyst **G2**.

Figure 4-3. Pictures of the polycatenane gels obtained from ROMP of complex **1**.[9]

Taking this as a starting point, we were interested in investigating the influence of the mechanical bond between the two macrocycles of catenate **1** on the gelation process. Our purpose was to study what happens when the analogous complex **2**, consisting of two non-interlocked macrocycles very similar to those of **1** (Figure 4-4), undergoes ring-opening metathesis polymerization when treated with catalyst **G2** under the same experimental conditions, the resulting supramolecular polymer[11] being exclusively held together by coordinative bonds (Figure 4-5).

RESULTS AND DISCUSSION

The choice of **2** as a non-interlocked model complex of catenate **1** was guided by a number of considerations. First of all, both complexes consist of two structurally analogous 28-membered macrocycles, $\mathbf{D_1}$ and $\mathbf{C_1}$ respectively, incorporating a 1,10-phenanthroline ligand (Figure 4-6).

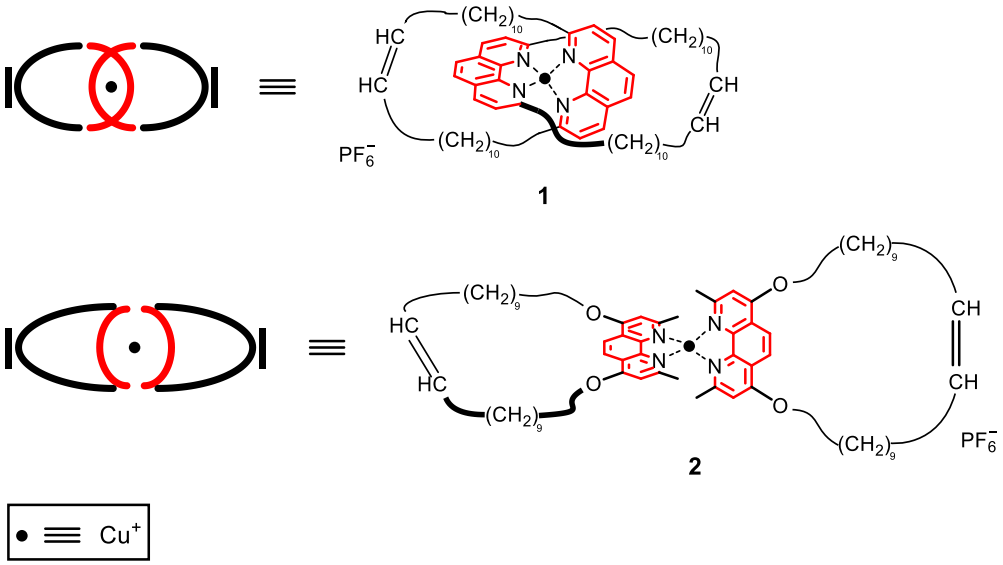

Figure 4-4. Comparison between the structures of catenated complex **1**[10] and model complex **2**.

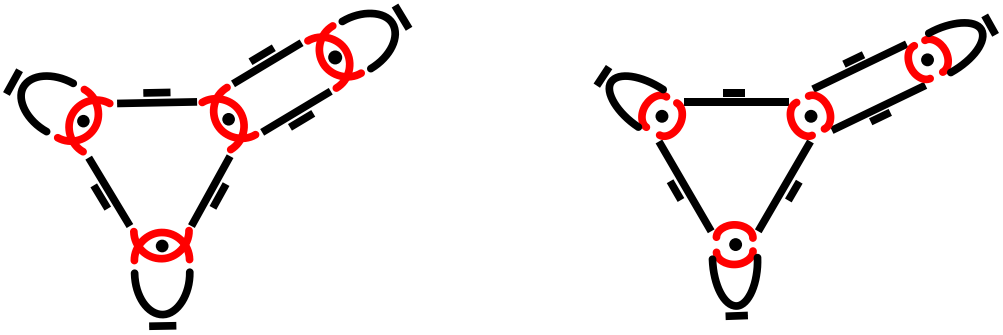

Figure 4-5. Examples of an oligomeric structure (a tetramer) obtainable from ROMP of **1** (left) and **2** (right) respectively.

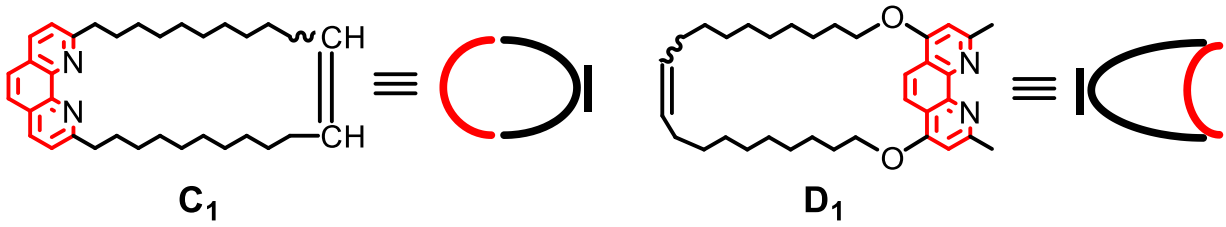

Figure 4-6. Structures of macrocycles $\mathbf{C_1}$ and $\mathbf{D_1}$.

Secondly, both $\mathbf{D_1}$ and $\mathbf{C_1}$ can be obtained by the ring-closure of linear precursors with the same number of rotatable single bonds, namely 22. Thirdly, $\mathbf{D_1}$ and $\mathbf{C_1}$ have the same number of tetrahedral and trigonal centers included in the cyclic structure. Apart from the methylene groups present in positions 2 and 9 of $\mathbf{D_1}$, the only difference between $\mathbf{D_1}$ and $\mathbf{C_1}$ lies in the presence of two oxygen atoms in $\mathbf{D_1}$ which are substituted with two methylene groups in $\mathbf{C_1}$. However, as it will be shown later, the lack of such correspondence will not

affect our analysis. The two oxygen atoms present in **D₁** are necessary for an easier synthetic route to this kind of macrocycle, otherwise hardly achievable.

Synthesis of the model complex 2

Macrocyclic alkene **D₁** was prepared by means of a two-step procedure starting from 2,9-dimethyl-4,7-dihydroxy-1,10-phenanthroline (**3**, Scheme 4-1), which, in turn, was synthesized according to a procedure reported by Buchwald *et al*..[12]

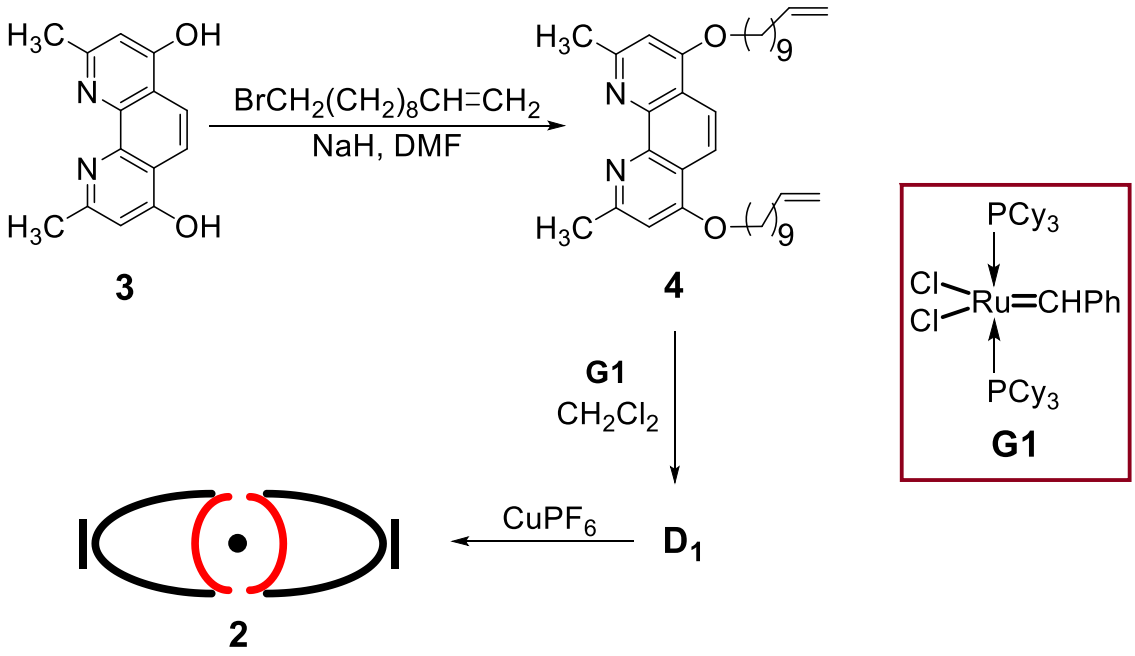

Scheme 4-1. Synthesis of model complex **2**.

Alkylation of **3** with 11-bromo-1-undecene gave the doubly alkylated compound **4**, which was then subjected to ring-closing metathesis (RCM) in a diluted dichloromethane solution (10 mM) at room temperature in presence of the 1st generation Grubbs' catalyst **G1** (Scheme 4-1). The less robust catalyst **G1** was preferred to **G2** to minimize the incursion of cross-metatheses involving **D₁**.[13] Chromatographic purification of the crude product afforded macrocycle **D₁** as a mixture of *cis* and *trans* isomers. It should be stressed here that the presence of the two methyl groups in positions 2 and 9 of the 1,10-phenanthroline moiety is crucial to obtain macrocycle **D₁**, since their presence provides the steric hindrance that is necessary to prevent the phenanthroline nitrogen atoms to interact with the ruthenium(II) metal center and dramatically reduce catalyst activity.[14] Macrocycle **D₁** was then reacted with half molar equivalent of tetrakis(acetonitrile)copper(I) hexafluorophosphate under argon atmosphere and complex **2** was obtained as a red solid.[15]

Comparison between ROMP equilibrations from macrocycles C_1 and D_1

The *cis*/*trans* mixture of geometrical isomers of **D_1** was subjected to ring-opening metathesis polymerization (dichloromethane, 30 °C) catalyzed by **G2** at various initial concentration of monomer **D_1** (c_{mon}), from 10 to 120 mM. **G2** was chosen in this case because its high robustness and activity make it one of the catalysts of choice for ROMP experiments under thermodynamic control.[13] Occasional ^{1}H NMR monitoring of the equilibrating mixtures indicated that equilibrium was reached in all cases after 24 h from start, in line with previous investigations on similar olefin systems under the same conditions.[10,14] The formation of dynamic covalent libraries (DCLs) of cyclic oligomers with higher polymerization degrees (**D_i** with $i \geq 2$, see Figure 4-7a) in the reaction mixtures was verified by mass spectrometry (Figure 4-8).[16]

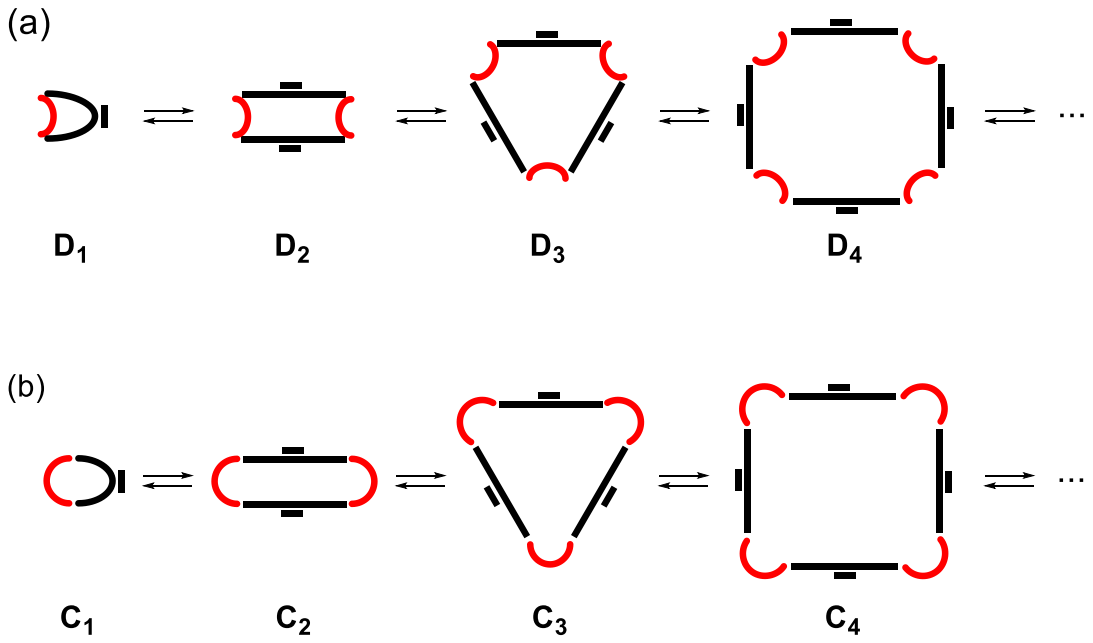

Figure 4-7. Dynamic library of macrocyclic oligomers generated by ROMP of (a) **D_1** and (b) **C_1**.

The DCLs generated in these equilibration experiments can be described in terms of the Jacobson-Stockmayer theory for reversible macrocyclization equilibria,[17] which predicts that the concentration of each cyclic oligomer **D_i** increases on increasing c_{mon} until a critical value c_{mon}* is reached. While below c_{mon}* a DCL contains cyclic oligomers only (Equation 1, which holds when $c_{mon} \leq c_{mon}$*), above c_{mon}* only the concentration of linear species **M_i** increases on increasing c_{mon} (Equation 2), whereas the concentration of cyclic species **D_i** remains constant (Equation 3). The limiting value [**D_i**]* approached by [**D_i**] when c_{mon} approaches c_{mon}* is the equilibrium effective molarity EM_i of **D_i**.[18] The equilibrium effective molarity of a

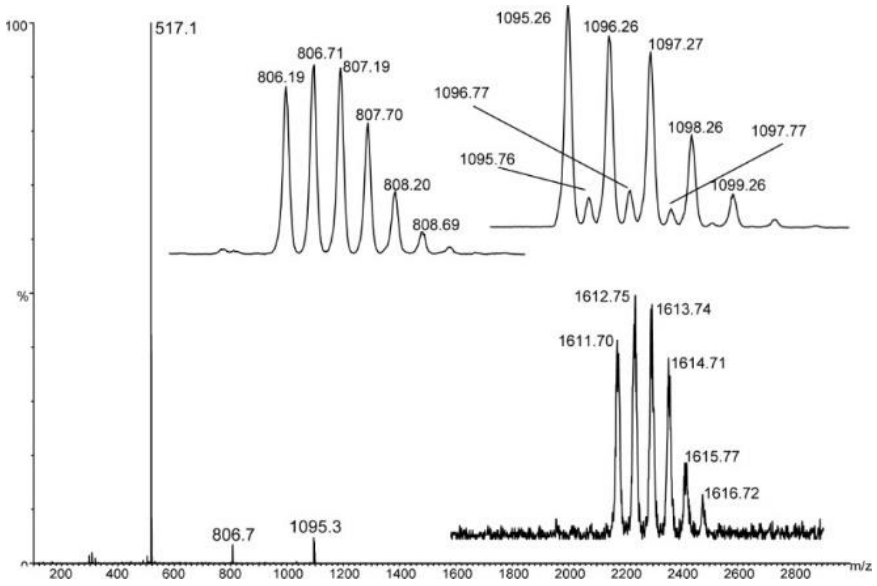

Figure 4-8. ROMP of $\mathbf{D_1}$ in the presence of **G2**. Typical ESI-TOF mass spectrum of a reaction mixture at equilibrium (m/z = 517 is attributed to $\mathbf{D_1}$ + H^+, m/z = 806 to $\mathbf{D_3}$ + H^+ + Cu^+, m/z = 1095 to $\mathbf{D_2}$ + Cu^+, the doubly charged m/z = 1095 to $\mathbf{D_4}$ + 2 Cu^+, m/z = 1611 to $\mathbf{D_3}$ + Cu^+). Copper(I)-containing species possibly arise from trace amounts of Cu^+ in the methanol used to prepare the samples (see reference 14).

macrocycle is a physical quantity that measures the ease of its formation from a linear precursor and correlates to the stability of the macrocycle.

$$\sum_{i=1}^{\infty} i[D_i] = c_{mon} \quad (1)$$

$$\sum_{i=1}^{\infty} i[M_i] = c_{mon} - c^*_{mon} \quad (2)$$

$$\sum_{i=1}^{\infty} i[D_i]^* = c^*_{mon} \quad (3)$$

In Figure 4-9a the equilibrium concentration of monomer $\mathbf{D_1}$ in the dynamic libraries $\mathbf{D_i}$ (Figure 4-7a) is reported as a function of the total monomer concentration c_{mon} whereas Figure 4-9b, which is reported for the sake of comparison, shows the analogous profile for the equilibrium concentration of $\mathbf{C_1}$ in the dynamic libraries $\mathbf{C_i}$ (Figure 4-7b).The limiting value 28 mM (Figure 4-9a) represents the *EM* for $\mathbf{D_1}$ (*cis* + *trans* mixture) which has to be compared with the limiting value 22 mM (Figure 4-9b),[19,20] the *EM* for $\mathbf{C_1}$ (*cis* + *trans* mixture).

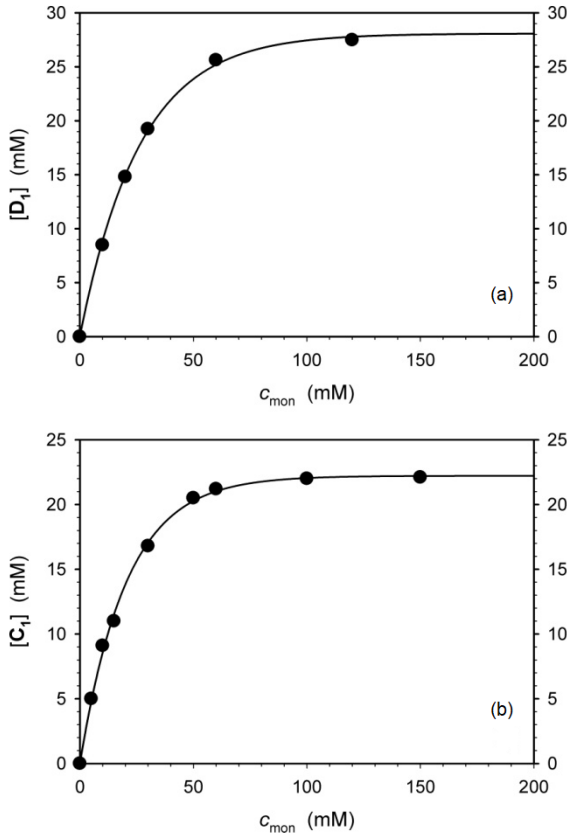

Figure 4-9. Equilibrium concentrations of (a) **D₁** and (b) **C₁** in the dynamic libraries represented in Figure 4-7a and Figure 4-7b, respectively, as a function of total monomer concentration c_{mon}. Data in Figure 4-9b are taken from Table 1 of reference 10.

Although **C₁** and **D₁** are not isomers and their thermodynamic stabilities are not directly comparable, the almost identical values of their effective molarities ensure that the two macrocycles have almost identical strain energies, only differing by RT ln (28/22) = 0.14 kcal mol^{-1} at 30 °C. Since both macrocycles **C₁** and **D₁** can be obtained from very similar linear precursors with an identical number of rotatable single bonds,[18] namely 22, their behaviors regarding ROMP are expected to be fully superimposable. The difference between the strain energies of larger macrocycles **Dᵢ** and **C*ᵢ*** with the same polymerization degree i ≥ 2, is indeed expected to be practically 0, since such difference is already negligible in the case of the more strained monomers **D₁** and **C₁**.[19] Thus the DLs **Dᵢ** and **Cᵢ** must behave in the same way when c_{mon} is the same, meaning that very similar, if not identical, equilibrium distributions are generated at the same c_{mon}. Consequently, complex **2** is an optimal non-interlocked model to assess the importance of interlocking on the gelation phenomenon observed from ROMP of catenate **1**.

Comparison between ROMP-induced gelation of complexes 1 and 2

The ^{1}H NMR spectra of complexes **1** and **2** clearly show their topological difference. The signals in the high field region (1 ppm ≤ δ ≤ 0 ppm) in Figure 4-10b are the most clear-cut evidence for the mechanical bond between the two twin macrocycles of **1**.[10,21] Such signals are due to the shielding effect that the aromatic moieties exert on the methylenes of the chains crossing their shielding cones. In contrast, the 0-1 ppm range in the ^{1}H NMR spectrum of complex **2** (Figure 4-10a) is featureless due to the absence of interlocking between the two macrocycles.

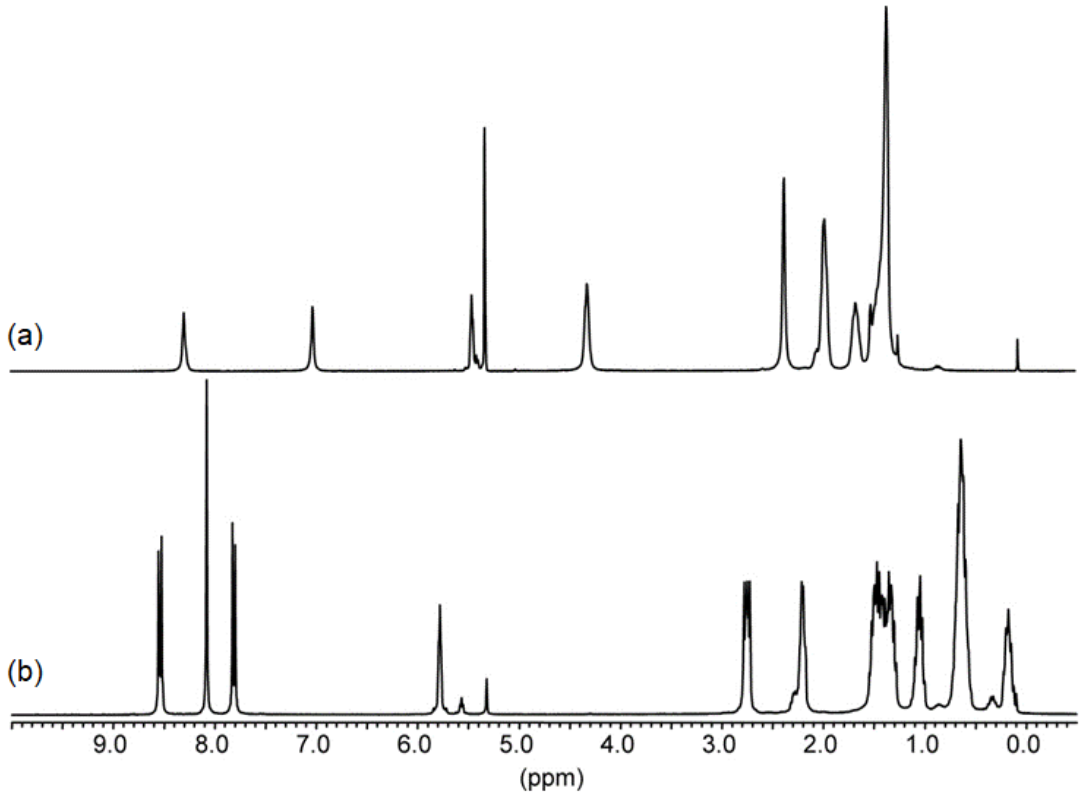

Figure 4-10. ^{1}H NMR spectrum of (a) complex **2** and (b) complex **1**.

As stated before, a red gel formed 30 min after the start of ROMP of complex **1** (30 mM in dichloromethane at 30 °C in the presence of 3 mol% 2nd generation Grubbs' catalyst **G2**).[9] On the contrary, when complex **2** was subjected to the same ROMP conditions no gel formed even after one month (Figure 4-11). Gelation was not observed within 30 min even when the concentration of **2** was increased from 30 mM to 45 mM. Finally, when the concentration of **2** was increased to values as high as 60 and 90 mM, we obtained a gel after 30 min from the addition of catalyst **G2**. The gel formation proved to be perfectly reproducible under these experimental conditions.

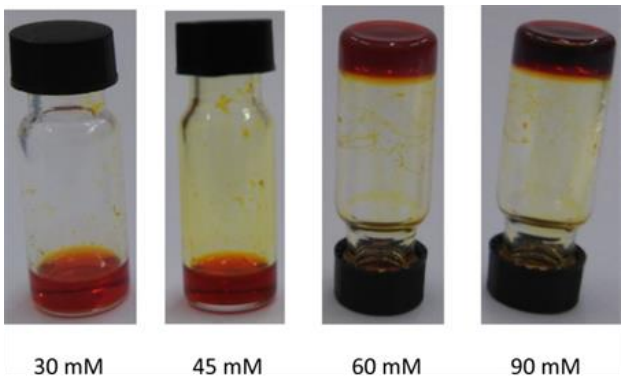

Figure 4-11. ROMP of complex **2** carried out at 30 °C in the presence of 3 mol% catalyst **G2**. Pictures are taken after 30 min from the addition of the catalyst.

Temperature dependence on the gelation behavior was not investigated due to the limited range explorable with dichloromethane. Other halogenated solvents were not considered since previous studies on similar phenanthroline-based systems[9,14] showed peculiar selectivities even between two very similar solvents such as dichloromethane and chloroform, the latter of which was found to be not suitable for gelation.

The choice of **2** as a non-interlocked model compound of **1** was widely discussed above. In particular, it has been shown that the close analogy between the DCLs $\mathbf{D_i}$ and $\mathbf{C_i}$ allows to obtain very similar, if not identical, distribution of cyclic species (and hence cross-links in the metallo-supramolecular polymer) at a given c_{mon}.[22] Although the lengths of the alkyl spacers are identical and olefin metathesis reaches thermodynamic equilibrium in both systems, severe backfolding of these methylene linkers to generate interlocked species is very unlikely in the DCLs $\mathbf{D_i}$ explored. Thus, the difference in the polymeric structures formed and gelation outcomes for the two systems has to be ascribed only to the mechanical bond present in **1** and absent in **2** (Figure 4-12).

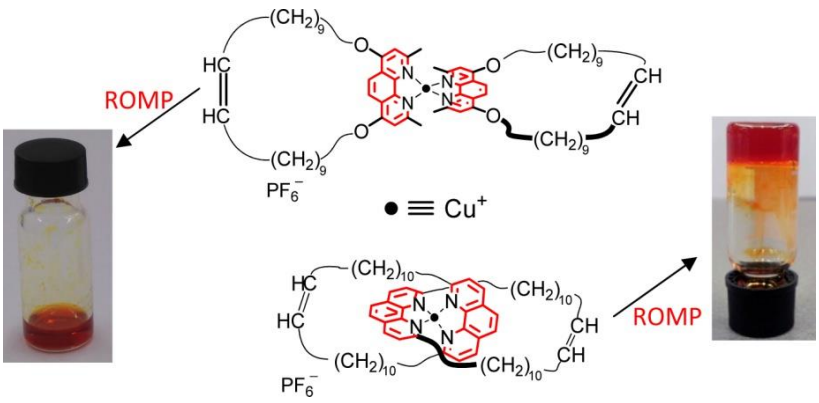

Figure 4-12. Comparison between the outcome of ROMP experiments (30 mM) for **2** (left) and **1** (right).

The *endo*-coordination accessible when macrocycles **C$_i$** are at the base of the polymerization process (complex **1** as the monomer for the polymerization reaction), strongly favors the formation of a polymeric gel-like material which was demonstrated to be mainly consisting of interlocked cyclic species.[9] The *exo*-coordination[23] for which macrocycles **D$_i$** are prompt to (complex **2** as the monomer for the polymerization reaction), clearly does not encourage the interlocking of macrocyclic species. Keeping in mind that the demetalated polycatenane is not able to produce a gel,[9] we can hypothesize that the presence of the mechanical bond should not only reinforce the coordination between Cu^+ and the two phenanthroline ligands (catenand effect)[24] but it should also bring additional stiffness to the metallo-supramolecular polymer, consequently increasing its extension in space. For this reason, we can speculate that for the less rigid non-interlocked model system gelation occurs only at higher concentrations, because a higher polymerization degree and branching is needed in the supramolecular polymer to be able to establish a sufficient number of physical cross-links to induce the transition to the gel state.

CONCLUSIONS

In conclusion, the influence of concatenation of the two identical macrocycles of complex **1** on the gelation behavior under ring-opening metathesis polymerization conditions has been evaluated by comparing the behavior of the non-interlocked complex **2** under the same conditions. The use of complex **2** as a non-interlocked model of complex **1** is justified in terms of molecular structure and effective molarity (*EM*). Concatenation plays a pivotal role in the gelation outcome, which is strongly favored by the endotopic, interlocked coordination of complex **1** in comparison with the exotopic, non-interlocked coordination of complex **2**. As a result, higher concentrations of the non-interlocked complex are required to form a gel.

EXPERIMENTAL SECTION

Instruments, general methods and materials

NMR spectra were recorded with a 300 MHz spectrometer at room temperature unless otherwise stated and were internally referenced to the residual proton solvent signal. Mass spectra were recorded with an ESI-TOF mass spectrometer. UV-vis spectra were recorded with a double-beam spectrophotometer using a standard quartz cell (path length: 1 cm) at room temperature.

All reagents and solvents were purchased at the highest commercial quality and were used without further purification unless otherwise stated. The glassware was either flame- or oven-dried. 2,9-Dimethyl-4,7-dihydroxy-1,10-phenanthroline **3** was prepared according to a literature procedure[12] starting from *o*-phenylenediamine, 2,2-dimethyl-1,3-dioxane-4,6-dione (Meldrum's acid) and trimethyl orthoacetate. 2,9-Dimethyl-4,7-bis(undec-10-en-1-yloxy)-1,10-phenanthroline **4** was synthesized as shown below, adapting a literature procedure.[25] Sodium hydride (60 wt% dispersion in mineral oil) was washed thrice with pentane immediately prior to use. Dichloromethane used in the olefin metathesis experiments was filtered through basic alumina just before use.

Preparation of 2,9-dimethyl-4,7-bis(undec-10-en-1-yloxy)-1,10-phenanthroline 4

2,9-Dimethyl-4,7-dihydroxy-1,10-phenanthroline (**3**; 1.71 g, 7 mmol) was added to a suspension of sodium hydride (1.72 g, 60 wt% in mineral oil, 43 mmol) in *N*,*N*-dimethylformamide (137 mL) at 0 °C and the mixture was stirred for 30 min under an inert atmosphere. Then 11-bromo-1-undecene (9.4 mL, 43 mmol) and sodium iodide (0.65 g, 4.3 mmol) were added and the mixture was stirred overnight at room temperature. Next, the reaction was quenched with water and the resulting mixture extracted three times with dichloromethane. The organic phases were collected, washed with brine, dried with sodium sulfate and filtered. The solvent was evaporated and the crude obtained was subjected to column chromatography (basic alumina, ethyl acetate/petroleum ether 4:6) to afford pure **4** (2.7 g, 5 mmol, yield: 70%). Mp: 120-122 °C. ^{1}H NMR (300 MHz, $CDCl_3$) δ (ppm): 8.08 (s, 2H), 6.82 (s, 2H), 5.75-5.88 (m, 2H), 4.91-5.02 (m, 4H), 4.19 (t, ^{3}J = 6 Hz, 4H), 2.86 (s, 6H), 1.91-2.08 (m, 8H), 1.52-1.62 (m, 4H), 1.25-1.41 (m, 20H). ^{13}C{^{1}H} NMR (75 MHz, $CDCl_3$) δ (ppm): 161.61, 160.01, 145.87, 139.09, 119.38, 117.82, 114.03, 103.16, 63.81, 33.68, 29.40, 29.31, 29.24, 29.00, 28.89, 28.81, 26.43, 26.03. UV-vis (CH_3OH) ε (mol^{-1} dm^3 cm^{-1}): 1600 at 340 nm, 2400 at 325 nm, 11000 at 308 nm, 11300 at 298 nm, 43000 at 256 nm. HRMS (ESI-TOF, *m*/*z*): $[M + H]^+$ calcd for $C_{36}H_{53}N_2O_2$, 545.4107; found, 545.4102.

Preparation of cyclic monomer D_1

Compound **4** (0.51 g, 0.9 mmol) was dissolved in dichloromethane (90 mL) and the solution was degassed by freeze-pump-thaw cycles, then 1st generation Grubbs' catalyst **G1** (0.04 g, 0.05 mmol) was added. The resulting mixture was stirred at room temperature for 3 d under an inert atmosphere, monitoring the reaction by ESI-TOF MS. The solvent was evaporated and the crude material was subjected to column chromatography (basic alumina, ethyl acetate/*n*-hexane 5.5:4.5) to give **D_1** as a mixture of *cis* and *trans* isomers (0.237 g,

0.46 mmol, yield: 50%). Mp: 202-204 °C. ^{1}H NMR (300 MHz, CD_2Cl_2) δ (ppm): 8.12-8.14 (s, 2H), 6.87 (s, 2H), 5.38-5.46 (m, 2H), 4.25 (t, ^{3}J = 5 Hz, 4H), 2.80 (s, 6H), 1.90-2.01 (m, 8H), 1.62-1.72 (m, 4H), 1.37-1.48 (m, 20H). $^{13}C\{^{1}H\}$ NMR (75 MHz, CD_2Cl_2) δ (ppm): 161.61, 159.50, 145.79, 130.22, 129.69, 119.47, 117.81, 103.02, 68.41, 32.32, 29.58, 29.47, 29.21, 29.14, 28.94, 28.88, 26.59, 25.69. UV-vis (CH_2Cl_2) ε (mol^{-1} dm^3 cm^{-1}): 1700 at 342, 2400 at 326 nm, 11700 at 310 nm, 13000 at 299 nm, 48000 at 256 nm. HRMS (ESI-TOF, *m*/*z*): $[M + H]^+$ calcd for $C_{34}H_{49}N_2O_2$, 517.3794; found, 517.3784.

Preparation of complex 2

Compound **D$_1$** (0.101 g, 0.2 mmol) was dissolved in dichloromethane (4 mL) and the solution was degassed by freeze-pump-thaw cycles. Then $[Cu(CH_3CN)_4]PF_6$ (0.036 g, 0.1 mmol) was added and the mixture was stirred for 24 h at room temperature under an inert atmosphere. The solvent was evaporated and the resulting solid was washed with water to afford complex **2** as a mixture of three isomers (0.120 g, 0.1 mmol, yield: quantitative). Mp: 248-250 °C. ^{1}H NMR (300 MHz, CD_2Cl_2) δ (ppm): 8.29 (m, 4H), 7.03 (s, 4H), 5.40-5.47 (m, 4H), 4.33 (t, ^{3}J = 6 Hz, 8H), 2.39 (s, 12H), 2.00 (m, 16H), 1.69 (m, 8H), 1.27-1.54 (m, 40H). $^{13}C\{^{1}H\}$ NMR (75 MHz, CD_2Cl_2) δ (ppm): 162.13, 158.95, 143.86, 130.25, 129.70, 120.00, 118.57, 104.67, 69.59, 69.36, 32.33, 29.65, 29.37, 29.28, 29.21, 29.11, 28.94, 28.90, 28.70, 27.03, 26.54, 25.91. UV-vis (CH_2Cl_2) ε (mol^{-1} dm^3 cm^{-1}): 10000 at 424 nm, 22500 at 300 nm, 77000 at 265 nm, 87000 at 254 nm. HRMS (ESI-QTOF, *m*/*z*): $[M - PF_6^-]^+$ calcd for $C_{68}H_{96}N_4O_4Cu$, 1095.6728; found, 1095.6609.

General procedure for ROMP equilibration experiments

An appropriate amount of cyclic monomer **D$_1$** was weighed in an NMR tube and dissolved in CD_2Cl_2. Then a calculated volume of a stock solution of 2nd generation Grubbs' catalyst **G2** in CD_2Cl_2 was added to reach the desired cyclic monomer (10 mM, 20 mM, 30 mM, 60 mM, 120 mM) and catalyst (3 mol%; final volume: 600 µL) concentration. The reactions were run at 30 °C and monitored by ^{1}H NMR spectroscopy.

General procedure for the gelation experiments

An appropriate amount of complex **2** was weighed in a screw-cap vial and dissolved in dichloromethane. Then a calculated volume of a stock solution of 2nd generation Grubbs' catalyst **G2** in dichloromethane was added to reach the desired complex (30 mM, 45 mM, 60 mM, 90 mM) and catalyst (3 mol%; final volume: 200 µL) concentration. The reactions were run at 30 °C.

NOTES AND REFERENCES

1 (a) C. J. Bruns, J. F. Stoddart, *The Nature of Mechanical Bond*, John Wiley & Sons, Hoboken, New Jersey (U.S.A.), **2017**; (b) J. F. Stoddart, *Chem. Soc. Rev.* **2009**, *38*, 1802-1820; (c) M. A. Olson, Y. Y. Botros, J. F. Stoddart, *Pure Appl. Chem.* **2010**, *82*, 1569-1574.

2 G. Gíl-Ramírez, David A. Leigh, A. J. Stephens, *Angew. Chem. Int. Ed.* **2015**, *54*, 6110-6150.

3 M. Xue, Y. Yang, X. Chi, X. Yan, F. Huang, *Chem. Rev.* **2015**, *115*, 7398-7501.

4 For the contributions of mechanically interlocked molecules in the field of artificial molecular machines, see for example: (a) V. Balzani, A. Credi, S. Silvi, M. Venturi, *Chem. Soc. Rev.* **2006**, *35*, 1135-1149; (b) J.-P. Sauvage, *Angew. Chem. Int. Ed.* **2017**, *56*, 11080-11093; (c) J. F. Stoddart, *Angew. Chem. Int. Ed.* **2017**, *56*, 11094-11125. For a deeper insight in the more general field of molecular machines, see for example: (d) V. Balzani, A. Credi, F. M. Raymo, J. F. Stoddart, *Angew. Chem. Int. Ed.* **2000**, *39*, 3348-3391; (e) S. Erbaş Çakmak, D. A. Leigh, C. T. McTernan, A. L. Nussbaumer, *Chem. Rev.* **2015**, *115*, 10081-10206; (f) S. Kassem, T. van Leeuwen, A. S. Lubbe, M. R. Wilson, B. L. Feringa, D. A. Leigh, *Chem. Soc. Rev.* **2017**, *46*, 2592-2621; (g) V. Balzani, M. Clemente-León, A. Credi, B. Ferrer, M. Venturi, A. H. Flood, J. F. Stoddart, *Proc. Natl. Acad. Sci. U.S.A.* **2006**, *103*, 1178-1183; (h) M. R. Wilson, J. Solà, A. Carlone, S. M. Goldup, N. Lebrasseur, D. A. Leigh, *Nature* **2016**, *534*, 235-241; (i) S. Erbaş Çakmak, S. D. P. Fielden, U. Karaca, D. A. Leigh, C. T. McTernan, D. J. Tetlow, M. R. Wilson, *Science* **2017**, *358*, 340-343.

5 (a) F. M. Raymo, J. F. Stoddart, *Chem. Rev.* **1999**, *99*, 1643-1663; (b) L. Fang, M. A. Olson, D. Benítez, E. Tkatchouk, W. A. Goddard III, J. F. Stoddart, *Chem. Soc. Rev.* **2010**, *39*, 17-29.

6 Z. Niu, H. Gibson, *Chem. Rev.* **2009**, *109*, 6024-6046.

7 A. Harada, A. Hashidzume, H. Yamaguchi, Y. Takashima, *Chem. Rev.* **2009**, *109*, 5974-6023.

8 Nonetheless, a major achievement has been reached very recently by Rowan *et al*., who reported the efficient and high-yield synthesis (≈ 75%) of poly[*n*]catenanes having remarkably high polymerization degree, estimated consisting of linear poly[7-27]catenanes (≈ 60%), branched poly[13-130]catenanes (≈ 24%) and cyclic poly[4-7]catenanes (≈ 16%): Q. Wu, P. M. Rauscher, X. Lang, R. J. Wojtecki, J. J. de Pablo, M. J. A. Hore, S. J. Rowan, *Science* **2017**, *358*, 1434-1439.

9 J. A. Berrocal, L. Pitet, M. M. L. Nieuwenhuizen, L. Mandolini, E. W. Meijer, S. Di Stefano, *Macromolecules* **2015**, *48*, 1358-1363.

10 J. A. Berrocal, M. M. L. Nieuwenhuizen, L. Mandolini, E. W. Meijer, S. Di Stefano, *Org. Biomol. Chem.* **2014**, *12*, 6167-6174.

11 On supramolecular polymers, see for example: (a) *Supramolecular Polymer Chemistry* (editor: A. Harada), Wiley VCH Verlag, Weinheim (Germany), **2012**; (b) L. Brunsveld, B. J. B. Folmer, E. W. Meijer, R. P. Sijbesma, *Chem. Rev.* **2001**, *101*, 4071-4097; (c) L. Yang, X. Tan, Z. Wang, X. Zhang, *Chem. Rev.* **2015**, *115*, 7196-7239.

12 R. A. Altman, S. L. Buchwald, *Org. Lett.* **2006**, *8*, 2779-2782.

13 (a) S. Monfette, D. E. Fogg, *Chem. Rev.* **2009**, *109*, 3783-3816; (b) G. C. Vougioukalakis, R. H. Grubbs, *Chem. Rev.* **2010**, *110*, 1746-1787; (c) S. H. Hong, A. G. Wenzel, T. T. Salguero, M. W. Day, R. H. Grubbs, *J. Am. Chem. Soc.* **2007**, *129*, 7961-7968.

14 J. A. Berrocal, S. Albano, L. Mandolini, S. Di Stefano, *Eur. J. Org. Chem.* **2015**, 7504-7510.

15 An alternative procedure to obtain complex **2** was also attempted. The purpose was to carry out its preparation by double cyclization of the 2:1 complex Cu(**4**)$_2$PF$_6$, which has been successfully prepared. The subsequent double cyclization reaction was performed in the presence of catalyst **G1** in dichloromethane. The reaction crude showed a good yield in complex **2**, however any attempt to purify this compound through normal phase column chromatography failed.

16 Each member $\mathbf{D_i}$ of the DCL will be present as a mixture of geometrical isomers because each double bond can have either a *cis* or *trans* configuration. This means that two isomers are possible for $\mathbf{D_1}$, three for $\mathbf{D_2}$, four for $\mathbf{D_3}$, six for $\mathbf{D_4}$ and so on.

17 (a) H. Jacobson, W. H. Stockmayer, *J. Chem. Phys.* **1950**, *18*, 1600-1606; (b) G. Ercolani, L. Mandolini, P. Mencarelli, S. Roelens, *J. Am. Chem. Soc.* **1993**, *115*, 3901-3908; (c) S. Di Stefano, *J. Phys. Org. Chem.* **2010**, *23*, 797-805.

18 (a) L. Mandolini, *Adv. Phys. Org. Chem.* **1986**, *22*, 1-111; (b) S. Di Stefano, G. Ercolani, *Adv. Phys. Org. Chem.* **2016**, *50*, 1-76.

19 *EM* values of 28 mM or 22 mM are those expected for macrocycles of such dimensions, in which very low strain energy is present (see reference 18b).

20 For *EM* values of other macrocycles of comparable size, see for example: (a) K. Ito, Y. Hashizuka, Y. Yamashita, *Macromolecules* **1977**, *10*, 821-824; (b) Y. Yamashita, J. Mayumi, Y. Kawakami, K. Ito, *Macromolecules* **1980**, *13*, 1075-1080; (c) A. T. ten Cate, H. Kooijman, A. L. Spek, R. P. Sijbesma, E. W. Meijer, *J. Am. Chem. Soc.* **2004**, *126*, 3801-3808; (d) R. Cacciapaglia, S. Di Stefano, L. Mandolini, *J. Am. Chem. Soc.* **2005**, *127*, 13666-13671; (e) R. Cacciapaglia, S. Di Stefano, L. Mandolini, P. Mencarelli, F. Ugozzoli, *Eur. J. Org. Chem.* **2008**, 186-195; (f) R. Cacciapaglia, S. Di Stefano, G. Ercolani, L. Mandolini, *Macromolecules* **2009**, *42*, 4077-4083; (g) J. A. Berrocal, R. Cacciapaglia, S. Di Stefano, *Org. Biomol. Chem.* **2011**, *9*, 8190-8194; (h) J. A. Berrocal, R. Cacciapaglia, S. Di Stefano, L. Mandolini, *New J. Chem.* **2012**, *36*, 40-43.

21 (a) J. A. Berrocal, C. Biagini, L. Mandolini, S. Di Stefano, *Angew. Chem. Int. Ed.* **2016**, *55*, 6997-7001; (b) C. Biagini, S. Albano, R. Caruso, L. Mandolini, J. A. Berrocal, S. Di Stefano, *Chem. Sci.* **2018**, *9*, 181-188.

22 A glance at Figure 4-9 clearly shows that critical concentrations (c_{mon}*) for both DCLs $\mathbf{D_i}$ and $\mathbf{C_i}$ are well above 100 mM, thus when c_{mon} = 30 mM or 45 mM both DCLs are only composed by cyclic species.

23 For reviews on *exo*-coordination see: (a) S. Park, S. Y. Lee, K. M. Park, S. S. Lee, *Acc. Chem. Res.* **2012**, *45*, 391-403; b) E. Lee, S. Y. Lee, L. F. Lindoy, S. S. Lee, *Coord. Chem. Rev.* **2013**, *2*, 3125-3138. For the synthesis and self-assembly of exotopic phenanthroline-based macrocycles see: (c) M. Schmittel, C. Michel, A. Ganz, M. Herderich, *J. Prakt. Chem.* **1999**, *341*, 228-236; (d) M. Schmittel, H. Ammon, *Synlett* **1999**, *6*, 750-752; (e) V. Kalsani, H. Ammon, F. Jäckel, J. P. Rabe, M. Schmittel, *Chem. Eur. J.* **2004**, *10*, 5481-5492.

24 (a) D. H. Busch, N. A. Stephenson, *Coord. Chem. Rev.* **1990**, *100*, 119-154; (b) A.-M. Albrecht-Gary, Z. Saad, C. O. Dietrich-Buchecker, J.-P. Sauvage, *J. Am. Chem. Soc.* **1985**, *107*, 3205-3209; (c) M. Cesario, C. O. Dietrich, A. Edel, J. Guilhem, J.-P. Kintzinger, C. Pascard, J.-P. Sauvage, *J. Am. Chem. Soc.* **1986**, *108*, 6250-6254.

25 X. Liu, X. Li, Y. Chen, Y. Hu, Y. Kishi, *J. Am. Chem. Soc.* **2012**, *134*, 6136-6139.

5. An Attempt to Study Statistical Catenation with Dynamic Combinatorial Chemistry

ABSTRACT

An attempt to study the statistical formation of catenanes was performed in order to verify novel theoretical predictions within the framework of Jacobson-Stockmayer theory. The choice of the reversible chemistry used and the compounds employed in the study has been thoroughly justified. The problems encountered in the DCL formation as well as in the analytical part of the work are discussed in detail.

INTRODUCTION

The synthesis of topologically non-trivial molecules[1] has long been a fascinating target for synthetic chemists. For example, the first successful effort to prepare catenanes, mechanically interlocked cyclic molecules, dates back to a work published in 1960 by Wasserman.[2] Indeed, a catenane was obtained, albeit in very low yields (≈ 1%),[3] by simply performing a cyclization reaction of a linear long-chain diester molecule in presence of a large excess of a 34-membered cyclic hydrocarbon (Scheme 5-1).

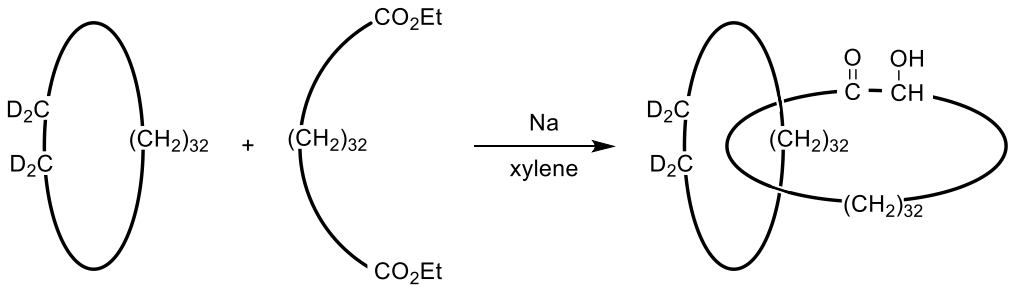

Scheme 5-1. First reported synthesis of a catenane.[2]

There were also other attempts at catenane synthesis using similar statistical approaches, namely methods that do not rely on attractive interactions between the catenane precursors but only on the probability of a linear bifunctional molecule to thread a large macrocycle in a concentrated solution before undergoing cyclization,[1c-d] but failures or low yields necessarily fostered to look for alternatives. Directed synthesis methods were also developed shortly after Wasserman's first catenane,[4] however it was not until the breakthrough of template-directed synthesis pioneered by Sauvage (Figure 5-1),[5] that chemists developed the most suitable tools and strategies to efficiently prepare catenanes (other than rotaxanes and molecular knots).[1b-c,e-f]

Interestingly, in a recent paper by Di Stefano and Ercolani,[6] an extension to the classical Jacobson-Stockmayer theory[7] for ring-chain equilibria has been proposed (see Chapter 3). The statistical formation of [2]catenanes in polymerization equilibria has been incorporated in the mass-balance equation for the total monomer concentration and thoroughly examined on the basis of the knowledge of the expression for the catenation constant.[8] Two different possibilities are taken in consideration. In the case of a "thin" system (dsDNA, for example), in which a polymer chain is characterized by negligible Kuhn segment[9] thickness with respect to its length, statistical formation of [2]catenanes is expected even for values of the

equilibrium constant of the intermolecular reaction K_{inter} as low as 10^2 mol^{-1} L (Figure 5-2a-b).

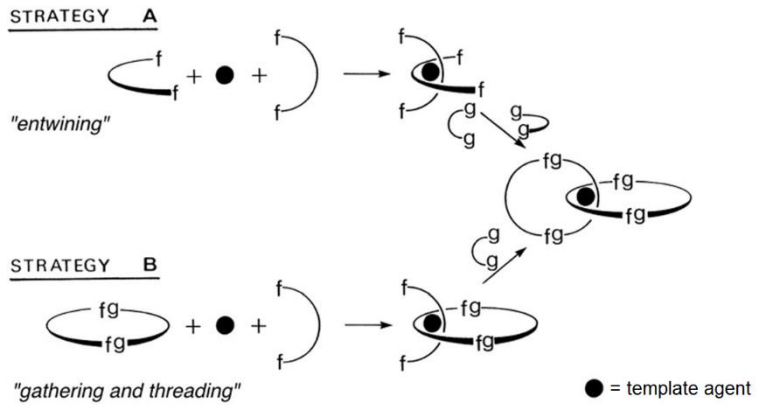

Figure 5-1. Synthetic strategies first described by Sauvage *et al.* for the synthesis of catenanes.[5]

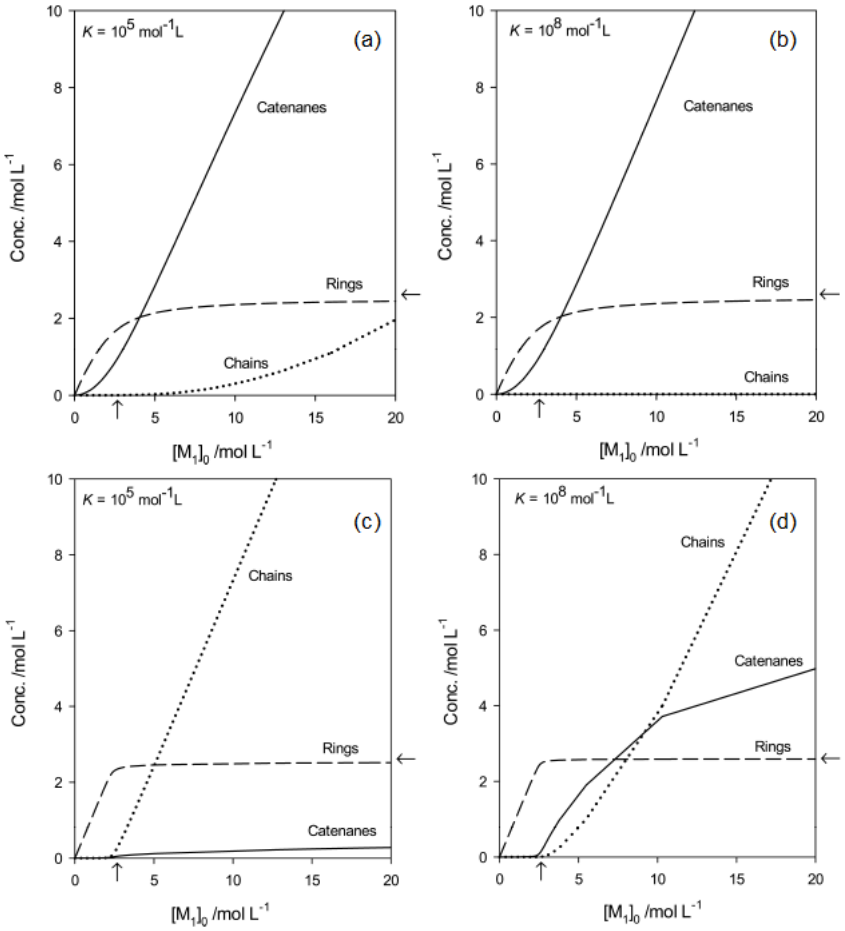

Figure 5-2. Weighted equilibrium concentrations of chains (dotted line), rings (dashed line), and catenanes (solid line) for a “thin” chain (top) and a “thick” chain (bottom). Distributions are reported as a function of $[M_1]_0$ for K_{inter} = 10^5 mol^{-1} L (a and c) and K_{inter} = 10^8 mol^{-1} L (b and d). Arrows on abscissa and ordinate point to the value of 2.612 mol L^{-1}.

The origin of this behavior is considered to be the absence of excluded volume effects for these type of locally rigid polymer chains. On the contrary, in the case of a “thick” system (a polymethylene chain, for example), in which a flexible chain is characterized by non-negligible Kuhn segment thickness with respect to its length, statistical formation of [2]catenanes is predicted to be significant only for very high values of K_{inter}, ≈ 10^8 mol^{-1} L or even more, and in correspondence of the critical monomer concentration (Figure 5-2c-d). As a matter of fact, in this case the excluded volume effects are shown to be relevant, hindering the catenation of macrocycles. Moreover, for K_{inter} tending to infinity, it is expected that above the critical monomer concentration all linear species are converted into catenanes, the concentration of ring species remaining constant (Figure 5-3).

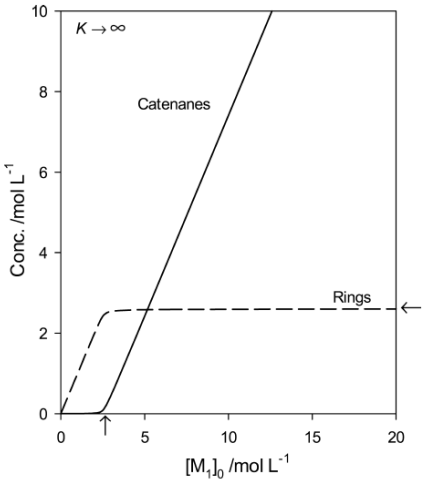

Figure 5-3. Weighted equilibrium concentrations of rings (dashed line) and catenanes (solid line) for a “thick” chain as a function of $[M_1]_0$, calculated for $K_{inter} \rightarrow \infty$. Arrows on the abscissa and ordinate point to the value of 2.612 mol L^{-1}.

The work reported here aimed at experimentally confirming these theoretical predictions. The goal was to study the statistical occurrence of catenane species in concentrated DCLs built from long chain bifunctional monomers as starting materials, by qualitatively and quantitatively analyzing the libraries obtained at different values of the total monomer concentration using liquid chromatography (LC) coupled to UV and mass spectrometry (MS) detection. The choice of the reversible reaction to employ fell on disulfide exchange, one of the most widely used reactions in DCC.[10] This reaction can be performed, for example, starting from thiol compounds in presence of a base catalyst to accelerate both thiol oxidation by atmospheric oxygen (Equation 1) and thiol-disulfide exchange (Equation 2).[11]

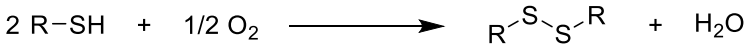

(1)

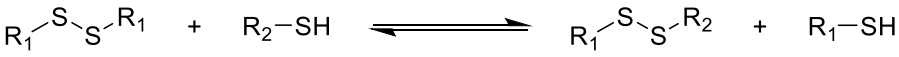

(2)

The reason behind the choice of this reaction resided in the possibility to obtain disulfide mixtures under thermodynamic control together with the feasible complete oxidation of thiol groups. We hypothesized that this second feature was of particular interest for our purpose, being of fundamental importance to have a large K_{inter} value in order to maximize the statistical formation of catenanes (Figures 5-2 and 5-3).[6] In this case, indeed, the reaction that forms a new S−S bond is the oxidation of thiols, an irreversible one. If oxidation of thiols is driven to completion, while equilibrium of the disulfides is reached through thiol-disulfide exchange reactions, then we should find ourselves in the most suitable conditions to be able to see statistically formed catenanes, according to the theory. The dithiol monomers chosen to carry on this study regarding the statistical formation of catenanes in concentrated DCLs of disulfides[12] were compounds **1** and **2**.

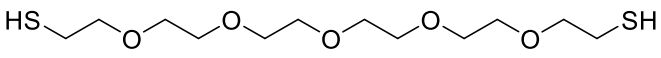

1

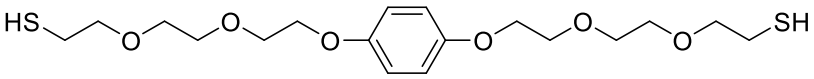

2

These long “thick” chain-type structures were chosen in order to build libraries composed of large macrocycles, thus helping in the formation of catenanes. Rough estimates of the expected c_{mon}^{*} value for the two systems were found to be, respectively, 114 mM and 97 mM.[13] The very simple and almost featureless structures were needed to minimize the possibility of intramolecular or intermolecular interactions, the latter eventually templating the formation of interlocked structures. Moreover, the ethylene glycol chains were meant to favor solubility in polar solvents needed for reverse phase LC and ionizability for MS detection. Finally, the phenylene ring present in monomer **2** should allow for UV spectrophotometric quantification of the different library members.

RESULTS AND DISCUSSION

Screening of reaction conditions

Hexaethylene glycol dithiol (**1**), prepared according to literature procedures,[14] was first used to test reaction conditions for DCC experiments at high concentration (near to the estimated value of c_{mon}^{*}, namely 114 mM; see Figure 5-2c-d and Figure 5-3), to verify the eventual occurrence of solubility problems.

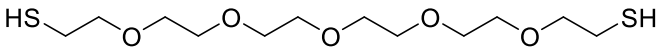

1

For a single experiment, a weighed amount of **1** was introduced in a vial with a magnetic stirring bar, then a solvent and a base to promote oxidation and disulfide metathesis were added in proper amounts and the reaction was monitored over time visually and with ultra-high performance LC-MS (UHPLC-MS). Disulfide exchange reactions are commonly performed in aqueous solution at near neutral or slightly basic pH (usually between 7 and 9), to allow for the formation of a sufficient amount of thiolate to promote thiol-disulfide exchange. These mild conditions and exposure of solution to air are usually enough to achieve relatively fast oxidation of thiols and equilibration of disulfides.[11] Moreover, only a few examples of disulfide exchange reactions in organic solvents are reported in the literature.[15] Therefore, the first attempts with monomer **1** were performed in aqueous solution with different type of additives for the formation of thiolates (Table 5-1),[16] but all of them ended up with the separation of a second phase, not compatible with the requirement to have a mixture of compounds under thermodynamic control.

Table 5-1. Screening of the conditions for DCL formation from **1** in aqueous solutions.

Entry	**1** (mM)	Reaction conditions	Solubility
1	74	water, phosphate buffer (pH = 7.5) 50 mM	-
2	76	water, 10% mol NaOH	-
3	100	water, 10% mol NH_4OH	-
4	102	water, 10% mol $NHMe_2$	-

For this reason, all the subsequent efforts were focused on finding the conditions to achieve complete oxidation of thiols in polar organic solvents (compatible with reverse-phase LC analysis) for a relatively wide range of concentrations and in the presence of a base (to hopefully promote disulfide exchange). Experiments in methanol showed phase-separation, despite an initially encouraging experiment at 120 mM concentration of **1** with 10% mol of tetrabutylammonium hydroxide (Table 5-2, Entry 1). Oxidation of thiols was found to be complete, demonstrated by disappearance over time of linear species observed through UHPLC-MS analysis, but increasing the concentration of monomer up to 192 mM caused phase-separation (Entry 2). Experiments in acetonitrile, dimethylsulfoxide/methanol mixtures and pure dimethylsulfoxide (Table 5-2, Entries 4-9), instead, showed a different problem. Despite all these libraries remained soluble, oxidation stopped over time as observed in the LC-MS chromatograms showing mixtures of linear and cyclic species. The addition of a small aliquot of base was in all cases able to restart oxidation, but only for a short time interval. We speculated that consumption of the base along with lack of a sufficient amount of oxygen in the headspace of the vial could be an explanation for incomplete oxidation,[17] the experiment of Entry 1 being only a fortuitous case of complete oxidation.

Table 5-2. Screening of the conditions for DCL formation from **1** in polar organic solvents.

Entry	**1** (mM)	Reaction conditions	Solubility
1	120	MeOH, 10% mol Bu_4NOH	yes
2	193	MeOH, 10% mol Bu_4NOH	-
3	134	MeOH, 10% mol NaOMe	-
4	137	MeCN, 10% mol Bu_4NOH	yes
5	131	DMSO/MeOH 1:1, 10% mol Bu_4NOH	yes
6	141	DMSO/MeOH 1:1, 10% mol NaOMe	yes
7	153	DMSO/MeOH 1:1, 20% mol Bu_4NOH	yes
8	141	DMSO, 10% mol NaH	yes
9	130	DMSO, NaH 130 mM	yes

Therefore, to push oxidation to completion, we decided to perform experiments either in presence of a catalyst for the oxidation (e.g. iodine) and an oxidant (DMSO),[18] or with an air balloon connected to a needle piercing the septum of the vial cap (see Experimental section for a picture of the experimental setup). The three procedures tested (Table 5-3) were adapted from literature reports on preparative methods for disulfide synthesis.[18-20]

Table 5-3. Screening of the conditions for DCL formation from **1** in organic solvents adapted from preparative procedures for disulfide synthesis.

Entry	**1** (mM)	Reaction conditions	Solubility
1	130	DMSO, 20% mol I_2	yes
2[19]	128	DMF, NEt_3 260 mM, 80 °C, air balloon	yes
3[20]	128	TMG, air balloon	-

The experiment of Entry 1 (performed in a closed vial) gave slow oxidation, still largely incomplete after a week, whereas the experiment performed in tetramethylguanidine (TMG) with the aid of an air balloon (Entry 3) produced in the early stages a phase-separation. In contrast, the experiment performed in *N*,*N*-dimethylformamide with two molar equivalents of triethylamine with respect to the molar amount of **1** and an air balloon at 80 °C afforded complete oxidation of the monomer in four days (Figure 5-4). However, no catenane species were identified in the final chromatogram at this concentration. Without having sufficient time to further study the effect of an added base and an air balloon in the DMSO/I_2 system, we decided to focus on the DMF/NEt_3 system at 80 °C, encouraged by the apparent absence of unoxidized species in the MS analysis for every peak present in the chromatogram and by the presence of a big amount of base that, in a polar aprotic solvent like *N*,*N*-dimethylformamide should be able to promote fast disulfide exchange.[11b]

Library experiments at different monomer concentration

At this point, the conditions found for the oxidation of monomer **1**, were used for monomer **2**, that was prepared according to literature procedures (Table 5-3).[21,22] Indeed, this was the preferred monomer to use for our studies, due to the presence of a phenylene ring that should allow for UV spectrophotometric quantitative analysis of the composition of the DCLs through UHPLC analysis.

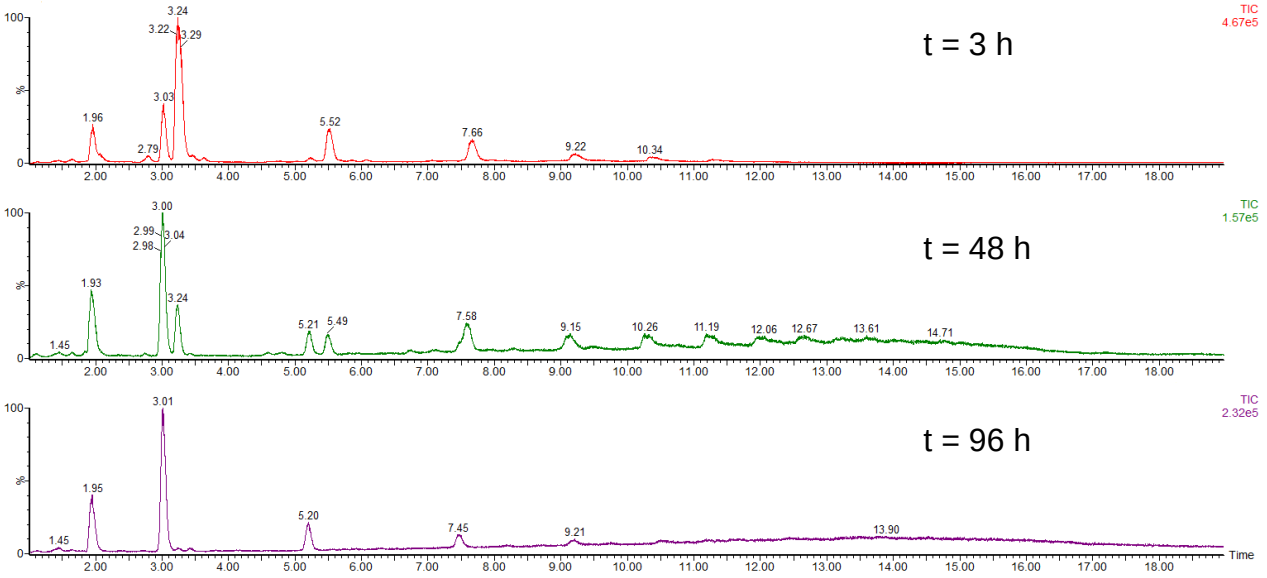

Figure 5-4. Portion of the LC-MS chromatograms for the experiment of Entry 2 of Table 5-3, respectively after 3 h, 48 h and 96 h from the beginning of the experiment. After 96 h, unreacted **1** (unresolved peak at t = 2.03 min), linear dimer (t = 3.24 min) and linear trimer (t = 5.49 min) disappeared, leaving only the related cyclic species (being, respectively, the unresolved peak at t = 1.96 min, the peak at t = 3.01 min and the peak at t = 5.20 min).

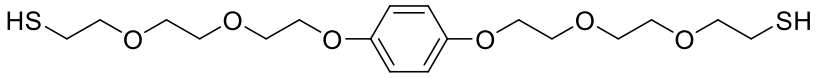

2

Table 5-4. Screening of the conditions for DCL formation from **2** in DMF/NEt_3.

Entry	**2** (mM)	Reaction conditions	Solubility
1	128 mM	DMF, NEt_3 260 mM, 80 °C, air balloon	-
2	250 mM	DMF, NEt_3 500 mM, 80 °C, air balloon	-

Unfortunately, both experiments at high concentrations of **2** gave some solubility problems and as a consequence we had to turn back to monomer **1** for the preparation of disulfide DCL at different concentrations and investigate the eventual formation of statistical catenanes.

So, eight libraries were built starting from monomer **1** (Table 5-5), using the following general conditions: *N*,*N*-dimethylformamide as the solvent, two molar equivalents of triethylamine with respect to the molar amount of **1**, an air balloon and reaction temperature of 80 °C. Both libraries at higher and lower concentrations with respect to the estimated c_{mon}^* value of 114 mM were prepared, to check if the behavior of cyclic species could be found to adhere

to classical Jacobson-Stockmayer predictions, even in case of eventual absence of catenanes. In this case, indeed, the otherwise expected catenane material[6] should form other oxidized species, supposing that oxidation is pushed to completion (namely cyclic species).

Table 5-5. DCLs prepared from monomer **1**.

Library	**1** (mM)	Reaction conditions
1	31	DMF, NEt_3 62 mM, 80 °C, air balloon
2	51	DMF, NEt_3 102 mM, 80 °C, air balloon
3	74	DMF, NEt_3 148 mM, 80 °C, air balloon
4	93	DMF, NEt_3 186 mM, 80 °C, air balloon
5	117	DMF, NEt_3 234 mM, 80 °C, air balloon
6	137	DMF, NEt_3 274 mM, 80 °C, air balloon
7	161	DMF, NEt_3 322 mM, 80 °C, air balloon
8	192	DMF, NEt_3 384 mM, 80 °C, air balloon

Libraries were daily monitored via UHPLC-MS until total oxidation was reached after four days, when no linear species were detectable in the MS of every peak of the chromatograms. Unfortunately, no catenane was detected even at the highest concentration employed, namely 192 mM. Moreover, another feature of the experiments became evident at high concentration domains and with the method used to analyze these libraries (see Experimental section):[23] the formation of a highly polydisperse polymeric material eluted at high retention times, whose nature (either linear, cyclic or catenated) was not possible to be determined (Figure 5-5). The addition of a reducing agent, tris(2-carboxyethyl)phosphine hydrochloride (TCEP), to an oxidized library proved that the polymeric material was formed by hexaethylene glycol dithiol subunits (Figure 5-6). Formation of this polymer possibly indicates that the conditions employed for the reaction do not allow to reach thermodynamic equilibrium in the disulfide mixtures.

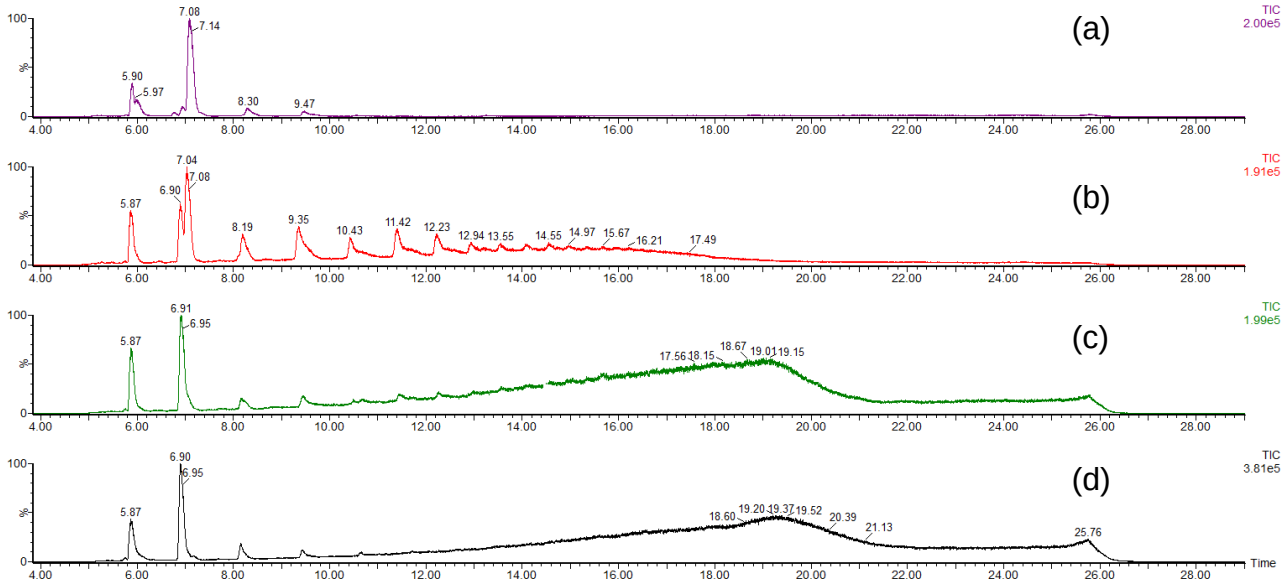

Figure 5-5. LC-MS monitoring of Library 8 (total monomer concentration: 192 mM), respectively, after (a) 1 d, (b) 2 d, (c), 3 d and (d) 4 d. The polymer maximum appears at 19 min.

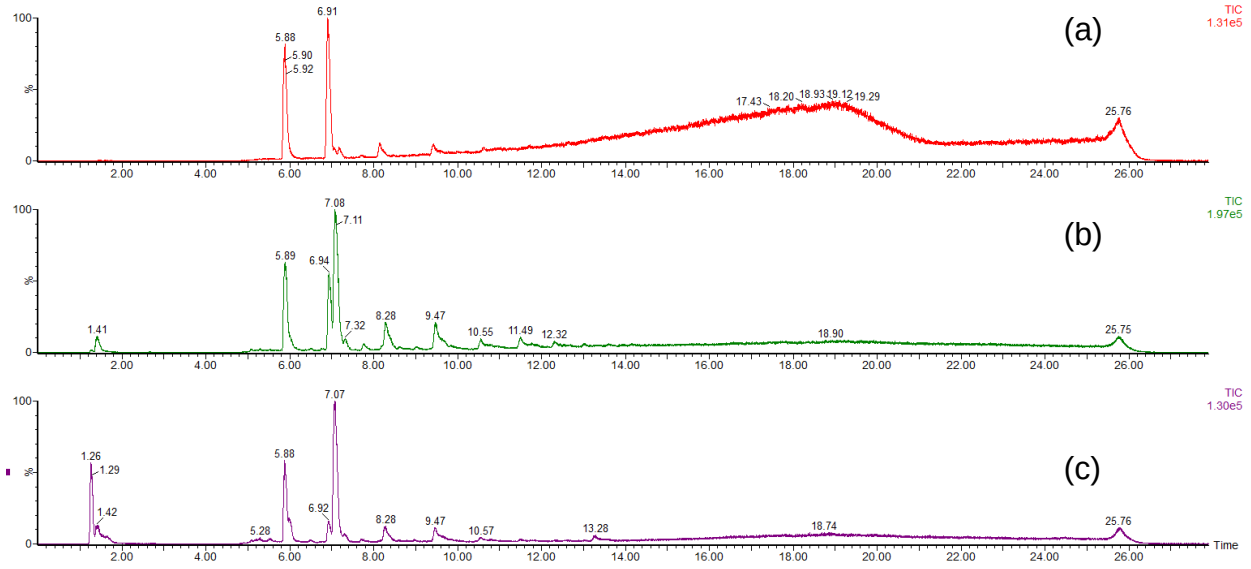

Figure 5-6. LC-MS traces relative to a reduction experiment of oxidized Library 8: (a) after 4 d from the beginning of the experiment; (b) after the addition of 50% mol TCEP and (c) after further addition of 100% mol TCEP. Polymer disappears upon addition of the reducing agent and peaks of lower oligomers grow due to the reductive depolymerization.

In UHPLC-UV chromatograms the polymer peak was not visible, no difference could be detected between the traces of the libraries and the ones for control experiments (without **1**) at high retention times. This was probably due to a combination of the wide breadth for the polymer peak and the general weak UV absorption power of the disulfide chromophores. However, based on the different relative intensities of the various cyclic oligomers in the UHPLC-MS and in the UHPLC-UV chromatograms (Figure 5-7), we speculated that MS

analysis might, to some extent, amplify the polymer peak due to elevated ionizability of the polymer.

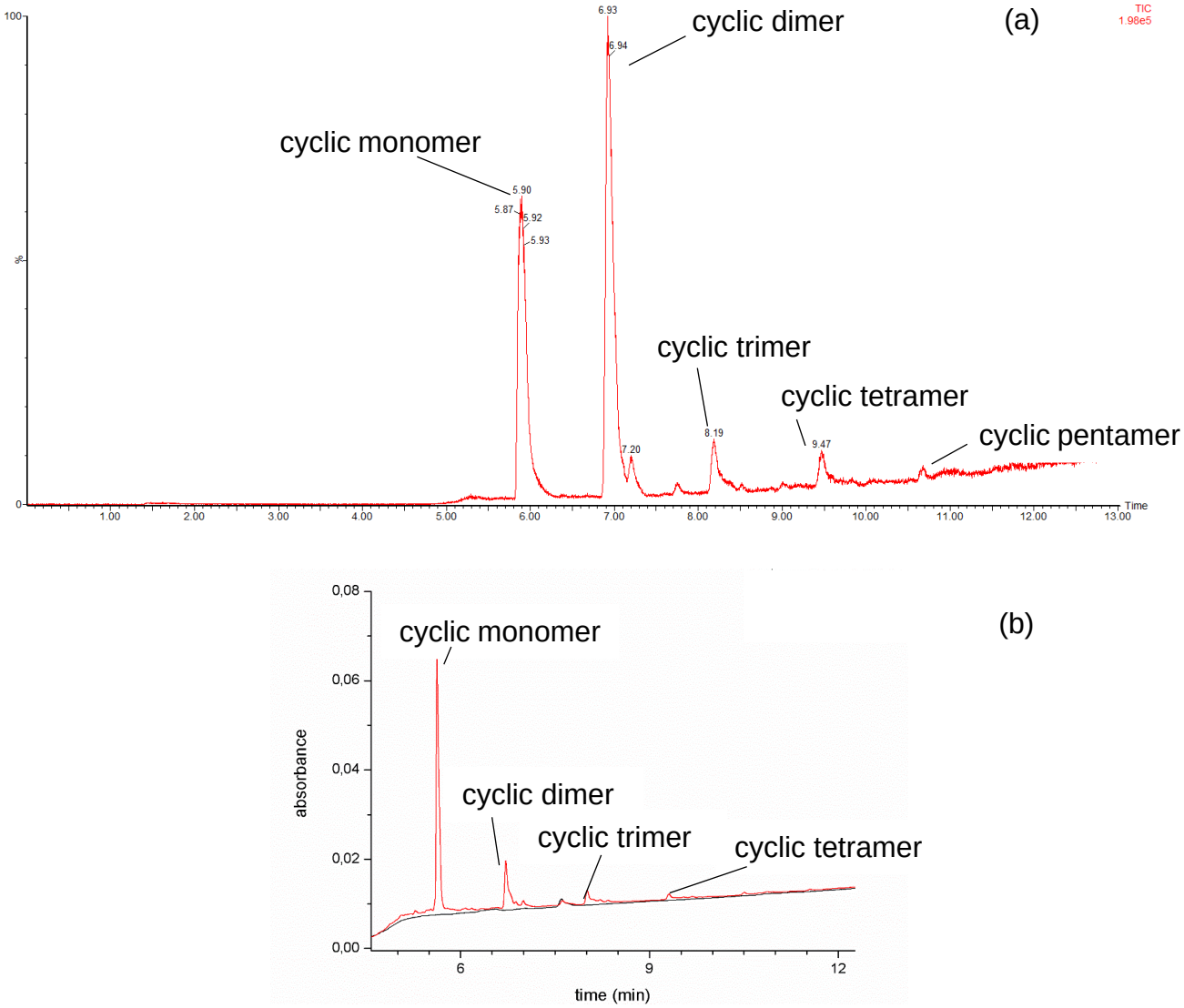

Figure 5-7. Library 7 (total monomer concentration: 161 mM) after 4 d. Portion of (a) the UHPLC-MS chromatogram and (b) the UHPLC-UV chromatograms, control (black trace) and experiment (red trace). Please note that the cyclic dimer appears to be more abundant than the cyclic monomer in the DCL, according to MS.

Therefore, based on the hypothesis that the polymer fraction might not be much relevant, an attempt at studying the distribution of the various species in the eight libraries was made, by integrating the peak areas of every visible cyclic oligomer and reporting the total peak area in each UHPLC-UV trace to the total monomer concentration of that experiment. In Figure 5-8 the concentrations thus determined for the first four cyclic oligomers are plotted against total monomer concentration.

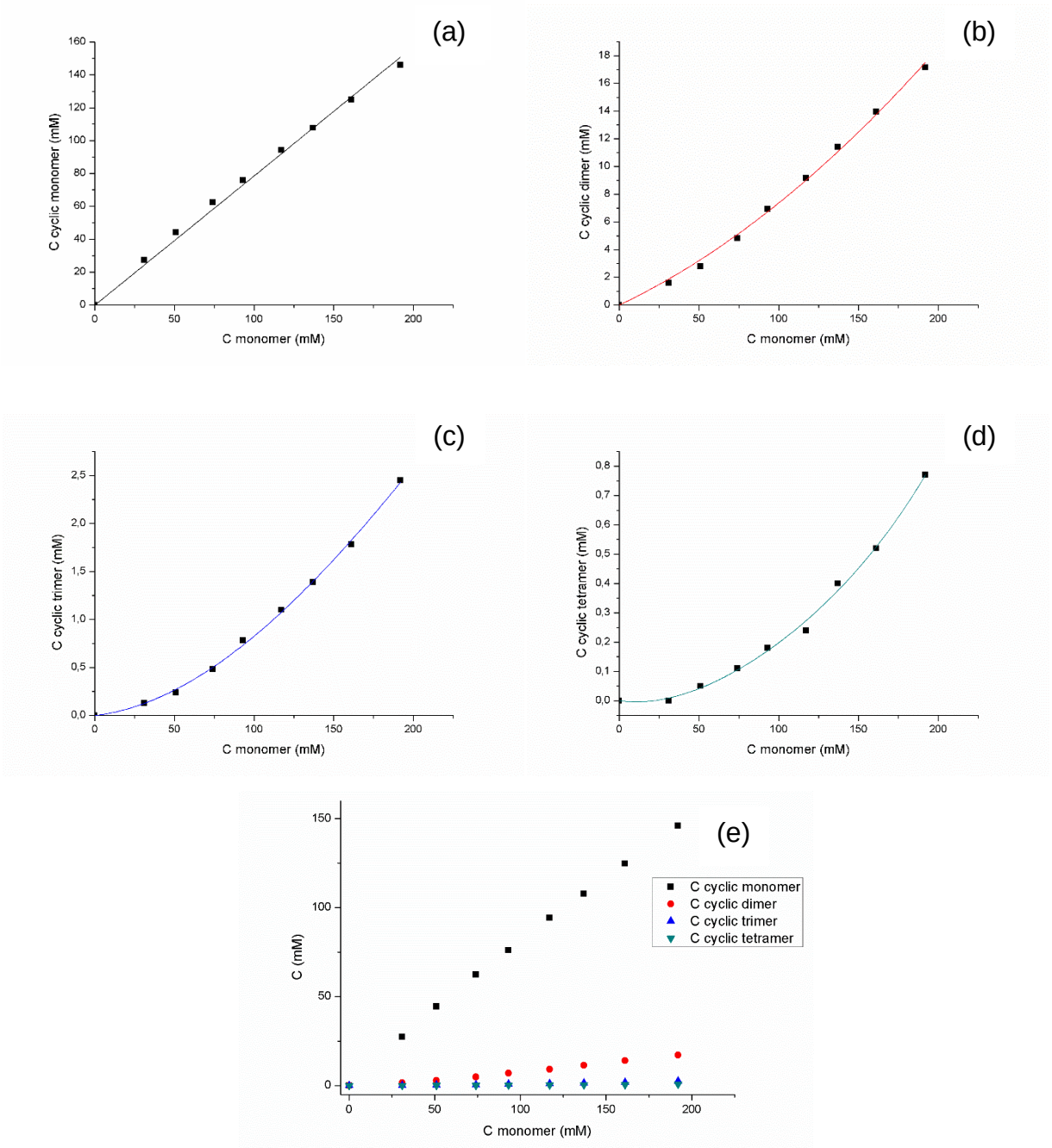

Figure 5-8. Plots of the estimated concentrations of (a) cyclic monomer, (b) cyclic dimer, (c) cyclic trimer and (d) cyclic tetramer against total monomer concentration, and (e) the combined data. Curves are meant as a guide to the eye.

The concentration trends for these species were not found to be amenable neither to any classical Jacobson-Stockmayer behavior for cyclic oligomers, that is saturation curves up to maximum values representing the respective EM_i, nor to any other theoretical explanation. The main reason behind these results is likely to be ascribed to the impossibility of determining accurate values of the absolute concentration of the species in the adopted conditions, due to the unwanted formation of a polymeric material of unknown nature.

CONCLUSIONS AND PERSPECTIVES

An attempt to study the statistical formation of catenanes in concentrated disulfide libraries prepared from long bifunctional dithiol monomers was made, in order to verify novel theoretical predictions within the framework of Jacobson-Stockmayer theory for reversible polymerization reactions.[6]

Due to low solubility of concentrated disulfide libraries of hexaethylene glycol dithiol (**1**) in aqueous solutions, a screening process to search for suitable conditions in polar organic solvents was performed, due to the shortage of procedures for disulfide exchange in this type of solvents in the literature. A possible solution to this problem was found by adapting a reported procedure for disulfide preparation.[19] Therefore, eight libraries were built at different total concentrations of **1** employing these reaction conditions, monomer **2** being not soluble in these conditions. However, no catenane was found at any of the initial monomer concentrations tested, according to LC-MS analysis of the oxidized libraries. Moreover, the unoptimized conditions adopted were found to be unsuitable for the aim of this study, due to the uncontrolled formation of a polymeric material, whose nature (either cyclic, linear or catenated) was not possible to be determined. This prevented any attempt to perform some quantitative analysis on the species constituting the oxidized libraries in the employed conditions.

On future efforts aimed at studying the statistical formation of catenanes using disulfide exchange, that in our view still represents probably the best candidate for this purpose, it will surely be useful to prepare the ground with preliminary studies on the reaction in organic solvents from which to draw fully for reliable procedures to achieve thermodynamically controlled mixtures of disulfides. Additionally, for very simple monomeric structures like **1**, the possibility to use alternative analytical techniques for the quantitative analysis of the mixtures should be investigated.

EXPERIMENTAL SECTION

Instruments, general methods and materials

NMR spectra were recorded with a 300 MHz or a 400 MHz spectrometer at room temperature and were internally referenced to the residual proton solvent signal. Flash chromatography was performed using a Reveleris® X2 flash chromatography system equipped with evaporative light-scattering (ELS) and UV detectors. UHPLC-MS

measurements were performed using a Waters Acquity UPLC® H-class system coupled to a Waters Xevo-G2 TOF. The mass spectrometer was operated in the positive electrospray ionization mode with the following ionization parameters: i) capillary voltage: 2.5 kV; ii) sampling cone voltage: 30 V; iii) extraction cone voltage: 4 V; iiii) source gas temperature: 150 °C; v) desolvation gas temperature: 500 °C; vi) cone gas flow (nitrogen): 5 L h^{-1}; vii) desolvation gas flow (nitrogen): 800 L h^{-1}. UHPLC-UV measurements were performed on a Waters Acquity UPLC® H-class system equipped with a photo-diode array (PDA) detector, at a detection wavelength of 250 nm. UHPLC analyses were performed on an Acquity UPLC® BEH C8 1.7 µm column (150 × 2.1 mm) using ULC-MS grade water (eluent A) and ULC-MS grade acetonitrile (eluent B), each containing 0.1% v/v formic acid as a modifier. A flow rate of 0.3 mL min^{-1} and a column temperature of 35 °C were applied. Dilution of all samples was always performed with the same solvent used in the experiment and right before injection in the UHPLC instruments. Libraries 1-8 were diluted to have ≈ 1 mg mL^{-1} samples for UHPLC analysis. The method used for the analysis of Libraries 1-8 for both types of UHPLC analysis is shown in Table 5-6.

Table 5-6. Chromatographic method used to analyze Libraries 1-8.

t (min)	% A	% B
0	90	10
2	90	10
3	50	50
18	5	95
23	5	95
24	50	50
26	50	50
27	90	10
30	90	10

All reagents and solvents were purchased at the highest commercial quality and were used without further purification, unless otherwise stated. Hexaethylene glycol (> 98%) was supplied by TCI. The glassware was either flame- or oven-dried. Hexaethylene glycol dibromide was prepared according to a literature procedure.[14a-b] Hexaethylene glycol dithiol (**1**) was prepared adapting a literature procedure.[14c] Monomer **2** was prepared adapting some literature procedures.[21]

Preparation of hexaethylene glycol dibromide

Under inert atmosphere, bromine (1 mL, 19.6 mmol) was added dropwise to a suspension of triphenylphosphine (4.7 g, 17.9 mmol) in acetonitrile (16.5 mL) and the resulting mixture was stirred for 10 min at 0 °C. Then, a solution of hexaethylene glycol (2.5 g, 8.9 mmol) in acetonitrile (8.5 mL) was added and the reaction mixture was left stirring for 48 h at room temperature. The white precipitate was filtered off as quickly as possible and the solvent was evaporated under vacuum. The thick residue obtained was extracted thoroughly with four portions of *n*-hexane (30 mL), and the combined organic phases were evaporated under vacuum to afford a colorless oil containing minor traces of triphenylphosphine oxide (1.79 g, yield: ≈ 50%) that was used without further purification. ^{1}H NMR (300 MHz, $CDCl_3$) δ (ppm): 3.81 (t, ^{3}J = 6 Hz, 4H), 3.67 (m, 16H), 3.48 (t, ^{3}J = 6 Hz, 4H).

Preparation of hexaethylene glycol dithiol (1)

In a two-neck round-bottomed flask equipped with a reflux condenser and containing an hexaethylene glycol dibromide (1.79 g of the colorless oil, ≈ 4.4 mmol) solution in ethanol (8.7 mL), thiourea (1 g, 13 mmol) was added and the reaction mixture was refluxed for 5 h. Then solvent was evaporated and freshly degassed aqueous sodium hydroxide (34 mL, 20% wt/v, 170 mmol) was introduced. The resulting reaction mixture was refluxed for 4 h. After cooling, aqueous hydrochloric acid (10% wt/wt) was slowly added until acidic pH. This non-homogenous mixture was extracted with three portions of diethyl ether (35 mL), then the ethereal phases were collected, dried with sodium sulfate, filtered and evaporated to afford a yellowish liquid (1.13 g). Reverse-phase flash column chromatography (C18 column, water + 0.1% v/v TFA/acetonitrile + 0.1% v/v TFA 0 → 100) allowed to obtain pure hexaethylene glycol dithiol (**1**) as a colorless liquid (0.66 g, yield: 48%). ^{1}H NMR (400 MHz, $CDCl_3$) δ (ppm): 3.66 (m, 20H), 2.70 (dt, $^{3}J_1$ = 8 Hz, $^{3}J_2$ = 6.4 Hz, 4H), 1.57 (t, ^{3}J = 6.4 Hz, 2H).

Preparation of 1,4-bis[2-[2-(2-hydroxyethoxy)ethoxy]ethoxy]benzene bis-(methylbenzenesulfonate)

Under inert atmosphere, a suspension of potassium carbonate (15.2 g, 110 mmol) in anhydrous acetonitrile (150 mL), distilled over calcium hydride, has been prepared in a two-neck round-bottomed flask equipped with a reflux condenser. Triethylene glycol ditosylate (12.1 g, 26.3 mmol) and hydroquinone (1.5 g, 13.9 mmol) were added and the reaction mixture was refluxed for seven days under inert atmosphere. After cooling, the mixture was filtered and the solid was washed with acetonitrile (50 mL). The organic layer was combined with the previously obtained filtrate and the solvent removed under vacuum. The crude

product was subjected to column chromatography (silica gel, *n*-hexane/ethyl acetate 9:1) to afford pure 4-bis[2-[2-(2-hydroxyethoxy)ethoxy]ethoxy]benzene bis(methylbenzene sulfonate) as a colorless oil (1.2 g, 1.8 mmol, yield: 13%). ^{1}H NMR (300 MHz, $CDCl_3$) δ (ppm): 7.79 (m, 4H), 7.32 (m, 4H), 6.83 (s, 4H), 4.16 (m, 4H), 4.05 (m, 4H), 3.79 (m, 4H), 3.65 (m, 12H), 2.43 (s, 6H).

Preparation of 1,4-bis[2-[2-(2-mercaptoethoxy)ethoxy]ethoxy]benzene diacetate

Potassium thioacetate (4.7 g, 40.9 mmol) was added to a solution of 4-bis[2-[2-(2-hydroxyethoxy)ethoxy]ethoxy]benzene bis-(methylbenzene sulfonate) (1.2 g, 1.8 mmol) in N,N-dimethylformamide (60 mL) under inert atmosphere, and the reaction mixture was stirred for seven days at room temperature. Dichloromethane (150 mL) was added and the resulting mixture was thoroughly washed with four portions of distilled water (300 mL). The solvent was evaporated and the reaction crude was subjected to column chromatography (silica gel, *n*-hexane/ethyl acetate 6:4) to afford pure 1,4-bis[2-[2-(2-mercapto-ethoxy)ethoxy]ethoxy]benzene diacetate (0.507 mg, 1.0 mmol, yield: 57%). ^{1}H NMR (400 MHz, $CDCl_3$) δ (ppm): 6.84 (s, 4H), 4.08 (m, 4H), 3.83 (m, 4H), 3.71 (m, 4H), 3.65 (m, 4H), 3.61 (t, ^{3}J = 6.4 Hz, 4H), 3.09 (t, ^{3}J = 6.4 Hz, 4H), 2.33 (s, 6H).

Preparation of compound 2

1,4-bis[2-[2-(2-mercaptoethoxy)ethoxy]ethoxy]benzene diacetate (0.507 mg, 1.0 mmol) was dissolved in a freshly degassed solution of methanol (9 mL) and aqueous hydrochloric acid (1 ml, 37% wt./wt.) under inert atmosphere, and the reaction mixture was refluxed overnight. After cooling, dichloromethane (20 mL) was added and the solution was washed with distilled water (30 mL), dried with sodium sulfate and filtered. The solvent was evaporated under vacuum and the crude subjected to reverse-phase flash column chromatography (C18 column, water + 0.1% v/v TFA/acetonitrile + 0.1% v/v TFA 0 → 100) to afford pure **2** as a colorless oil (0.285 g, 0.7 mmol, yield: 65%). ^{1}H NMR (400 MHz, $CDCl_3$) δ (ppm): 6.84 (s, 4H), 4.08 (m, 4H), 3.84 (m, 4H), 3.72 (m, 4H), 3.66 (m, 4H), 3.63 (t, ^{3}J = 6.4 Hz, 4H), 2.70 (dt, $^{3}J_1$ = 8 Hz, $^{3}J_2$ = 6.4 Hz, 4H). 1.58 (t, ^{3}J = 6.4 Hz, 2H).

General procedure for disulfide exchange experiments

A stock solution of dithiol monomer in dichloromethane was introduced in a weighed 4 mL vial, and the solvent was carefully evaporated under vacuum to accurately measure the weight of the dithiol introduced. A magnetic stirring bar is introduced in the vial, then the

proper amounts of solvents and base were added up to a total volume of 0.5 mL, the vial was closed with a screw-cap and the reaction mixture was stirred at room temperature.

General procedure for Libraries 1-8 experiments

A stock solution of **1** in dichloromethane was introduced in a weighed 4 mL vial, and the solvent was carefully evaporated under vacuum to accurately measure the weight of the dithiol introduced. A magnetic stirring bar is introduced in the vial, then the proper amounts of 1 M triethylamine stock solution in *N*,*N*-dimethylformamide and pure *N*,*N*-dimethylformamide were added up to a total volume of 0.5 mL and an air balloon was attached through a needle to the vial having a septum-equipped cap. The reaction mixture was stirred at 80 °C for 4 d.

NOTES AND REFERENCES

1 (a) G. Schill, *Catenanes, Rotaxanes, and Knots*, Academic Press, London (U.K.), **1971**; (b) *Molecular Catenanes, Rotaxanes and Knots* (editors: J.-P. Sauvage, C. O. Dietrich-Buchecker), Wiley-VCH, Weinheim (Germany), **1999**; (c) C. J. Bruns, J. F. Stoddart, *The Nature of Mechanical Bond*, John Wiley & Sons, Hoboken, New Jersey (U.S.A.), **2017**; (d) H. L. Frisch, E. Wasserman, *J. Am. Chem. Soc.* **1961**, *83*, 3789-3795; (e) G. Gil-Ramírez, D. A. Leigh, A. J. Stephens, *Angew. Chem. Int. Ed.* **2015**, *54*, 6110-6150; (f) S. D. P. Fielden, D. A. Leigh, S. L. Woltering, *Angew. Chem. Int. Ed.* **2017**, *56*, 11166-11194.

2 E. Wasserman, *J. Am. Chem. Soc.* **1960**, *82*, 4433-4434.

3 For a disambiguation statement by Wasserman on the reported yield value, see note 7 in: D. A. Ben-Efraim, C. Batich, E. Wasserman, *J. Am. Chem. Soc.* **1970**, *92*, 2133-2135.

4 G. Schill, A. Lüttringhaus, *Angew. Chem. Int. Ed. Engl.* **1964**, *3*, 546-547.

5 C. O. Dietrich-Buchecker, J. P. Sauvage, J.-P. Kintzinger, *Tetrahedron Lett.* **1983**, *24*, 5095-5098.

6 S. Di Stefano, G. Ercolani, *J. Phys. Chem. B* **2017**, *121*, 649-656.

7 (a) H. Jacobson, W. H. Stockmayer, *J. Chem. Phys.* **1950**, *18*, 1600-1606; (b) G. Ercolani, L. Mandolini, P. Mencarelli, S. Roelens, *J. Am. Chem. Soc.* **1993**, *115*, 3901-3908.

8 S. Di Stefano, G. Ercolani, *Macromol. Theory Simul.* **2016**, *25*, 63-73.

9 The Kuhn segment of an ideal polymer chain is defined as the shortest portion of an equivalent freely-jointed polymer chain that is able to explore freely any direction in space. See: M. Rubinstein, R. H. Colby, *Polymer Physics*, Oxford University Press, Oxford (U.K.), **2003**, pp. 53-54.

10 See for example: (a) S. P. Black, J. K. M. Sanders, A. R. Stefankiewicz, *Chem. Soc. Rev.* **2014**, *43*, 1861-1872; (b) H. Hioki, W. C. Still, *J. Org. Chem.* **1998**, *63*, 904-905; (c) S. Otto, R. L. E. Furlan, J. K. M. Sanders, *J. Am. Chem. Soc.* **2000**, *122*, 12063-12064; (d) S. Otto, S. Kubik, *J. Am. Chem. Soc*. **2003**, *125*, 7804-7805 (e) S. Ladame, A. M. Whitney, S. Balasubramanian, *Angew. Chem. Int. Ed.* **2005**, *44*, 5736-5739; (f) J. M. A. Carnall, C. A. Waudby, A. M. Belenguer, M. C. A. Stuart, J. J.-P. Peyralans, S. Otto, *Science* **2010**, *327*, 1502-1506; (g) N. Ponnuswamy, F. B. L. Cougnon, J. M. Clough, G. D. Pantoş, J. K. M. Sanders, *Science* **2012**, *338*, 783-785.; (h) P. Nowak, M. Colomb-Delsuc, S. Otto, J. Li, *J. Am. Chem. Soc.* **2015**, *137*, 10965-10969; (i) J. W. Sadownik, E. Mattia, P. Nowak, S. Otto, *Nat. Chem.* **2016**, *8*, 264-269; (j) B. M. Matysiak, P. Nowak, I. Cvrtila, C. G. Pappas, B. Liu, D. Komáromy, S. Otto, *J. Am. Chem. Soc.* **2017**, *139*, 6744−6751; (k) F. B. L. Cougnon, K. Caprice, M. Pupier, A. Bauzá, A. Frontera, *J. Am. Chem. Soc.* **2018**, *140*, 12442-12450.

11 For more information on oxidation of thiols by molecular oxygen and thiol-disulfide exchange reaction, see for example: (a) G. Capozzi, G. Modena, *Oxidation of Thiols* in *The Chemistry of Functional Groups - The Chemistry of the Thiol Group, Part 2* (editor: S. Patai), John Wiley & Sons, Chichester (U.K.), **1974**; (b) R. Singh, G. M. Whitesides, *Thiol-Disulfide Interchange* in *The Chemistry*

of Functional Groups - Supplement S: The Chemistry of Sulphur-Containing Functional Groups (editors: S. Patai, Z. Rappoport), John Wiley & Sons, Chichester (U.K.), **1993**; (c) H. Gilbert, *Methods Enzymol.* **1995**, *251*, 8-28; (d) T. J. Wallace, A. Schriesheim, W. Bartok, *J. Org. Chem.* **1963**, *28*, 1311-1314; (e) W. J. Lees, G. M. Whitesides, *J. Org. Chem.* **1993**, *58*, 642-647.

12 Some research work suggesting statistical formation of catenanes and polycatenanes in 1,2-dithiane bulk polymerization by means of disulfide metathesis (radical mechanism) has already been reported in the literature. See for example: (a) K. Endo, T. Shiroi, N. Murata, G. Kojima, T. Yamanaka, *Macromolecules* **2004**, *37*, 3143-3150; (b) K. Endo, T. Shiroi, N. Murata, *Polym. J.* **2005**, *37*, 512-516.

13 These values were obtained hypothesizing that only strainless rings are formed from monomers **1** and **2**, having respectively 18 and 20 rotors. Thus, Equation 10 in Chapter 3 becomes

$$c^*_{\mathrm{mon}} = 2.612B$$

where the expression of *B* was shown in reference 6 of Chapter 3. *B* values for the two chains were calculated by using the average values of 1.54 x 10^{-9} dm and 8 for *l* and C_∞, respectively. See: (a) Y. Yamashita, J. Mayumi, Y. Kawakami, K. Ito, *Macromolecules* **1980**, *13*, 1075-1080; (b) L. Mandolini, *Adv. Phys. Org. Chem.* **1986**, *22*, 1-111; (c) S. Di Stefano, G. Ercolani, *Adv. Phys. Org. Chem.* **2016**, *50*, 1-76.

14 (a) E. Biron, F. Otis, J.-C. Meillon, M. Robitaille, J. Lamothe, P. Van Hove, M.-E. Cormier, N. Voyer, *Bioorg. Med. Chem.* **2004**, *12*, 1279-1290; (b) B. Maji, K. Kumar, K. Muniyappa, S. Bhattacharya, *Org. Biomol. Chem.* **2015**, *13*, 8335-8348; (c) J. S. Bradshaw, K. E. Krakowiak, R. M. Izatt, R. L. Bruening, B. J. Tarbet, *J. Heterocyclic Chem.* **1990**, *27*, 347-349.

15 For examples of base-induced disulfide exchange in halogenated solvents, see reference 10b and: (a) A. L. Kieran, A. D. Bond, A. M. Belenguer, J. K. M. Sanders, *Chem. Commun.* **2003**, 2674-2675; (b) A. T. ten Cate, P. Y. W. Dankers, R. P. Sijbesma, E. W. Meijer, *J. Org. Chem.* **2005**, *70*, 5799-5803. For an example of disulfide metathesis in a polar solvent, see: (c) M. Arisawa, M. Yamaguchi, *J. Am. Chem. Soc.* **2003**, *125*, 6624-6625.

16 2-Mercaptoethanol, a structurally analogous thiol with respect to **1** and **2**, has a pK_a value of 9.72. See: *Ionisation constants of organic acids in aqueous solution* (editors: E. P. Serjeant, B. Dempsey), Pergamon Press, Oxford (U.K.), **1979**.

17 For 0.5 mL of a 130 mM dithiol solution the total amount of thiols is 1.3 x 10^{-4} mol. If the solution is contained in a 4 mL closed vial, the headspace of the vial should be approximately 3.5 mL. From the ideal gas law, using T = 298 K, P = 1 atm, R = 0.082 L atm K^{-1} mol^{-1} and a relative molar concentration of molecular oxygen in air equal to 20%, we find n_{O_2} = 2.86 x 10^{-5} mol. If this is the case, the amount of oxygen would not be enough for the oxidation of all thiols present in the solution, according to the stoichiometry of Equation 1.

18 L. Bettanin, S. Saba, F. Z. Galetto, G. A. Mike, J. Rafique, A. L. Braga, *Tetrahedron Lett.* **2017**, *58*, 4713-4716.

19 J. L. García Ruano, A. Parra, J. Alemán, *Green Chem.* **2008**, *10*, 706-711.

20 T. J. Wallace, N. Jacobson, A. Schriesheim, *Nature* **1964**, *201*, 609-610.

21 (a) L. Sheeney-Haj-Ichia, I. Willner, *J. Phys. Chem. B* **2002**, *106*, 13094-13097; (b) P. R. Ashton, J. Huff, S. Menzer, I. W. Parsons, J. A. Preece, J. F. Stoddart, M. S. Tolley, A. J. P. White, D. J. Williams, *Chem. Eur. J.* **1996**, *2*, 31-44; (c) D. J. Keddie, J. B. Grande, F. Gonzaga, M. A. Brook, T. R. Dargaville, *Org. Lett.* **2011**, *13*, 6006-6009.

22 Some tests in methanol with 10% mol Bu_4NOH were also conducted, but the DCLs formed with this monomer were found to be not soluble even at monomer concentrations as low as 100 mM. Experiments performed in DMSO/MeOH mixtures in conditions like the ones described in Entries 5-7 of Table 5-2 gave the same outcome as for monomer **1**.

23 At this stage of the work a different chromatographic method was used (see Experimental section) with respect to the one used in the screening phase (e.g. the one used for LC-MS traces shown in Figure 5-4). The reason for this change was to let the peak of the cyclic monomer elute at higher retention times, to avoid the superposition with the peak ascribable to DMF/NEt_3 (after comparison with the trace of a control experiment, without **1**) observed in the UHPLC traces, allowing for integration of the peak in order to perform quantitative analyses.

List of publications

Publications included in this work

I. S. Albano, G. Olivo, L. Mandolini, C. Massera, F. Ugozzoli, S. Di Stefano, *J. Org. Chem.* **2017**, *82*, 3820-3825;

II. S. Albano, A. Fantozzi, J. A. Berrocal, S. Di Stefano, *J. Polym. Sci. Part A: Polym. Chem.* **2017**, *55*, 1237-1242.

Publications not included in this work

I. J. A. Berrocal, S. Albano, L. Mandolini, S. Di Stefano, *Eur. J. Org. Chem.* **2015**, 7504-7510;

II. C. Biagini, S. Albano, R. Caruso, L. Mandolini, J. A. Berrocal, S. Di Stefano, *Chem. Sci.* **2018**, *9*, 181-188.